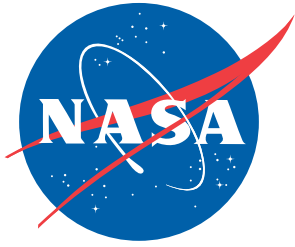


NASA/TM-2010-216839



Design of 8-ft-diameter Barrel Test Article Attachment Rings for Shell Buckling Knockdown Factor Project

*Andrew E. Lovejoy and Mark W. Hilburger
Langley Research Center, Hampton, Virginia*

August 2010

NASA STI Program . . . in Profile

Since its founding, NASA has been dedicated to the advancement of aeronautics and space science. The NASA scientific and technical information (STI) program plays a key part in helping NASA maintain this important role.

The NASA STI program operates under the auspices of the Agency Chief Information Officer. It collects, organizes, provides for archiving, and disseminates NASA's STI. The NASA STI program provides access to the NASA Aeronautics and Space Database and its public interface, the NASA Technical Report Server, thus providing one of the largest collections of aeronautical and space science STI in the world. Results are published in both non-NASA channels and by NASA in the NASA STI Report Series, which includes the following report types:

- **TECHNICAL PUBLICATION.** Reports of completed research or a major significant phase of research that present the results of NASA programs and include extensive data or theoretical analysis. Includes compilations of significant scientific and technical data and information deemed to be of continuing reference value. NASA counterpart of peer-reviewed formal professional papers, but having less stringent limitations on manuscript length and extent of graphic presentations.
- **TECHNICAL MEMORANDUM.** Scientific and technical findings that are preliminary or of specialized interest, e.g., quick release reports, working papers, and bibliographies that contain minimal annotation. Does not contain extensive analysis.
- **CONTRACTOR REPORT.** Scientific and technical findings by NASA-sponsored contractors and grantees.

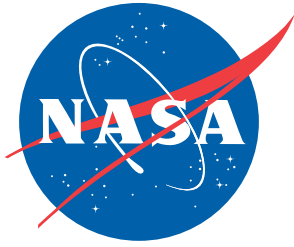
- **CONFERENCE PUBLICATION.** Collected papers from scientific and technical conferences, symposia, seminars, or other meetings sponsored or co-sponsored by NASA.
- **SPECIAL PUBLICATION.** Scientific, technical, or historical information from NASA programs, projects, and missions, often concerned with subjects having substantial public interest.
- **TECHNICAL TRANSLATION.** English-language translations of foreign scientific and technical material pertinent to NASA's mission.

Specialized services also include creating custom thesauri, building customized databases, and organizing and publishing research results.

For more information about the NASA STI program, see the following:

- Access the NASA STI program home page at <http://www.sti.nasa.gov>
- E-mail your question via the Internet to help@sti.nasa.gov
- Fax your question to the NASA STI Help Desk at 443-757-5803
- Phone the NASA STI Help Desk at 443-757-5802
- Write to:
NASA STI Help Desk
NASA Center for AeroSpace Information
7115 Standard Drive
Hanover, MD 21076-1320

NASA/TM-2010-216839



Design of 8-ft-diameter Barrel Test Article Attachment Rings for Shell Buckling Knockdown Factor Project

*Andrew E. Lovejoy and Mark W. Hilburger
Langley Research Center, Hampton, Virginia*

National Aeronautics and
Space Administration

Langley Research Center
Hampton, Virginia 23681-2199

August 2010

The use of trademarks or names of manufacturers in the report is for accurate reporting and does not constitute an official endorsement, either expressed or implied, of such products or manufacturers by the National Aeronautics and Space Administration.

Available from:

NASA Center for AeroSpace Information
7115 Standard Drive
Hanover, MD 21076-1320
443-757-5802

Preface

The Shell Buckling Knockdown Factor Project (SBKF), NESC Assessment #: 07-010-E, was established in March of 2007 by the NASA Engineering and Safety Center (NESC) in collaboration with the NASA Constellation Program (CxP). The SBKF Project has the goal of developing and experimentally validating improved (i.e., less-conservative, more robust) shell buckling design factors (a.k.a. knockdown factors) and design technologies for launch vehicle structures.

Preliminary design studies indicate that implementation of these new knockdown factors can enable significant weight savings in these vehicles and will help mitigate some of NASA's future launch vehicle development and performance risks, e.g., reduced reliance on large-scale testing, high-fidelity estimates of as-built structural performance, increased payload capability, and improved structural reliability.

To this end, a series of detailed Project Reports are being published to document all results from the SBKF Project and including design trade studies, test article and test facility design, analysis and test data, technology development white papers and state-of-the-art assessments, and finally shell design guidelines to update and/or augment the existing NASA SP series publications for the design of buckling-critical thin-walled shell structures. A select group of significant results, in whole or in part, will be published as NASA Technical Memorandums (TM).

Any documents, that are published as a part of this series, that refer to or report specific designs or design, analysis, and testing methodologies are to be regarded as guidelines and not as NASA requirements or criteria, except as specified in formal project specifications.

Comments concerning the technical content of this NASA TM are welcomed.

The following Project Report was used to create this TM:

SBKF-P2-TR-2008-007

Table of Contents

Nomenclature	viii
1.0 Introduction	1
2.0 Summary of Results	1
3.0 Physical Description of Test Setup/Test Assembly	1
4.0 Design/Test Requirements and Criteria	2
4.1 Structural Design	2
4.2 Factors of Safety and Knockdown Factors	5
4.3 Margin Calculations	5
4.4 Material Properties	6
4.5 Loads	6
5.0 Approach	6
5.1 Purpose	6
5.2 Assumptions	7
5.3 Rationale	8
6.0 Results	8
6.1 Bolt Patterns	8
6.2 Multiple-Piece Designs	9
6.3 Single-Piece Design	22
7.0 Conclusions	27
8.0 References	28
 Appendix A: Closed-Form Solution Spreadsheet Description	 29
 Appendix B: Bolt Pattern Design FEM	 32
B-1 Two-Row, In-Line	32
B-2 Two-Row, Staggered	33
B-3 Two-Row, Staggered, Gapped	34
 Appendix C: Multiple-Piece Design FEM	 35
C-1 Design MP-1	35
C-2 Design MP-2	37
C-3 Design MP-3	55
 Appendix D: Single-Piece Design FEM	 56

List of Figures

Figure 3.1. SBKF sub-scale cylinder test assembly.....	2
Figure 4.1. Initial two-piece attachment ring design concept (MP-1).....	3
Figure 4.2. Two-piece attachment ring design concept with outer band (MP-2).....	3
Figure 4.3. Three-piece attachment ring design concept (MP-3).....	4
Figure 4.4. Single-piece attachment ring design concept (SP-1).....	4
Figure 5.1. Sketch depicting clamped boundary for finite element analyses (MP-1).....	8
Figure 6.1. Two-row bolt patterns investigated.	9
Figure 6.2. MP-1 design cross-section definition (not drawn to scale).....	10
Figure 6.3. MP-1 design inner and outer ring locations.....	11
Figure 6.4. MP-1 design circumferential bolt spacing.....	11
Figure 6.5. MP-2 Design cross-section definition (not drawn to scale).....	15
Figure 6.6. Typical MP-2 buckling mode, shown for $t_{w,L} = t_{w,B} = 0.5$ inch.....	16
Figure 6.7. Local solid model MP-2 design cross-section deformation at $N_x = 5,050$ lb/in (magnification factor of 5).....	17
Figure 6.8. Local solid model MP-2 design, L-shaped ring vonMises stresses at $N_x = 5,050$ lb/in.....	18
Figure 6.9. Local solid model MP-2 design, band vonMises stresses at $N_x = 5,050$ lb/in.	19
Figure 6.10. MP-2 design cross-section definition (not drawn to scale).....	21
Figure 6.11. SP-1 design cross-section definition (not drawn to scale).....	27
Figure A.1. Example spreadsheet for bolted joint in tension.....	29
Figure A.2. Example spreadsheet for bolted joint in single shear.	30
Figure A.3. Example spreadsheet for bolted joint in double shear.	31
Figure B.1. Two-row, in-line bolt pattern FEM (compression case).....	32
Figure B.2. Two-row, staggered bolt pattern FEM (compression case).....	33
Figure B.3. Two-row, staggered, gapped bolt pattern FEM (compression case).....	34
Figure C.1. MP-1 FEM.....	35
Figure C.2. MP-1 FEM isometric view.....	36
Figure C.3. MP-1 FEM applied load.....	37
Figure C.4. MP-2 FEM to examine thickness of L-bracket web and band.....	38
Figure C.5. Close-up of MP-2 FEM to determine required thickness of L-bracket web and band.	39
Figure C.6. Use of dummy ply to remove offsets.....	40
Figure C.7. Nonlinear deformation for design MP-2 at 2,300 lb/in with $t_{w,L} = t_{w,B} = 0.25$ inch (contours indicate radial displacement).....	41
Figure C.8. vonMises stress for design MP-2 at 2,300 lb/in with $t_{w,L} = t_{w,B} = 0.25$ inch, test article weld land inner surface.	42
Figure C.9. vonMises stress for design MP-2 at 2,300 lb/in with $t_{w,L} = t_{w,B} = 0.25$ inch, test article weld land outer surface.	43
Figure C.10. vonMises stress for design MP-2 at 2,300 lb/in with $t_{w,L} = t_{w,B} = 0.25$ inch, test article skin inner surface.....	44
Figure C.11. vonMises stress for design MP-2 at 2,300 lb/in with $t_{w,L} = t_{w,B} = 0.25$ inch, test article skin outer surface.....	45
Figure C.12. vonMises stress for design MP-2 at 2,300 lb/in with $t_{w,L} = t_{w,B} = 0.25$ inch, test article stringer Z_1 ("bottom" of element) surface.	46
Figure C.13. vonMises stress for design MP-2 at 2,300 lb/in with $t_{w,L} = t_{w,B} = 0.25$ inch, test article stringer Z_2 ("bottom" of element) surface.	47
Figure C.14. vonMises stress for design MP-2 at 2,300 lb/in with $t_{w,L} = t_{w,B} = 0.25$ inch, test article L-shaped ring web inner surface.....	48
Figure C.15. vonMises stress for design MP-2 at 2,300 lb/in with $t_{w,L} = t_{w,B} = 0.25$ inch, test article L-shaped ring web outer surface.....	49

Figure C.16. vonMises stress for design MP-2 at 2,300 lb/in with $t_{w,L} = t_{w,B} = 0.25$ inch, test article band inner surface.	50
Figure C.17. vonMises stress for design MP-2 at 2,300 lb/in with $t_{w,L} = t_{w,B} = 0.25$ inch, test article band outer surface.	51
Figure C.18. Local MP-2 FEM to examine contact response of L-bracket web and band.	52
Figure C.19. Locations of bolts (black) in local MP-2 FEM.	53
Figure C.20. Contact surface locations for local MP-2 FEM.	54
Figure C.21. Attachment ring modeled in MP-3 shell FEM.	55
Figure D.1. SP-1 ABAQUS™ shell FEM.	57
Figure D.2. SP-1 ABAQUS™ shell FEM, laminated end.	58
Figure D.3. SP-1 ABAQUS™ shell FEM, bolted end.	59
Figure D.4. SP-1 ABAQUS™ shell FEM attachment bolt beams (shown in black).	60
Figure D.5. SP-1 nonlinear deformed shape, LC1 at 2220 lb/in, AISI 1025 steel attachment rings (deformations magnified x50).	61
Figure D.6. SP-1 nonlinear deformed shape with radial deflection contours, LC1 at 2220 lb/in, AISI 1025 steel attachment rings (deformations magnified x50).	62
Figure D.7. SP-1 vonMises stress (psi) in inner flange inner surface at laminated end, LC1 at 2220 lb/in, AISI 1025 steel attachment rings.	63
Figure D.8. SP-1 vonMises stress (psi) in inner flange outer surface at laminated end, LC1 at 2220 lb/in, AISI 1025 steel attachment rings.	64
Figure D.9. SP-1 vonMises stress (psi) in inner flange inner surface at bolted end, LC1 at 2220 lb/in, AISI 1025 steel attachment rings.	65
Figure D.10. SP-1 vonMises stress (psi) in inner flange outer surface at bolted end, LC1 at 2220 lb/in, AISI 1025 steel attachment rings.	66
Figure D.11. SP-1 vonMises stress (psi) in outer flange inner surface at laminated end, LC1 at 2220 lb/in, AISI 1025 steel attachment rings.	67
Figure D.12. SP-1 vonMises stress (psi) in outer flange outer surface at laminated end, LC1 at 2220 lb/in, AISI 1025 steel attachment rings.	68
Figure D.13. SP-1 vonMises stress (psi) in outer flange inner surface at bolted end, LC1 at 2220 lb/in, AISI 1025 steel attachment rings.	69
Figure D.14. SP-1 vonMises stress (psi) in outer flange outer surface at bolted end, LC1 at 2220 lb/in, AISI 1025 steel attachment rings.	70
Figure D.15. SP-1 vonMises stress (psi) in weld land inner surface, LC1 at 2220 lb/in, AISI 1025 steel attachment rings.	71
Figure D.16. SP-1 vonMises stress (psi) in weld land outer surface, LC1 at 2220 lb/in, AISI 1025 steel attachment rings.	72
Figure D.17. SP-1 vonMises stress (psi) in acreage skin inner surface, LC1 at 2220 lb/in, AISI 1025 steel attachment rings.	73
Figure D.18. SP-1 vonMises stress (psi) in acreage skin outer surface, LC1 at 2220 lb/in, AISI 1025 steel attachment rings.	74
Figure D.19. SP-1 vonMises stress (psi) in intermediate skin inner surface, LC1 at 2220 lb/in, AISI 1025 steel attachment rings.	75
Figure D.20. SP-1 vonMises stress (psi) in intermediate skin outer surface, LC1 at 2220 lb/in, AISI 1025 steel attachment rings.	76
Figure D.21. SP-1 vonMises stress (psi) in ring inner surface, LC1 at 2220 lb/in, AISI 1025 steel attachment rings.	77
Figure D.22. SP-1 vonMises stress (psi) in ring outer surface, LC1 at 2220 lb/in, AISI 1025 steel attachment rings.	78
Figure D.23. SP-1 vonMises stress (psi) in stringer inner surface, LC1 at 2220 lb/in, AISI 1025 steel attachment rings.	79

Figure D.24. SP-1 vonMises stress (psi) in stringer skin outer surface, LC1 at 2220 lb/in, AISI 1025 steel attachment rings.	80
Figure D.25. SP-1 nonlinear contact region deformation at weld land, LC1 at 2220 lb/in, AISI 1025 steel attachment rings (deformations magnified x50).	81
Figure D.26. SP-1 nonlinear contact region deformation at acreage (center of panel), LC1 at 2220 lb/in, AISI 1025 steel attachment rings (deformations magnified x50).	82

List of Tables

Table 4.1. Attachment ring material properties.	6
Table 6.1. Bolt load distribution between bolt rows in two-row patterns.	9
Table 6.2. MS for MP-1 attachment ring design.	10
Table 6.3. Critical LC1 linear buckling loads for design MP-2, various attachment ring designs.	13
Table 6.4. Nonlinear LC1 instability loads for design MP-2, various attachment ring designs.	13
Table 6.5. Maximum LC1 nonlinear vonmises stresses for design MP-2, various attachment ring designs.	13
Table 6.6. MS for MP-2 attachment ring design, load case LC1.	14
Table 6.7. MS for MP-2 attachment ring design, load case LC2.	14
Table 6.8. MS for MP-3 attachment ring design, load case LC1.	20
Table 6.9. MS for MP-3 Attachment Ring Design, Load Case LC2.	20
Table 6.10. Response summary for SP-1 AISI 1025 steel attachment ring design.	23
Table 6.11. Response summary for SP-1 7075-T651 aluminum attachment ring design.	23
Table 6.12. MS for SP-1 AISI 1025 steel attachment ring design, LC1 scaled to 5050 lb/in.	24
Table 6.13. MS for SP-1 7075-T651 aluminum attachment ring design, LC1 scaled to 5050 lb/in.	24
Table 6.14. MS for SP-1 AISI 1025 steel attachment ring design, load case LC2.	25
Table 6.15. MS for SP-1 7075-T651 aluminum attachment ring design, load case LC2.	25
Table 6.16. MS for SP-1 AISI 1025 steel attachment ring design, load case LC3.	26
Table 6.17. MS for SP-1 7075-T651 aluminum attachment ring design, load case LC3.	26

Nomenclature

Acronyms

AISC	American Institute of Steel Construction
AISI	American Iron and Steel Institute
Al	Aluminum
Al-Li	Aluminum Lithium
ASTM	American Society for Testing and Materials
FEA	Finite Element Analysis
FEM	Finite Element Model
FS	Factor of Safety
IU	Instrument Unit
ksi	Thousand Pounds Per Square Inch
LC1	Load Case #1
LC2	Load Case #2
LC3	Load Case #3
LH ₂	Liquid Hydrogen
LOX	Liquid Oxygen
MP-1	Multiple-Piece Design #1
MP-2	Multiple-Piece Design #2
MP-3	Multiple-Piece Design #3
MS	Margin of Safety
Msi	Million Pounds Per Square Inch
MSFC	Marshall Space Flight Center
OML	Outer Mold Line
psi	Pounds Per Square Inch
SAE	Society of Automotive Engineers
SBKF	Shell Buckling Knockdown Factor
SF	Safety Factor
SP-1	Single-Piece Design #1

List of Symbols

A_{bond}	Bonding area (in ²)
E	Elastic modulus (psi, Msi)
I	Moment of inertia (in ⁴)
N_x	Uniform stress resultant (lb/in)
$N_{x,crit}$	Critical uniform stress resultant (lb/in)
$N_{x,unst}$	Nonlinear analysis unstable uniform stress resultant (lb/in)
$P_{applied}$	Applied load (lb)
S_y	Allowable shear stress, yield (psi)
$t_{w,B}$	Thickness of band (inch)
$t_{w,L}$	Thickness of L-shaped section web (inch)
Z_1	Finite element inner surface location
Z_2	Finite element outer surface location
ν	Poisson's ratio
σ_{allow}	Allowable stress (psi, ksi)
σ_{bru}	Allowable bearing stress, ultimate (psi, ksi)
σ_{bry}	Allowable bearing stress, yield (psi, ksi)
σ_{calc}	Calculated stress (psi)

σ_{shear}	Calculated shear stress in the adhesive layer
σ_u	Allowable stress, ultimate (psi, ksi)
σ_{vonM}	vonMises stress (psi)
σ_y	Allowable stress, yield (psi, ksi)

Abstract

The Shell Buckling Knockdown Factor (SBKF) project includes the testing of sub-scale cylinders to validate new shell buckling knockdown factors for use in the design of the Ares-I and Ares-V launch vehicles. Test article cylinders represent various barrel segments of the Ares-I and Ares-V vehicles, and also include checkout test articles. Testing will be conducted at Marshall Space Flight Center (MSFC) for test articles having an eight-foot diameter outer mold line (OML) and having lengths that range from three to ten feet long. Both ends of the test articles will be connected to the test apparatus using attachment rings. Three multiple-piece and one single-piece design for the attachment rings were developed and analyzed. The single-piece design was chosen and will be fabricated from either steel or aluminum (Al) depending on the required safety factors (SF) for test hardware. This report summarizes the design and analysis of these attachment ring concepts.

1.0 Introduction

The SBKF project includes the testing of sub-scale cylinders to validate new shell buckling knockdown factors for use in the design of the Ares-I and Ares-V launch vehicles. These sub-scale test articles represent various barrel segments of the Ares-I and Ares-V vehicles, and also include several checkout test articles. Testing will be conducted at MSFC on eight-foot diameter test articles having lengths that range from three to ten feet long. The test setup, described in detail in Section 3 and shown in Figure 3.1, and is designed to test articles of various length by using different length extension rods to attach the upper and lower portions of the test fixture at the load cell locations. The upper and lower portions of the test fixture are connected to the test article using attachment rings. These attachment rings act as the interface between the test article and the transition section sections of the test fixtures. This report summarizes the design and analysis of the test article attachment rings.

2.0 Summary of Results

Three multiple-piece and one single-piece attachment ring designs were developed and analyzed. While it is possible to use a multiple-piece design to satisfy strength requirements, manufacturing and assembly considerations lead to choosing the single-piece design. The single-piece design reported herein shows positive margins for the three design load cases examined. However, depending on SF requirements, the attachment ring will be fabricated from either American Institute of Steel Construction (AISI) 1025 steel or 7075-T651 Al. In particular, if a minimum $SF = 3$ for adhesive shear is required for the compression load case, then AISI 1025 steel is required for the current design. If a minimum $SF = 2$ is acceptable for the compression load case, then 7075-T651 Al can be used for the current design.

3.0 Physical Description of Test Setup/Test Assembly

Testing will be conducted at MSFC on sub-scale cylinder test articles. Test articles are representative of scaled Ares-I and Ares-V barrel segments such as the liquid oxygen (LOX) tank, liquid hydrogen (LH₂) tank and instrument unit (IU). Additionally, there will be checkout articles that will be used to verify the test setup and process. The basic test setup comprises the test towers and the test assembly. The test assembly comprises the test article, attachment rings, transition sections, struts, spider beams and eight load lines. The load lines connect the upper and lower spider beams, and comprise load cylinder, load cell, extension rods, adapters and clevises. Test articles of various lengths (approximately 3 feet, 6 feet and 10 feet) can be accommodated by using different length extension rods. The test assembly portion of the test setup, with a typical six-foot-long test article, is shown in Figure 3.1. The load lines attach to the

load spiders, which transfers load through the struts and transition sections into the test article. Attachment rings connect the test article to the upper and lower portions of the test fixture at the transition sections. The attachment rings that connect the test article to the transition sections are indicated in the figure, and are the focus of this design report.

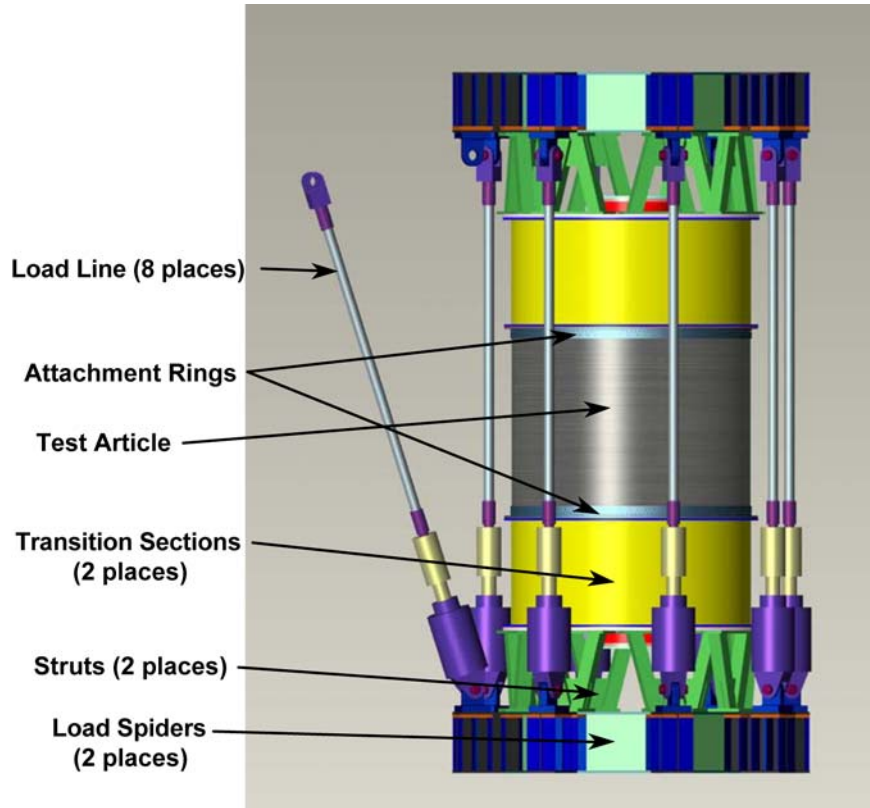


Figure 3.1. SBKF sub-scale cylinder test assembly.

4.0 Design/Test Requirements and Criteria

4.1 Structural Design

Four different attachment ring designs were investigated. Several designs were multiple-piece designs. One design is a single-piece ring design with an integrally-machined groove into which the test article is inserted. Descriptions of these two designs are given in the following subsections.

4.1.1 Multiple-Piece Designs

Three multiple-piece designs (MP) were examined. The initial multiple-piece design comprises two L-shaped rings that are attached to the inside and outside of the test article as shown in Figure 4.1. Subsequently, the outer L-shaped ring was replaced by a band as shown in Figure 4.2. Lastly, an annular ring was added to the base of the L-shaped rings to form a three-piece attachment fixture as shown in Figure 4.3 to aid in assembly and alignment. The two-piece design of Figure 4.1 was designated MP-1, the two-piece design of Figure 4.2 was designated MP-2 and the three-piece design of Figure 4.3 was designated MP-3. Designs MP-1 and MP-2 were designed to have all load transfer from the transition structure through bearing on the L-rings, then transfer load to the test article through bearing at bolts through the rings and test article. That is, no bearing of the test article end against the transition structure was permitted. The locations of the bolts are not indicated in the cross-section sketches depicted in the figures because they are dependent upon the bolt pattern development described in Section 6.1 and the

subsequent analyses. The MP-2 banded design was developed in an effort to reduce the manufacturing and installation complexity and cost. Design MP-3 was developed to assist in alignment of the parts, and to permit the test article to bear upon the annular ring, thus shifting the load transfer from bearing at bolts through the test article to bearing through the test article at the interface between the test article and the annular ring.

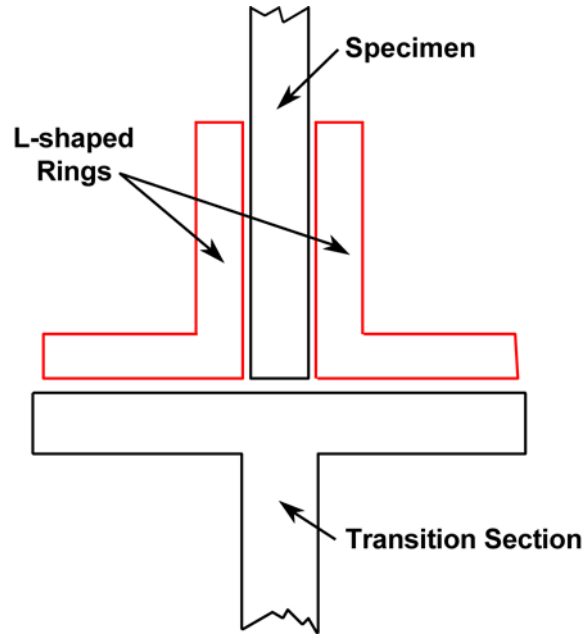


Figure 4.1. Initial two-piece attachment ring design concept (MP-1).

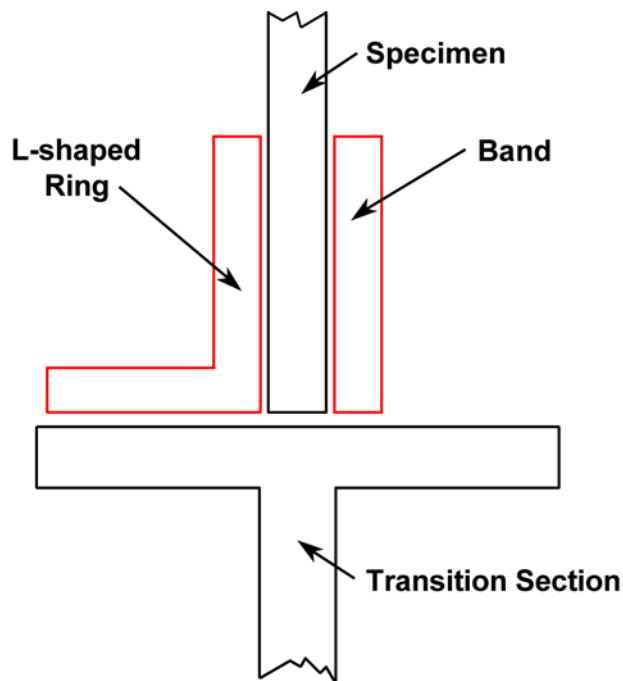


Figure 4.2. Two-piece attachment ring design concept with outer band (MP-2).

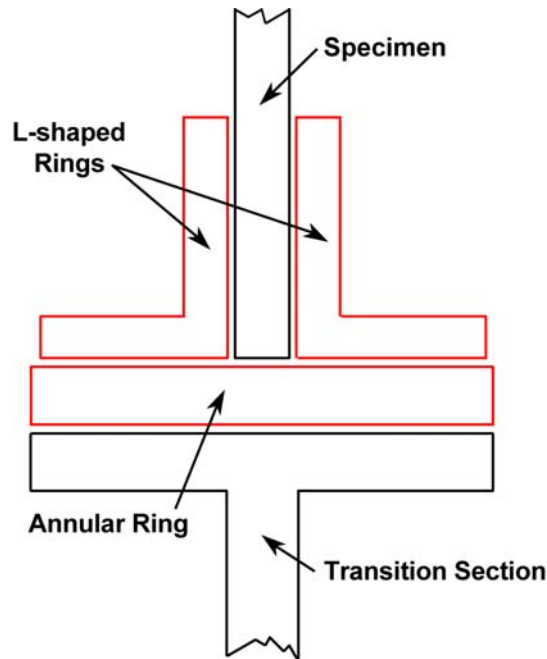


Figure 4.3. Three-piece attachment ring design concept (MP-3).

4.1.2 Single-Piece Design

Based upon the analysis and design of MP-3, a single-piece (SP) was developed in order to simplify assembly, reduce part count, and decrease cost. The single-piece design essentially takes the MP-3 design and makes it a single piece by integrally-machining the attachment ring from a single piece of material. This single-piece design concept is shown in Figure 4.4 and is designated SP-1. This design utilizes an adhesive/potting material in the gap between the test article and the attachment ring as the primary attachment mechanism in order to reduce bolt count. A small number of attachment bolts (not shown) are retained from previous designs for fail-safe purposes in the event that the adhesive potting material fails during handling or testing..

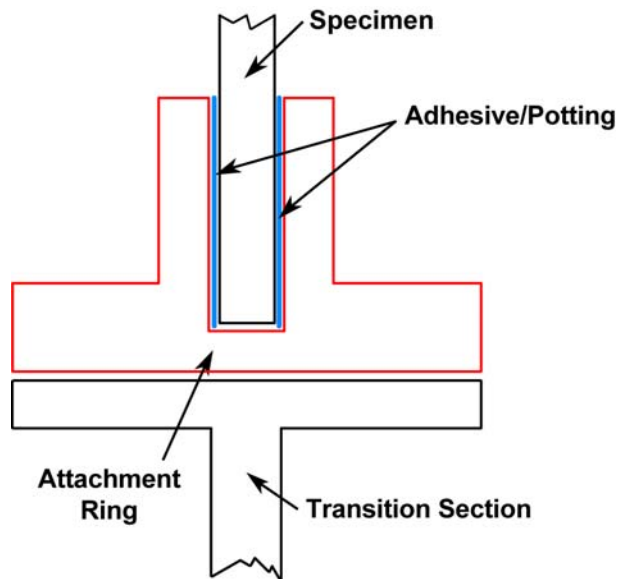


Figure 4.4. Single-piece attachment ring design concept (SP-1).

4.2 Factors of Safety and Knockdown Factors

SFs were used in the design process. Knockdown factors were not used in the design process as they were not applicable to the design of the attachment rings. The SFs were applied to numerous failure modes and included limit (yield) stress, bolt shear, test article and attachment ring bearing, net tension failure, shear out and tensile tear out. For the multiple-piece design, the SFs applied to the design analyses were as follows:

- Limit = 1 or 3
- Bolt Shear = 1
- Net Tension Failure = 1
- Bearing, Test Article = 1
- Bearing, Attachment Ring = 1
- Bolt Tension = 1

For the single-piece design, the SFs applied to the design analyses were the following:

- Limit = 1 or 3
- Bolt Shear = 1, 3 or 4
- Net Tension Failure = 1, 3 or 4
- Bearing, Test Article = 1, 3 or 4
- Bearing, Attachment Ring = 1, 3 or 4
- Bolt Tension = 1.5
- Adhesive Shear = 3 or 4

Multiple SFs were applied to some of the failure modes considered in the design analyses because it was uncertain what the required SFs were. Using multiple SFs provided the opportunity to evaluate the designs for SFs that were anticipated as potentially being required to meet imposed testing safety standards.

4.3 Margin Calculations

Margins of safety (MS) were calculated based upon allowable values or design requirements. Therefore, the generic form of the MS calculation equation is:

$$MS = \frac{\text{Specified_Value}}{SF(\text{Calculated_Value})} - 1$$

where SF represents the applicable SF. For example, a stress margin of safety calculation used the following equation:

$$MS = \frac{\sigma_{allow}}{SF(\sigma_{calc})} - 1$$

where σ_{allow} is the allowable stress (yield for limit and ultimate for ultimate), and σ_{calc} is the calculated stress. The attachment rings are not permitted to yield, so ultimate stress failure was not examined for the attachment rings.

4.4 Material Properties

Test article designs utilized Al alloy aluminum lithium (Al-Li)-2195. The properties for Al-Li-2195 were initially provided by MSFC, and are also found in References 1 and 2. Room temperature values used in the design study were $E = 11.0$ Msi (L-direction), $\nu = 0.33$, $\sigma_y = 66$ ksi (45°-direction) and $\sigma_u = 73$ ksi (45°-direction), and are for stock with a thickness range of 1.5-1.85 inches. The weight density was provided as 0.098 lb/in³ (Ref. 1).

Attachment rings were designed and analyzed as being fabricated from either steel or Al. Two steel alloys were chosen, AISI 4130 and AISI 1025, and the chosen Al alloy was 7075-T651. The properties for these three materials are shown in Table 4.1 and were obtained from Reference 3. Bolts used for all attachments were assumed to be Society of Automotive Engineers (SAE) 5, American Society for Testing and Materials (ASTM) A325 (Type 1) with $\sigma_y = 92$ ksi and $\sigma_u = 120$ ksi as obtained from Reference 4. The adhesive/potting material selected was Hysol EA-9394 manufactured by Henkel. Properties for EA-9394 were given as $E = 0.59$ Msi and $\nu = 0.37$ in Reference 5, and $S_y = 4.2$ ksi in Reference 6.

Table 4.1. Attachment ring material properties.

Property	AISI 4130 Steel	AISI 1025 Steel	7075-T651 Al
E (Msi)	29.0	29.0	10.3
ν	0.32	0.32	0.33
σ_y (ksi)	70.0	36.0	56.0
σ_u (ksi)	90.0	55.0	66.0
σ_{bry} (ksi) (e/D = 2.0)	120.	N/A	98.0
σ_{bru} (ksi) (e/D = 2.0)	190.	90.0	124.

4.5 Loads

Three load cases were used to design the attachment rings. The first load case (LC1) was a uniform running load of 5,050 lb/in, representing the maximum applied test load, which could be applied in either compression or tension. For designs MP-1 and MP-2, this was the only load case considered. The second load case (LC2) represents an assembly lifting load. The total weight to be lifted was assumed to be approximately 1160 lb. This weight comprises the test article and the complete attachment ring at one end, and represents the weight that is being lifted by the attachment ring at the opposite end. The resulting running load is $N_x = 3.846$ lb/in in this case. Using a 1-g acceleration during the lifting process with a factor of safety (FS) of 3, the design load becomes $N_x = 11.54$ lb/in for LC2. Lastly, a 10 psi internal pressure load case (LC3) was considered whereby pressure on the test assembly ends generates a tension load in the test article of $N_x = 240$ lb/in ($N_x = 720$ lb/in including FS = 3). Load cases LC2 and LC3 were included with LC1 for the analysis and sizing of designs MP-3 and SP-1.

5.0 Approach

The approach for designing the attachment rings used both closed-form and finite element solutions. First, closed-form solutions were used to provide the basic thicknesses of the attachment rings. Second, finite element analysis (FEA) was performed to verify the closed-form solutions and to examine detailed response not possible using the closed-form solutions.

5.1 Purpose

5.1.1 Closed-Form Solutions

Close-form solutions were used for calculating the response of the connection between the attachment rings and the test article and transition section. Primarily, this encompassed calculations to determine the bolt spacing and diameters, and the thickness of the parts involved. The equations used for the calculations were found in Reference 7, and were used to calculate bolt load factor (bolt in tension), bolt

shear, net tension failure, bearing (test article), bearing (attachment ring), shear out and tensile tear out. Shear out and tensile tear out are only important for situations where the bolt is close to the edge, so the designs developed were such that the distance from the bolt to the edge was at least two bolt diameters. Therefore, the shear out and tensile tear out calculations were not performed as they were deemed unnecessary. The closed-form, bolted-connection calculations were made by implementing the equations in Microsoft Excel workbooks, the details of which are presented in Appendix A.

Additional closed-form calculations were used to examine the response of the adhesive potting layer subjected to the second and third load cases, assembly and internal pressure, respectively. For these two load cases, the bond area was calculated, and the associated stress was calculated using the total load for the load case. Mathematically, this is equivalent to:

$$\sigma_{shear} = \frac{P_{applied}}{A_{bond}}$$

where σ_{shear} is the calculated shear stress in the adhesive layer, $P_{applied}$ is the applied total load, and A_{bond} is the bond area. Note that the bond area accounts for adhesive on both the internal and external test article surfaces, i.e., there are two bonding surfaces at each test article/attachment ring interface.

5.1.2 Finite Element Solutions

FEA was used for two main purposes. First, FEAs were performed to determine the effect of bolt pattern on the bolt load sharing. Second, the overall performance of the test article/attachment ring combination was examined using FEA. FEAs were performed using the NASTRAN™ (Ref. 8) or ABAQUS™ (Ref. 9) finite element codes.

5.2 Assumptions

5.2.1 Closed-Form Solutions

It was assumed that the thickness of the test article was 0.25 inch thick in the region where it interfaces with the attachment rings. Most assumptions related to the bolted connection calculations can be found in Reference 7 and are not repeated herein. Specific assumptions made about the bolt calculations for this report are described in Appendix A. It is important to recognize that the initial calculations assumed that the load was evenly distributed to all bolts in the pattern. In later calculations, that assumption was changed so that bolt load distribution was based on the FEA results for the bolt patterns as described in Section 6.1. The FEA led to the assumption that the load was distributed evenly among the bolts within each row. Finally, the assumption on the adhesive layer closed-form calculation was that the adhesive acts in shear, only.

5.2.2 Finite Element Solutions

It was assumed that the test article/attachment ring combination was clamped at the circumferential edges of the test article (see example in Figure 5.1 for design MP-1). This assumption requires that the transition section and attachment ring flange connection to the transition section be sufficiently stiff to approximate a clamped condition. It was determined that this boundary condition was sufficient for the design of the attachment ring and its components. Other assumptions were made for the various analyses and are described in the sections with their associated modeling descriptions and results.

5.3 Rationale

Both closed-form and finite element solutions were used to provide design data in the most efficient manner. The closed-form solutions were used to simplify analyses and provide design-level results in order to evaluate the designs. Finite element solutions were used where closed-form solutions were unavailable and where more detailed information was required.

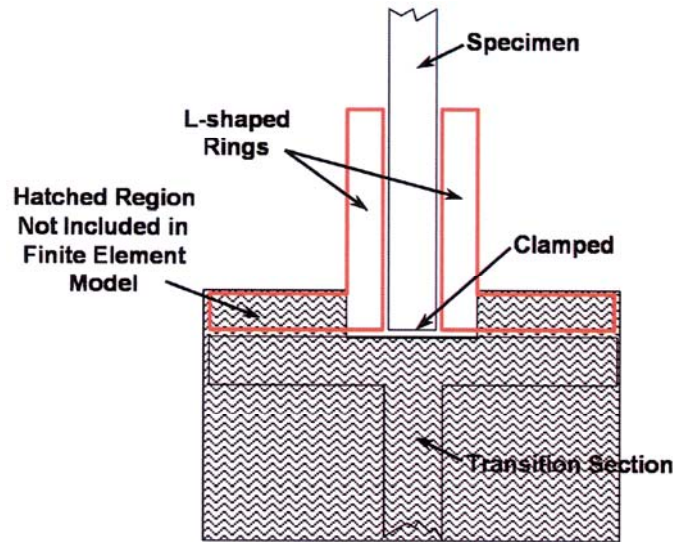


Figure 5.1. Sketch depicting clamped boundary for finite element analyses (MP-1).

6.0 Results

6.1 Bolt Patterns

Based on experience with the design of other test fixtures, it was assumed that the MP-1 design would have two rows of bolts of equal diameter. The primary purpose of the bolt pattern analysis was to examine the load sharing by the bolts. Therefore, FEAs were used to determine the pattern that would provide the most even distribution of load between the bolts in the two rows. Three bolt patterns were examined and are shown in Figure 6.1. The patterns of Figure 6.1a and Figure 6.1b have the same number of bolts in the two rows, while the pattern of Figure 6.1c has half as many bolts in the row interior to the test article as it does at the article edge. The finite element models (FEM) used in the analyses and their descriptions are provided in Appendix B. The load distribution between the two rows for the three bolt patterns are shown in Table 6.1. It is evident that for the in-line and staggered bolt patterns, the interior row carries a significant portion of the load. With equal numbers of bolts in the two rows, this means that the individual bolt load on the interior row is over three times that of the edge row. Conversely, the two rows carry nearly equal load in the staggered and gapped bolt pattern, so the individual bolt load on the inner row is only about two times that of the edge row since the inner row has half the number of bolts. Therefore, the staggered and gapped bolt pattern was chosen because the individual bolt loads are closer between the edge and inner rows, resulting in more efficient load sharing. Sizing of the MP-1 design was then performed on this staggered and gapped bolt pattern. In order to be conservative, sizing used only the load carried by the inner row of bolts. In the later designs (MP-2, MP-3 and SP-1), only a single row of bolts was used so the bolt row load distribution analysis was not needed.

Table 6.1. Bolt load distribution between bolt rows in two-row patterns.

Bolt Pattern	Edge Row, percent	Interior Row, percent
In-line	20.8	79.2
Staggered	23.1	76.9
Staggered, Gapped	48.4	51.6

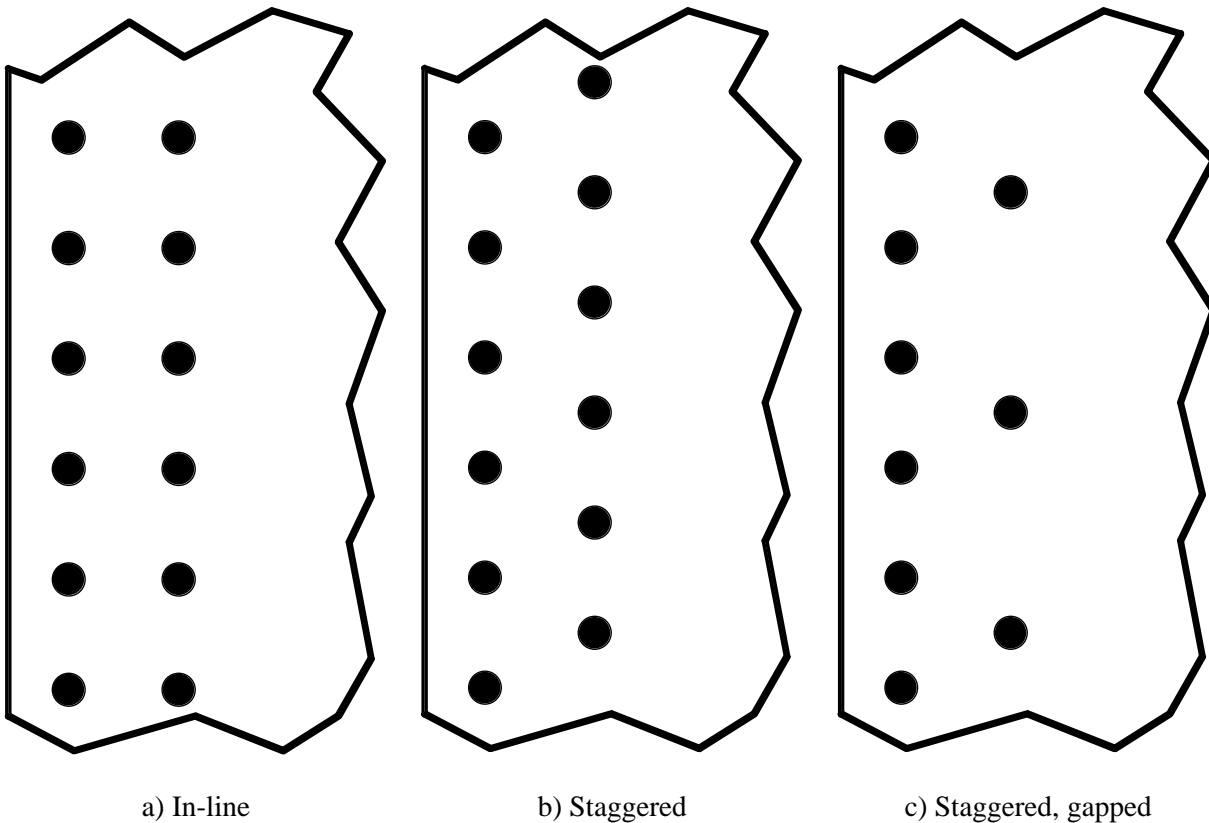


Figure 6.1. Two-row bolt patterns investigated.

6.2 Multiple-Piece Designs

Details of the analyses and the results for each of the three multiple-piece designs are presented in the following three sub-sections.

6.2.1 MP-1

Multiple-piece design MP-1, shown in Figure 4.1, was assumed to be fabricated from AISI 4130 steel. The cross-section for the design MP-1 is shown in Figure 6.2, and this cross-section was used for both the inner and outer L-section rings for the design. The locations of the inner and outer L-section rings are shown in Figure 6.3. MS were calculated using both the closed-form solutions and FEA. Closed-form solutions were used for all MS calculated at the bolt locations including the bolts, test article and attachment rings. FEA was used to examine the stresses within the attachment ring L-section. Details of the FEM and analysis are provided in Appendix C. Lastly, the bolt spacing and locations were developed

so as to satisfy the clearances needed for assembly by using the AISC stagger for impact wrench tightening requirement (Ref 10). The circumferential bolt spacing is shown in Figure 6.4.

MS were calculated using only the LC1 load case and are summarized in Table 6.2. For this design, all SF = 1.0 in the MS calculations. The most critical margin was bearing yield in the test article with a value of MS = 0.4625.

Table 6.2. MS for MP-1 attachment ring design.

Description	MS
Bolt shear, yield, attachment ring to test article	1.464
Bolt shear, ultimate, attachment ring to test article	2.213
Net tension failure, yield, attachment ring to test article	1.292
Net tension failure, ultimate, attachment ring to test article	1.535
Bearing - test article, yield, attachment ring to test article	0.4625
Bearing - test article, ultimate, attachment ring to test article	0.6176
Bearing - rings, yield, attachment ring to test article	3.653
Bearing - rings, yield, attachment ring to test article	4.983
Bolt tension, attachment ring to transition section	1.283
Attachment ring stress, yield	1.917
Attachment ring stress, ultimate	2.750

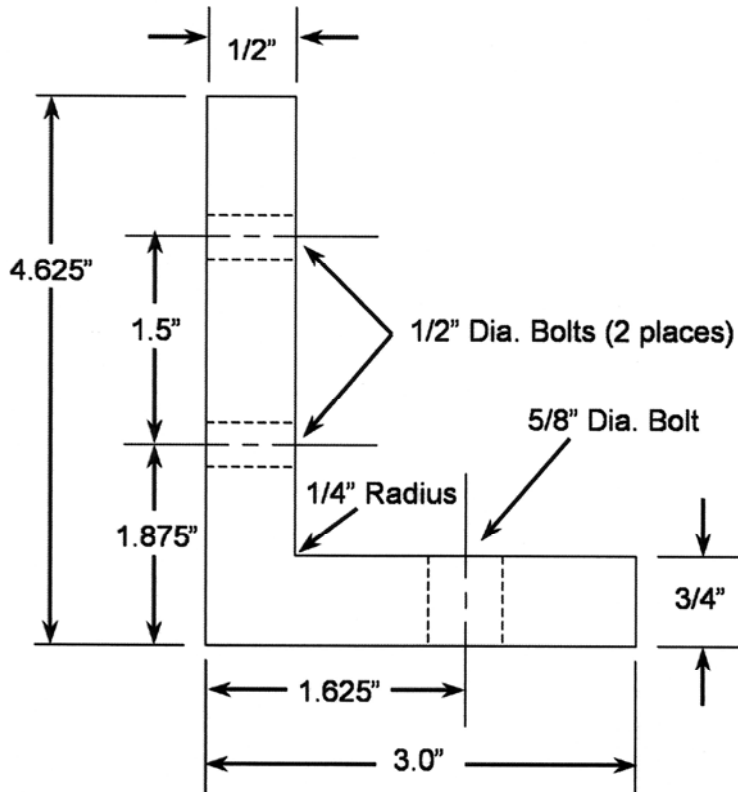


Figure 6.2. MP-1 design cross-section definition (not drawn to scale).

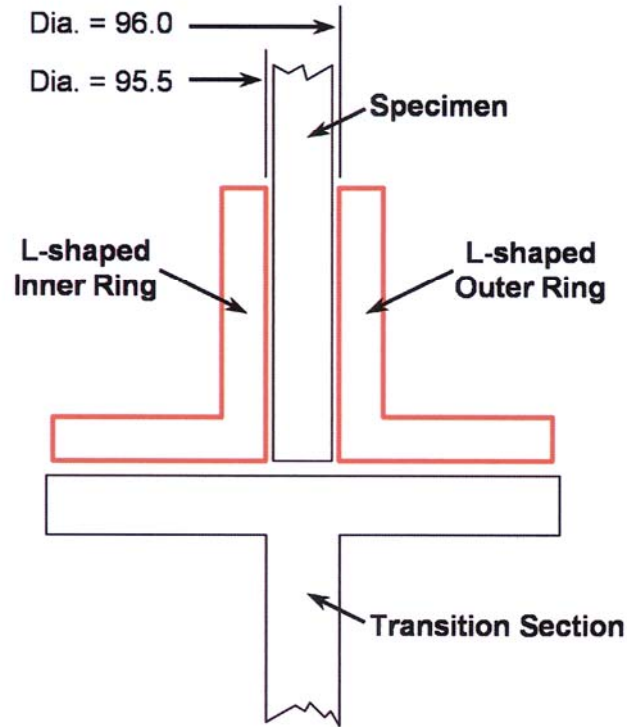


Figure 6.3. MP-1 design inner and outer ring locations.

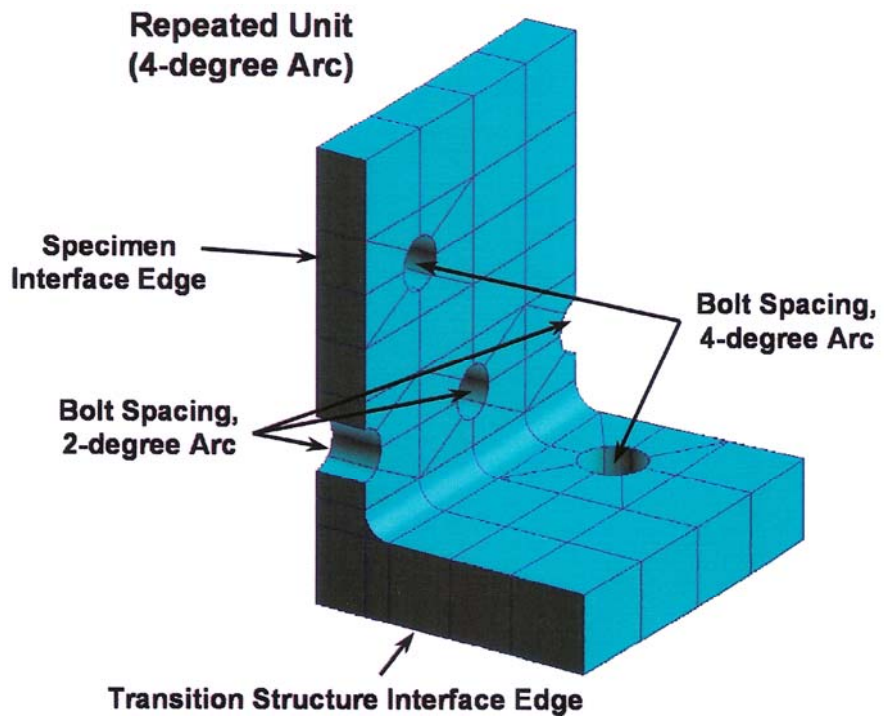


Figure 6.4. MP-1 design circumferential bolt spacing.

6.2.2 MP-2

Multiple-piece design MP-2, shown in Figure 4.2, was assumed to be fabricated from AISI 1025 steel. The cross-sections for the L-shaped ring and band for the MP-2 design are shown in Figure 6.5, where the L-shaped ring is internal to the test article and the band is external. Both the L-shaped ring and band were assumed to be adhesively bonded to the test article using EA-9394, but include bolts through the test article connection as a fail-safe measure. The web thicknesses that attaches to the test article are given thicknesses defined by $t_{w,L}$ and $t_{w,B}$. The values for $t_{w,L}$ and $t_{w,B}$ were set to be equal, and a design study was conducted where the values of these thicknesses ranged from 0.1 and 0.625 inch. The final thickness value was set to 0.25 inches. MS were calculated using both the closed-form solutions and FEA. Closed-form solutions were used for all MS calculated at the bolt locations including the bolts, test article and attachment rings. FEA was used to examine overall buckling of the test article, and the nonlinear stresses in the test article, the L-shaped ring and the band. Details of the FEM and analysis are provided in Appendix C. Lastly, the bolt spacing and locations were based upon the MP-1 design. The bolts attaching to the transition structure remain the same as those for MP-1 shown in Figure 6.4. However, the row of bolts closest to the L-section elbow (2-degree arc spacing) has been removed while the 4-degree arc spacing bolts through the test article remain.

A test article buckling analysis study was conducted using NASTRAN™ and the shell FEM, which is described in Appendix C. The study was used to examine the effect of the attachment ring on the overall buckling of the test article. For buckling of the test section only, which is defined as the portion of the test article not connected to the two attachment rings, the fundamental buckling load was 2,272 lb/in. Table 6.3 shows the buckling loads for various values of $t_{w,L}$ and $t_{w,B}$, and Figure 6.6 shows a typical fundamental buckling mode for a design where $t_{w,L}$ and $t_{w,B}$ are equal to 0.5 inch. It was determined from this study the thickness of the L-shaped ring web and the band have little effect on the overall buckling load. Therefore, the buckling response did not appear to drive the attachment ring design. Nonlinear analysis was then performed using NASTRAN™, and the LC1 loads at which the nonlinear analysis became unstable for various values of $t_{w,L}$ and $t_{w,B}$ are shown in Table 6.4. All web thicknesses shown result in designs that become unstable for a load slightly higher than 2,300 lb/in, so Table 6.5 shows the maximum vonMises stress for the various components at a load of 2,300 lb/in. Since the attachment ring components appear to behave linearly (very small deformations in this region), the stresses in Table 6.5 are scaled to a load of 5,050 lbs/inch (LC1 maximum expected load for all test articles) in the MS calculations for the attachment ring. Finally, a nonlinear analysis using ABAQUS™ and a local 24-degree arc section solid FEM described in Appendix C was used to examine the response if no adhesive was used between the attachment ring and test article, so that only the fail-safe bolts were attaching the components. ABAQUS™ was used to enforce contact relationships between the test article and attachment ring components. The nonlinear deformation from this analysis is seen in Figure 6.7 for 5,050 lb/in uniform axial compressive load, and separation between the attachment ring and test article are clearly evident. Attachment ring vonMises stresses are shown in Figures 6.8 and 6.9 for the L-shaped ring and band, respectively. The maximum vonMises stress observed in the L-shaped ring was 44,700 lbs/in² and in the band was 77,200 lb/in². These maximum values were concentrated in the region of the bolt locations, and were ignored due to the coarseness of the FEM at the bolt holes, and because the behavior in the vicinity of the bolt holes was determined using the closed-form solutions. The maximum values of vonMises stress used to calculate MS were taken to be body stresses removed from the bolt locations, and were 10,000 lb/in² and 22,000 lb/in² for the L-shaped ring and band, respectively.

MS were calculated using the LC1 and LC2 load cases and are summarized in Tables 6.6 and 6.7, respectively, for $t_{w,L}$ and $t_{w,B}$ a value of 0.5 inch is assigned. In the MS calculations, attachment ring stresses were scaled to a load of 5,050 lb/in for LC1. In the bolt MS calculations it was assumed that the inner L-shaped ring took all loads transferred from the test article as a fail-safe condition with no EA-9394. Additionally, for this MP-2 design, all SF = 1.0 inch the MS calculations. The most critical margin was yield due to joint bending of the test article with a value of MS = -0.6370 for LC1. These

calculations apply to a fail-safe condition so they may not be appropriate. However, examination of the remaining MS shows the bolt tension joint has a negative margin of $MS = -0.1336$ for LC1 in tension. Therefore, design MP-2 was deemed not satisfactory for the LC1 tension case, and design MP-3 was developed and analyzed.

Table 6.3. Critical LC1 linear buckling loads for design MP-2, various attachment ring designs.

$t_{w,L}$ and $t_{w,B}$ (inch)	$N_{x,crit}$ (lb/in)
0.1	2,285
0.125	2,288
0.25	2,293
0.375	2,298
0.5	2,302
0.625	2,305

Table 6.4. Nonlinear LC1 instability loads for design MP-2, various attachment ring designs.

$t_{w,L}$ and $t_{w,B}$ (inch)	$N_{x,unst}$ (lb/in)
0.1	2,367
0.125	2,383
0.25	2,320
0.375	2,313
0.5	2,344
0.625	2,344

Table 6.5. Maximum LC1 nonlinear vonmises stresses for design MP-2, various attachment ring designs.

$t_{w,L}$ and $t_{w,B}$ (inch)	Maximum σ_{vonM} (psi) at $N_x=2300$ lbs/in		
	L-shaped ring*	Band*	Test Article
0.1	13,900	16,200	44,500
0.125	11,900	14,100	44,500
0.25	6,800	8,200	44,500
0.375	4,750**	5,900***	46,000
0.5	3,700**	4,700***	45,600
0.625	3,050**	3,950***	45,700

*Occurs at the weld land locations.

** Adjusted from mid-surface value based on values seen in 0.1, 0.125 and 0.25 cases, added 200 psi.

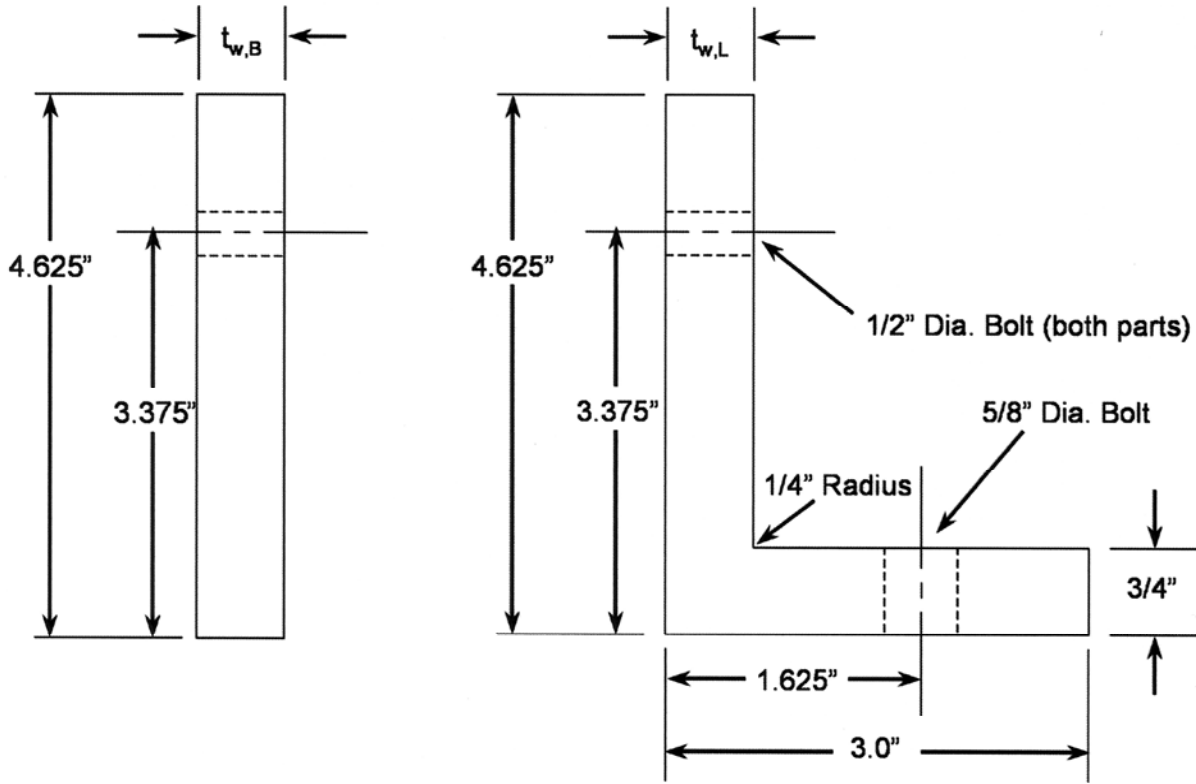
*** Adjusted from mid-surface value based on values seen in 0.1, 0.125 and 0.25 cases, added 900 psi.

Table 6.6. MS for MP-2 attachment ring design, load case LC1.

Description	MS
Bolt shear, yield, attachment ring to test article	-0.3841
Bolt shear, ultimate, attachment ring to test article	-0.1966
Net tension failure, yield, attachment ring to test article	1.780
Net tension failure, ultimate, attachment ring to test article	2.075
Bearing - test article, yield, attachment ring to test article	-0.2687
Bearing - test article, ultimate, attachment ring to test article	-0.1912
Bearing - rings, yield, attachment ring to test article	-0.2023
Bearing - rings, yield, attachment ring to test article	0.2188
Joint bending - bolt, yield	1.847
Joint bending - bolt, ultimate	2.713
Joint bending - test article, yield	-0.6370
Joint bending - test article, ultimate	-0.5985
Joint bending - L-shaped ring, yield	-0.2079
Joint bending - L-shaped ring, yield	0.2101
Bolt tension, attachment ring to transition section	0.1415
Attachment ring stress, L-shaped ring, yield	3.431
Attachment ring stress, L-shaped ring, ultimate	5.770
Attachment ring stress, band, yield	2.489
Attachment ring stress, band, ultimate	4.330
Test article stress, yield (at 2,300 lbs/in)	0.4474
Test article stress, ultimate (at 2,300 lbs/in)	0.6009

Table 6.7. MS for MP-2 attachment ring design, load case LC2

Description	MS
Bolt shear, yield, attachment ring to test article	268.5
Bolt shear, ultimate, attachment ring to test article	350.6
Net tension failure, yield, attachment ring to test article	1215.
Net tension failure, ultimate, attachment ring to test article	1344.
Bearing - test article, yield, attachment ring to test article	319.0
Bearing - test article, ultimate, attachment ring to test article	352.9
Bearing - rings, yield, attachment ring to test article	348.1
Bearing - rings, yield, attachment ring to test article	532.3
Joint bending - bolt, yield	1245.
Joint bending - bolt, ultimate	1624.
Joint bending - test article, yield	157.9
Joint bending - test article, ultimate	174.7
Joint bending - L-shaped ring, yield	345.6
Joint bending - L-shaped ring, yield	528.6
Bolt tension, attachment ring to transition section	499.5



a) Band

b) L-section

Figure 6.5. MP-2 Design cross-section definition (not drawn to scale).

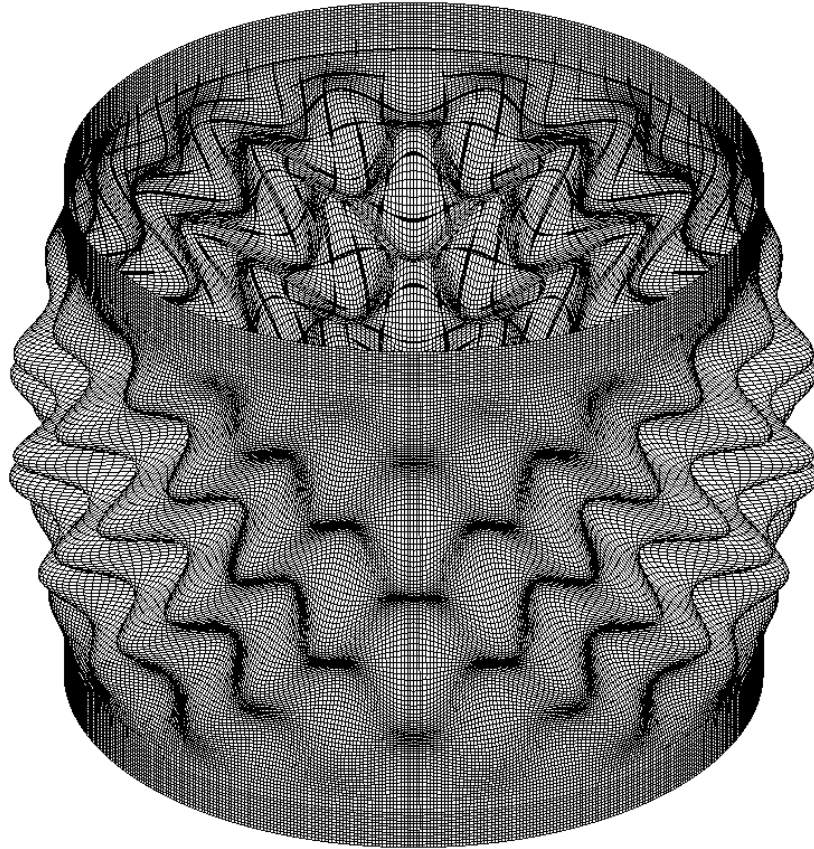


Figure 6.6. Typical MP-2 buckling mode, shown for $t_{w,L} = t_{w,B} = 0.5$ inch.

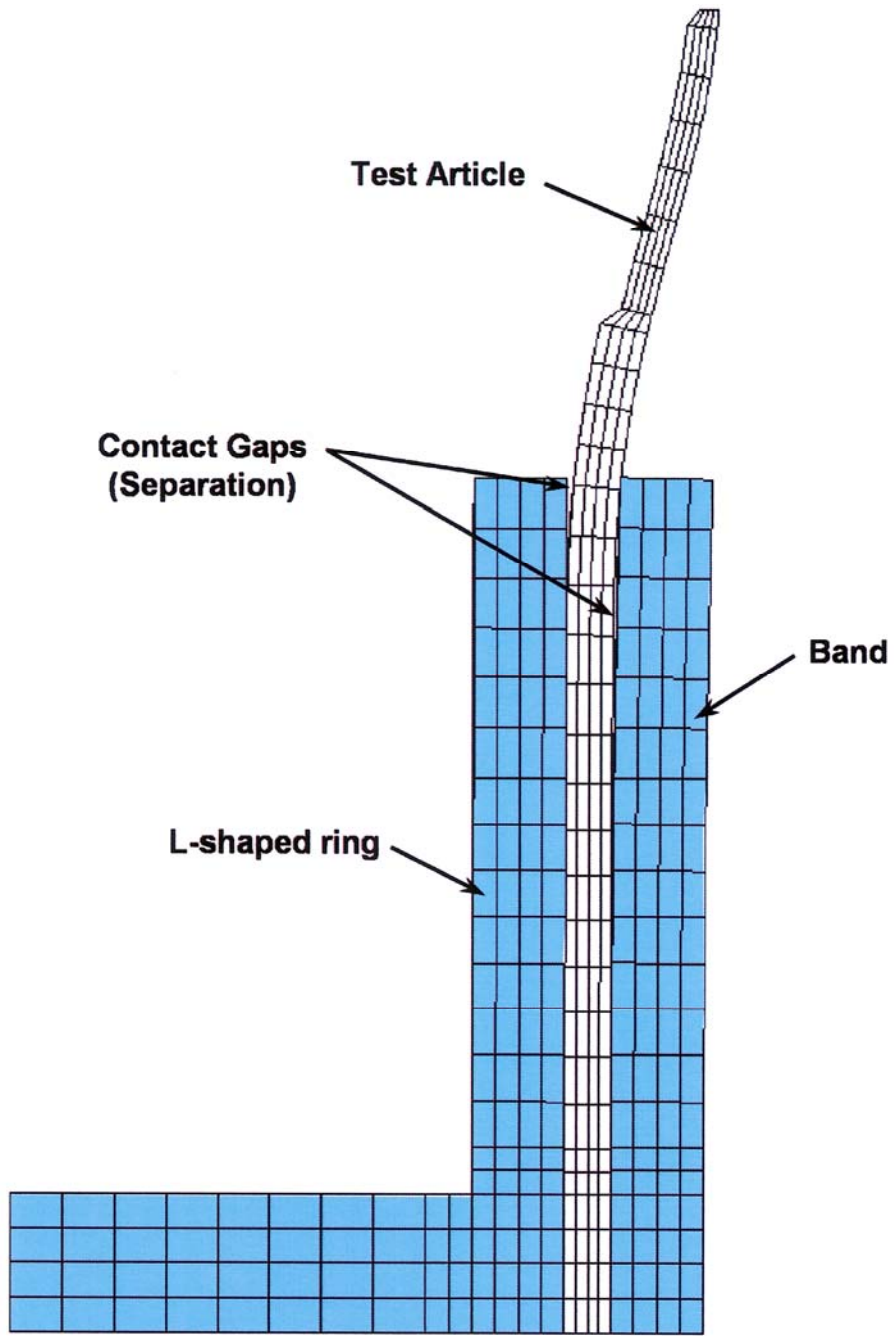


Figure 6.7. Local solid model MP-2 design cross-section deformation at $N_x = 5,050$ lb/in (magnification factor of 5).

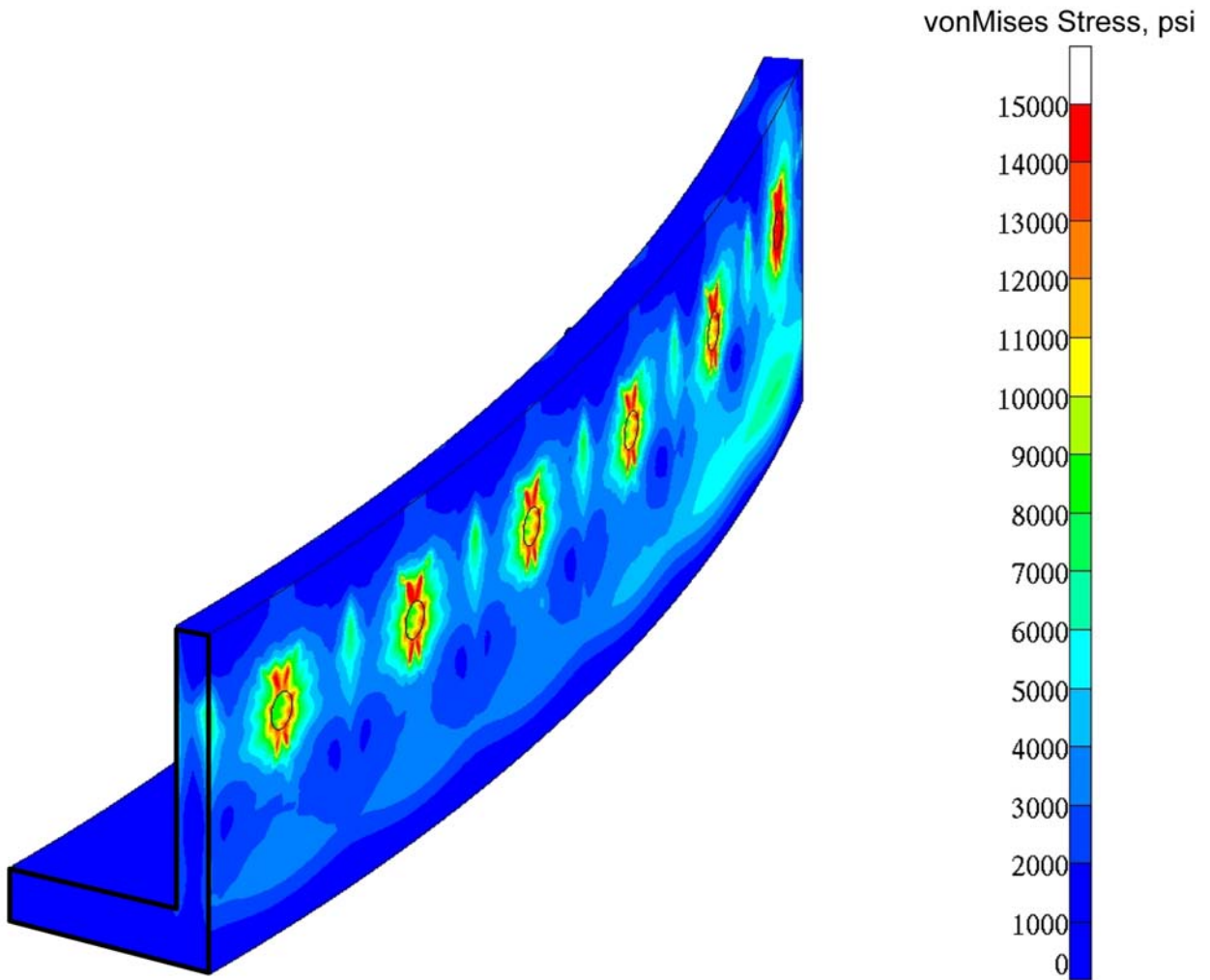


Figure 6.8. Local solid model MP-2 design, L-shaped ring vonMises stresses at $N_x = 5,050$ lb/in.

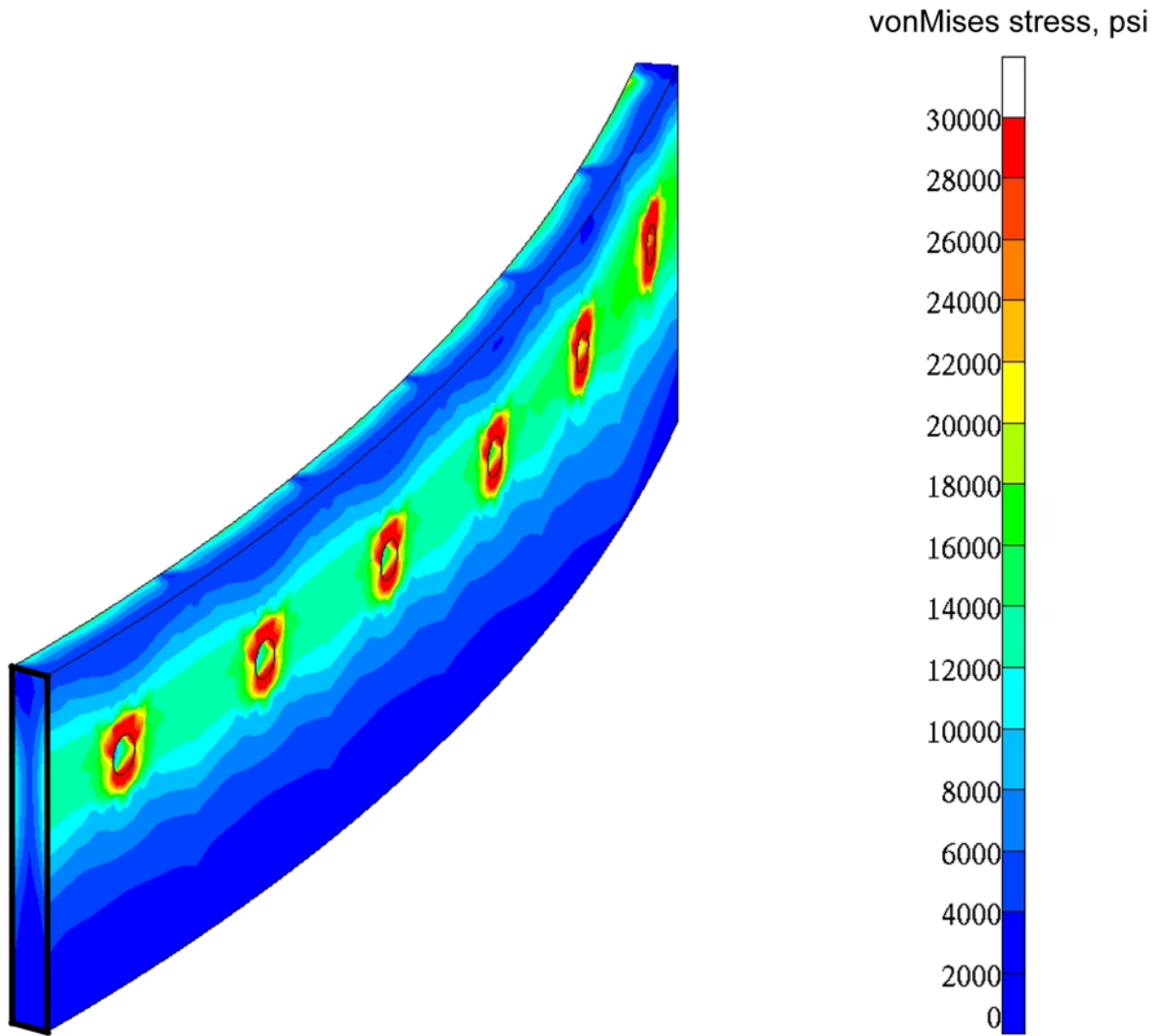


Figure 6.9. Local solid model MP-2 design, band vonMises stresses at $N_x = 5,050$ lb/in.

6.2.3 MP-3

Multiple-piece design MP-3 was assumed to be fabricated from AISI 1025 steel and is attached to the test article using both EA-9394 and bolts. The cross-section for the design MP-3 is shown in Figure 6.10. The L-shaped rings are attached to the annular ring, and are separated at a distance of 0.5 inch, which results in 0.125-inch regions of EA-9394 between the test article and L-shaped ring webs. MS were calculated using both the closed-form solutions and FEA. Closed-form solutions were used for all MS calculated at the bolt locations including the bolts, test article, and attachment rings. FEA was used to examine the stresses within the attachment ring L-section. Details of the FEM and analysis are provided in Appendix C. Lastly, the bolt spacing and locations were based upon the MP-2 design. The bolts attaching to the transition structure remain the same as those for MP-1 shown in Figure 6.4. The number of bolts through the test article was determined through analysis.

Closed-form solutions for design MP-3 are different than for design MP-2 for load case LC1 due to the double-shear condition in the attachment ring. However, assuming the test article bears on the transition sections, and that the adhesive connects the test article to the attachment ring, only the tension case of LC1 was analyzed for design MP-3. Also, due to the same FEM being used, finite element results for design MP-3 are identical to those for design MP-2 for load case LC1. Load case LC2 was examined as a

fail-safe condition where only the bolts hold the load for assembly. The number of bolts used around the test article circumference was varied, and included 90 (same as MP-2), 45, and 18. No adhesive calculations were performed for design MP-3.

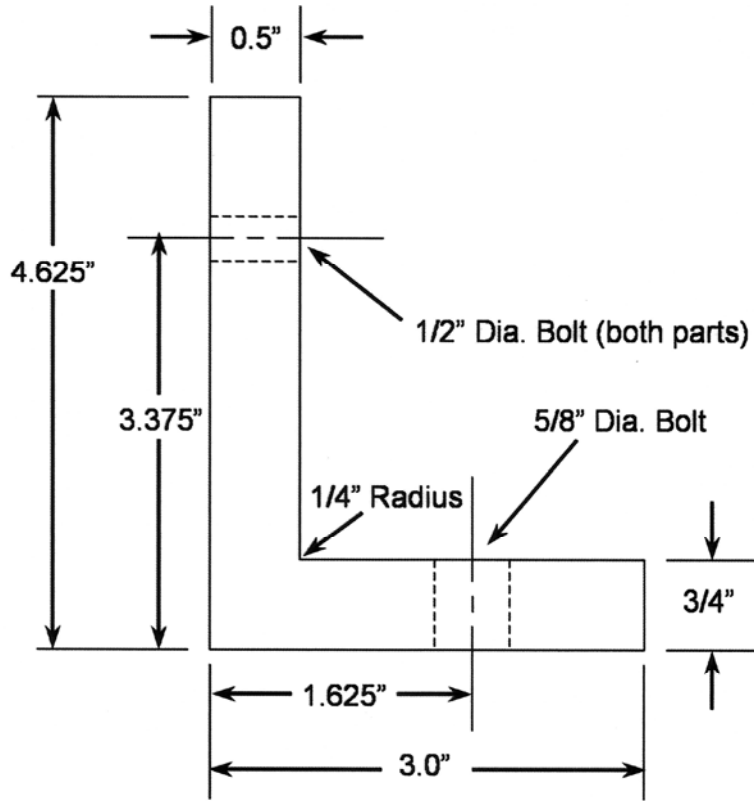
MS were calculated for design MP-3 for load cases LC1 and LC2. MS results for LC1 are summarized in Table 6.8. No calculations were performed for the bolts connecting the test article and attachment ring as it was assumed that the adhesive provided the connection. Also, no analysis of the adhesive was performed for MP-3. Minimum MS for LC2 for 90, 45, and 18 bolts were MS = 319.0, MS = 159.0 and MS = 63.00, respectively. Therefore, the closed-form bolt calculations yield significant positive margin when using 18 bolts, which corresponds to 20-degree arc spacing. Therefore, 18 test article/attachment ring bolts were chosen for design MP-3. MS results for LC2 are summarized in Table 6.9 for the 18-bolt design. As with design MP-2, SF = 1.0 was used in all of the MS calculations indicated in the tables. The most critical margin was test article yield at 2,300 lb/in load for LC1, with a value of MS = 0.4831.

Table 6.8. MS for MP-3 attachment ring design, load case LC1.

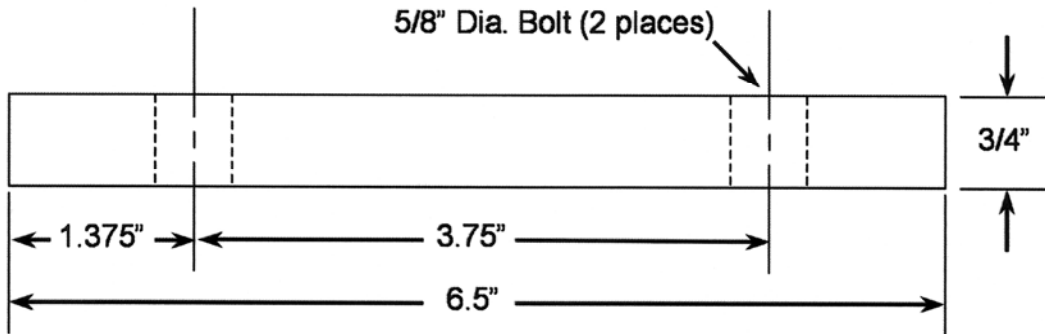
Description	MS
Bolt tension, attachment ring to transition section	2.283
Attachment ring stress, L-shaped ring, yield	3.431
Attachment ring stress, L-shaped ring, ultimate	5.770
Attachment ring stress, band, yield	2.489
Attachment ring stress, band, ultimate	4.330
Test article stress, yield (at 2,300 lbs/in.)	0.4474
Test article stress, ultimate (at 2,300 lbs/in.)	0.6009

Table 6.9. MS for MP-3 Attachment Ring Design, Load Case LC2

Description	MS
Bolt shear, yield, attachment ring to test article	106.8
Bolt shear, ultimate, attachment ring to test article	139.6
Net tension failure, yield, attachment ring to test article	1386.
Net tension failure, ultimate, attachment ring to test article	1533.
Bearing - test article, yield, attachment ring to test article	63.00
Bearing - test article, ultimate, attachment ring to test article	69.79
Bearing - rings, yield, attachment ring to test article	270.5
Bearing - rings, ultimate, attachment ring to test article	348.1
Bolt tension, attachment ring to transition section	999.0



a) Inner and outer L-shaped rings



b) Annular base ring

Figure 6.10. MP-2 design cross-section definition (not drawn to scale).

6.3 Single-Piece Design

Single-piece design SP-1 was assumed to be fabricated from either AISI 1025 steel or 7075-T651 Al. The purpose of SP-1 was to simplify the manufacturing process by reducing the part count and assembly by choosing a single-piece construction. Also, the two materials were examined to simplify machining of the attachment ring and to potentially lighten the fixture. The cross-section for the design SP-1 is shown in Figure 6.11. For this design, the webs attaching to the test article have been separated such that there are approximately 0.125-inches of EA-9394 between each web and the test article. The EA-9394 is assumed to provide all attachment strength between the test article and the attachment ring, and bolts were retained for fail-safe consideration. MS were calculated using both the closed-form solutions and FEA. Closed-form solutions were used for all MS calculated at the bolt locations including the bolts, test article and attachment rings. FEA was used to examine the stresses within the attachment ring. Details of the FEM and analysis are provided in Appendix C. Lastly, the bolt spacing and locations were identical to the MP-3 design. The 18 bolts around the circumference of the test article are only present as a fail-safe mechanism.

Closed-form and FEAs were conducted for load case LC1. As with design MP-3, assuming that the test article bears on the transition sections and that the adhesive connects the test article to the attachment ring, only the tension case of LC1 was analyzed using the closed-form solutions. The FEM was used to determine the stresses in the attachment ring webs and the test article for LC1. Only closed-form solutions were conducted for load cases LC2 and LC3. Load cases LC2 and LC3 were examined where either the EA-9394 or the bolts hold the entire load for assembly or pressure, respectively. Response summaries are shown in Tables 6.10 and 6.11 for the AISI 1025 steel and 7075-T651 Al attachment rings, respectively. Finite element results are provided for both the S4 and S4R5 elements at the load at which the nonlinear analysis becomes unstable, as indicated in the tables.

MS were calculated for all three load cases and are summarized in Tables 6.12 through 6.17, where SFs used in the calculations are indicated in the tables. Tables 6.12 and 6.13 show the MS values for load case LC1 using steel and Al, respectively. Tables 6.14 and 6.15 show the MS values for load case LC2 using steel and Al, respectively. Tables 6.16 and 6.17 show the MS values for load case LC3 using steel and Al, respectively. All margins are positive with the exception of shear stress in the adhesive for LC1 subjected to compression. For the steel attachment ring subjected to LC1 compressive loading, positive margin is shown in the adhesive for a SF of 3, but becomes negative for a SF of 4. For the Al attachment ring subjected to LC1 compressive loading, positive margin is shown in the adhesive for a SF of 2, but becomes negative for a SF of 3. For LC1 in tension, only an adhesive calculation was performed because, based on previous analyses, for a bolted-only connection having 18 bolts, large negative margins were expected to exist. For tension loading, the adhesive bond must be completely intact to yield the MS values reported, and no analysis of partial bonds was performed to determine when the MS would become negative. Therefore, if a SF of at least 2 is sufficient for the adhesive subjected to LC1 loading, then all margins are positive for both the steel and Al designs. If a minimum SF of 3 is required, then only the steel design satisfies the requirement. For LC2, all margins are positive and large, indicating that LC2 is not critical. For LC3, the critical margin for both the steel and Al designs is bearing in the test article, with a value of $MS = 0.02580$ when $SF = 3$ for bearing is used. If an acceptable value of FS for the adhesive in LC1 is chosen (2 for Al, 3 for steel), the critical margin for both the steel and Al designs is bearing in the test article at the bolt locations for LC3, with a value of $MS = 0.02580$ for $SF = 3$.

Table 6.10. Response summary for SP-1 AISI 1025 steel attachment ring design.

Load Case	Location	Description	Value
LC1*	Inner flange (S4)	Max. vonMises stress	4,230 psi
	Inner flange (S4R5)	Max. vonMises stress	3,820 psi
	Outer flange (S4)	Max. vonMises stress	4,860 psi
	Outer flange (S4R5)	Max. vonMises stress	4,590 psi
	Test article, stringer (S4)	Max. vonMises stress	49,500 psi
	Test article, stringer (S4R5)	Max. vonMises stress	41,800 psi
	Adhesive (S4)	Max. shear stress	542 psi
	Adhesive (S4R5)	Max. shear stress	487 psi
	Flange edge (S4)	Max. fixture displacement	0.00402 inch
	Flange edge (S4R5)	Max. fixture displacement	0.00393 inch
	Test article end (S4)	Max. test article end shortening	-0.137 inch
	Test article end (S4R5)	Max. test article end shortening	-0.133 inch
LC2	Each bolt	Bolt load	4,020 lb
	Adhesive	Adhesive shear stress	25.95 psi
LC3	Each bolt	Bolt load	193.3 psi
	Adhesive	Adhesive shear stress	2.00 psi

* LC1 results at 2,336 lb/in for S4 elements and at 2,220 lb/in for S4R5 elements

Table 6.11. Response summary for SP-1 7075-T651 aluminum attachment ring design.

Load Case	Location	Description	Value
LC1*	Inner flange (S4)	Max. vonMises stress	2,380 psi
	Inner flange (S4R5)	Max. vonMises stress	2,260 psi
	Outer flange (S4)	Max. vonMises stress	3,710 psi
	Outer flange (S4R5)	Max. vonMises stress	3,600 psi
	Test article, stringer (S4)	Max. vonMises stress	47,200 psi
	Test article, stringer (S4R5)	Max. vonMises stress	41,700 psi
	Adhesive (S4)	Max. shear stress	817 psi
	Adhesive (S4R5)	Max. shear stress	793 psi
	Flange edge (S4)	Max. fixture displacement	0.00831 inch
	Flange edge (S4R5)	Max. fixture displacement	0.00823 inch
	Test article end (S4)	Max. test article end shortening	-0.137 inch
	Test article end (S4R5)	Max. test article end shortening	-0.133 inch
LC2	Each bolt	Bolt load	4,020 lb
	Adhesive	Adhesive shear stress	25.95 psi
LC3	Each bolt	Bolt load	193.3 psi
	Adhesive	Adhesive shear stress	2.00 psi

* LC1 results at 2,290 lb/in for S4 elements and at 2,220 lb/in for S4R5 elements

Table 6.12. MS for SP-1 AISI 1025 steel attachment ring design, LC1 scaled to 5050 lb/in.

Element	Description	MS
S4R5	Adhesive (SF = 2) (yield, max. shear)	0.8956
	Adhesive (SF = 3) (yield, max. shear)	0.2637
	Adhesive (SF = 4) (yield, max. shear)	-0.05219
	Inner flange (yield, vonMises)	3.143
	Inner flange (SF = 3) (yield, vonMises)	0.3810
	Outer flange (yield, vonMises)	2.448
	Outer flange (SF = 3) (yield, vonMises)	0.1493
	Test article, (SF = 1) (yield, vonMises) (at 2,220 lb/in)	0.5789
	Bolt, tension, transition section (SF = 1.5)	0.8847
S4	Adhesive (SF = 2) (yield, max. shear)	0.7923
	Adhesive (SF = 3) (yield, max. shear)	0.1948
	Adhesive (SF = 4) (yield, max. shear)	-0.1039
	Inner flange (yield, vonMises)	2.937
	Inner flange (SF = 3) (yield, vonMises)	0.3123
	Outer flange (yield, vonMises)	2.426
	Outer flange (SF = 3) (yield, vonMises)	0.1422
	Test article, (SF = 1) (yield, vonMises) (at 2,336 lb/in)	0.3333
	Bolt, tension, transition section (SF = 1.5)	0.8847
N/A (Closed- Form))	Adhesive, tension load (SF = 2) (yield, max. shear)	2.847
	Adhesive, tension load (SF = 3) (yield, max. shear)	1.565
	Adhesive, tension load (SF = 4) (yield, max. shear)	0.9234

Table 6.13. MS for SP-1 7075-T651 aluminum attachment ring design, LC1 scaled to 5050 lb/in.

Element	Description	MS
S4R5	Adhesive (SF = 2) (yield, max. shear)	0.1641
	Adhesive (SF = 3) (yield, max. shear)	-0.2239
	Adhesive (SF = 4) (yield, max. shear)	-0.4179
	Inner flange (yield, vonMises)	9.893
	Inner flange (SF = 3) (yield, vonMises)	2.631
	Outer flange (yield, vonMises)	5.838
	Outer flange (SF = 3) (yield, vonMises)	1.279
	Test article, (SF = 1) (yield, vonMises) (at 2,220 lb /in.)	0.5827
	Bolt, tension, transition section (SF = 1.5)	0.1247
S4	Adhesive (SF = 2) (yield, max. shear)	0.2009
	Adhesive (SF = 3) (yield, max. shear)	-0.1994
	Adhesive (SF = 4) (yield, max. shear)	-0.3996
	Inner flange (yield, vonMises)	9.670
	Inner flange (SF=3) (yield, vonMises)	2.557
	Outer flange (yield, vonMises)	5.845
	Outer flange (SF=3) (yield, vonMises)	1.282
	Test article, (SF=1) (yield, vonMises) (at 2,336 lb/in)	0.3983
	Bolt, tension, transition section (SF = 1.5)	0.1247
N/A (Closed- Form))	Adhesive, tension load (SF = 2) (yield, max. shear)	2.847
	Adhesive, tension load (SF = 3) (yield, max. shear)	1.565
	Adhesive, tension load (SF = 4) (yield, max. shear)	0.9234

Table 6.14. MS for SP-1 AISI 1025 steel attachment ring design, load case LC2.

Description	MS
Bolt shear, yield, attachment ring to test article (SF = 1)	106.8
Bolt shear, ultimate, attachment ring to test article (SF = 1)	139.6
Net tension failure, yield, attachment ring to test article (SF = 1)	1386.
Net tension failure, ultimate, attachment ring to test article (SF = 1)	1533.
Bearing - test article, yield, attachment ring to test article (SF = 1)	63.00
Bearing - test article, ultimate, attachment ring to test article (SF = 1)	69.79
Bearing - rings, yield, attachment ring to test article (SF = 1)	138.6
Bearing - rings, ultimate, attachment ring to test article (SF = 1)	212.3
Bolt shear, yield, attachment ring to test article (SF = 4)	25.96
Bolt shear, ultimate, attachment ring to test article (SF = 4)	34.16
Net tension failure, yield, attachment ring to test article (SF = 4)	345.8
Net tension failure, ultimate, attachment ring to test article (SF = 4)	382.6
Bearing - test article, yield, attachment ring to test article (SF = 4)	15.00
Bearing - test article, ultimate, attachment ring to test article (SF = 4)	16.70
Bearing - rings, yield, attachment ring to test article (SF = 4)	33.92
Bearing - rings, yield, attachment ring to test article (SF = 4)	52.34
Bolt tension, attachment ring to transition section (SF = 1.5)	823.8
Adhesive (SF = 4)	524.0

Table 6.15. MS for SP-1 7075-T651 aluminum attachment ring design, load case LC2.

Description	MS
Bolt shear, yield, attachment ring to test article (SF = 1)	106.8
Bolt shear, ultimate, attachment ring to test article (SF = 1)	139.6
Net tension failure, yield, attachment ring to test article (SF = 1)	1386.
Net tension failure, ultimate, attachment ring to test article (SF = 1)	1533.
Bearing - test article, yield, attachment ring to test article (SF = 1)	63.00
Bearing - test article, ultimate, attachment ring to test article (SF = 1)	69.79
Bearing - rings, yield, attachment ring to test article (SF = 1)	216.2
Bearing - rings, ultimate, attachment ring to test article (SF = 1)	255.0
Bolt shear, yield, attachment ring to test article (SF = 4)	25.96
Bolt shear, ultimate, attachment ring to test article (SF = 4)	34.16
Net tension failure, yield, attachment ring to test article (SF = 4)	345.8
Net tension failure, ultimate, attachment ring to test article (SF = 4)	382.6
Bearing - test article, yield, attachment ring to test article (SF = 4)	15.00
Bearing - test article, ultimate, attachment ring to test article (SF = 4)	16.70
Bearing - rings, yield, attachment ring to test article (SF = 4)	53.31
Bearing - rings, yield, attachment ring to test article (SF = 4)	63.01
Bolt tension, attachment ring to transition section (SF = 1.5)	491.2
Adhesive (SF = 4)	524.0

Table 6.16. MS for SP-1 AISI 1025 steel attachment ring design, load case LC3.

Description	MS
Bolt shear, yield, attachment ring to test article (SF = 1)	4.184
Bolt shear, ultimate, attachment ring to test article (SF = 1)	5.762
Net tension failure, yield, attachment ring to test article (SF = 1)	65.70
Net tension failure, ultimate, attachment ring to test article (SF = 1)	72.77
Bearing - test article, yield, attachment ring to test article (SF = 1)	2.077
Bearing - test article, ultimate, attachment ring to test article (SF = 1)	2.404
Bearing - rings, yield, attachment ring to test article (SF = 1)	5.714
Bearing - rings, ultimate, attachment ring to test article (SF = 1)	9.258
Bolt shear, yield, attachment ring to test article (SF = 3)	0.7280
Bolt shear, ultimate, attachment ring to test article (SF = 3)	1.254
Net tension failure, yield, attachment ring to test article (SF = 3)	21.23
Net tension failure, ultimate, attachment ring to test article (SF = 3)	23.59
Bearing - test article, yield, attachment ring to test article (SF = 3)	0.02580
Bearing - test article, ultimate, attachment ring to test article (SF = 3)	0.1346
Bearing - rings, yield, attachment ring to test article (SF = 3)	1.238
Bearing - rings, yield, attachment ring to test article (SF = 3)	2.419
Bolt tension, attachment ring to transition section (SF = 1.5)	39.66
Adhesive (SF = 4)	39.46

Table 6.17. MS for SP-1 7075-T651 aluminum attachment ring design, load case LC3.

Description	MS
Bolt shear, yield, attachment ring to test article (SF = 1)	4.184
Bolt shear, ultimate, attachment ring to test article (SF = 1)	5.762
Net tension failure, yield, attachment ring to test article (SF = 1)	65.70
Net tension failure, ultimate, attachment ring to test article (SF = 1)	72.77
Bearing - test article, yield, attachment ring to test article (SF = 1)	2.077
Bearing - test article, ultimate, attachment ring to test article (SF = 1)	2.404
Bearing - rings, yield, attachment ring to test article (SF = 1)	9.445
Bearing - rings, ultimate, attachment ring to test article (SF = 1)	11.31
Bolt shear, yield, attachment ring to test article (SF = 3)	0.7280
Bolt shear, ultimate, attachment ring to test article (SF = 3)	1.254
Net tension failure, yield, attachment ring to test article (SF = 3)	21.23
Net tension failure, ultimate, attachment ring to test article (SF = 3)	23.59
Bearing - test article, yield, attachment ring to test article (SF = 3)	0.02580
Bearing - test article, ultimate, attachment ring to test article (SF = 3)	0.1346
Bearing - rings, yield, attachment ring to test article (SF = 3)	2.482
Bearing - rings, yield, attachment ring to test article (SF = 3)	3.103
Bolt tension, attachment ring to transition section (SF = 1.5)	23.67
Adhesive (SF = 4)	39.46

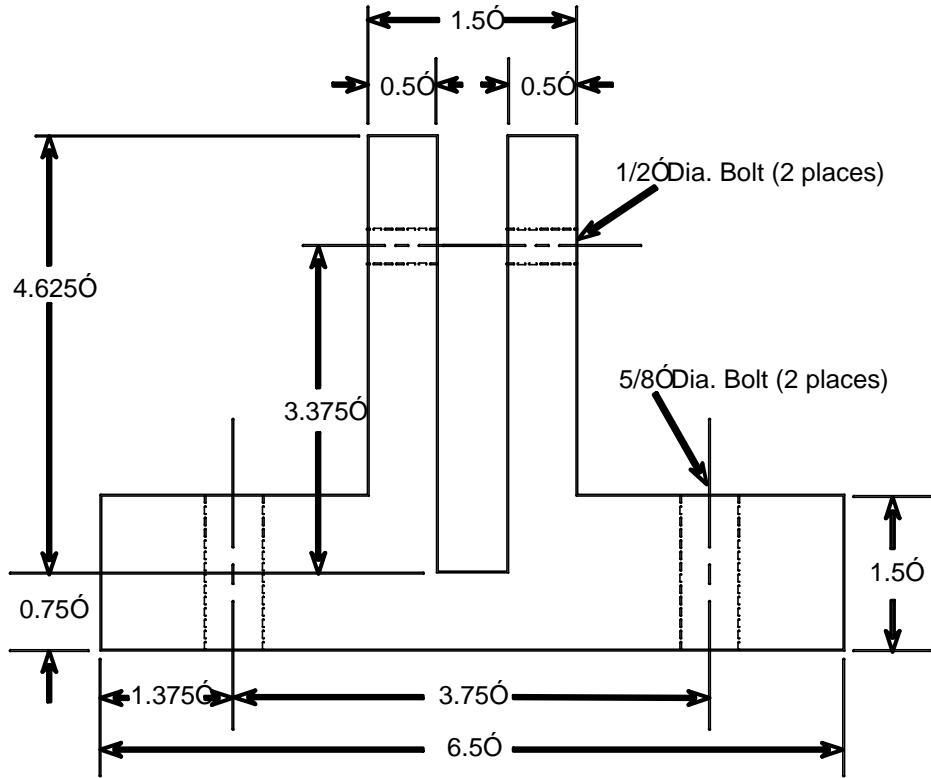


Figure 6.11. SP-1 design cross-section definition (not drawn to scale).

7.0 Conclusions

Analysis and design was performed on several attachment ring concepts to connect a test article to the test assembly transition sections. Three multi-piece designs and one single-piece design were examined, and three material systems were considered, namely AISI 4130 steel, AISI 1025 steel and 7075-T651 Al. Designs MP-1 and MP-2 are not satisfactory particularly design MP-2 which shows many negative margins. Design MP-3 shows positive margins for those calculated, but in the analyses of MP-3, LC3 was not considered and no analysis of the adhesive was performed for any load case. However, because of the similarity between the two designs, the response of MP-3 is expected to be identical to SP-1 for LC3 and for the analyses of adhesive for all load cases. Despite the similarity in margins between designs MP-3 and SP-1, the SP-1 single-piece design is the design of choice because not only are all MS positive, the single-piece design simplifies the manufacturing and assembly processes. However, the material from which the SP-1 attachment ring design is made depends upon the SFs required. Provided that a minimum SF of 2 is acceptable for load case LC1, the attachment ring can be made from either the 7075-T651 Al or the AISI 1025 steel. If a minimum SF of 3 is required for the adhesive subjected to LC1 loading, then the attachment ring must be made from the AISI 1025 steel.

8.0 References

1. *Design Allowables Handbook for Aluminum-Lithium 2195 Plates, Extrusions, Forgings, & Welds*. MSFC-HDBK-3513 (Baseline).
2. *ET Project – Design Values for Aluminum Allow 2195*. MMC-ET-SE64-H, Michoud Space Systems, Lockheed Martin, April 1999.
3. *Metallic Materials Properties Development and Standardization (MMPDS)*. DOT/FAA/AR-MMPDS-01, Office of Aviation Research, Washington, D.C., January 2003.
4. *Standard Specification for Structural Bolts, Steel, Heat Treated, 120/105 ksi Minimum Tensile Strength*. A 325-06, ASTM International, West Conshohocken, Pennsylvania, August 1, 2006.
5. Guess, T. R.; Reedy, E.D.; and Stavig, M. E.: *Mechanical Properties of Hysol EA-9394 Structural Adhesive*. SAND95-0229, Sandia National Laboratories, Albuquerque, New Mexico, February 1995.
6. *Hysol EA 9394 Epoxy Paste Adhesive*. Henkel Corporation, Bay Point, California, Rev. 6/02.
7. Shigley, J. E.; and Mischke, C. R.: *Mechanical Engineering Design*. Fifth, Ed., McGraw-Hill, New York, New York 1989.
8. MSC.NASTRAN 2005 manuals, MSC Software, Santa Ana, California, 2004.
9. ABAQUS V6.7 manuals, Desselault Systemes, SIMULIA Worldwide Headquarters, Providence, Rhode Island, 2007
10. *Manual of Steel Construction – Load & Resistance Factor Design*. First Ed., American Institute of Steel Construction, Inc., Chicago, Illinois, 1986.

Appendix A: Closed-Form Solution Spreadsheet Description

Closed-form solutions for the bolted joints were performed using an MS Excel spreadsheet and the design equations from Reference 7. Three spreadsheets were developed. The first spreadsheet was for a bolted joint subjected to tension, an example of which is shown in Figure A.1. The second spreadsheet was for a bolted joint with a bolt subjected to single shear, an example of which is shown in Figure A.2. Lastly, a spreadsheet for a bolted joint with a bolt subjected to double shear was developed, an example of which is shown in Figure A.3. Assumptions inherent in the spreadsheets are noted in the figures.

Bolt Grade: SAE 5, ASTM A325 (Type 1)

INPUT

Bolt Diameter (in.)	0.625
Bolt Yield (psi)	92000
Bolt Ultimate (psi)	120000
Bolt Young's Modulus (ksi)	30000
Proof Stress (psi)	85000
At (in.^2) (Table 8-2 in Shigley & Mischke)	0.226
Washer Thickness (in.)	0
Cylinder Radius (in.)	48
Bolt Distance from OML	1.25
Arc per Bolt (degrees)	4
Row Spacing (in.)	1.75
L-bracket Flange Thickness (in.)	1.5
L-bracket Yield (psi)	56000
L-bracket Ultimate (psi)	66000
L-bracket Young's Modulus (ksi)	10300
Trans. Cyl. Flange Thickness (in.)	0.75
Trans. Cyl. Flange Yield (psi)	36000
Trans. Cyl. Flange Ultimate (psi)	55000
Trans. Cyl. Young's Modulus (ksi)	29000
Axial Running Load (lbs./in.)	5050
Pressure Fruntrum Angle (degrees)	30
Safety Factor	1.5

OUTPUT

Cylinder Circumference (in.)	301.592895
Bolt Line Circumference (in.)	309.446876
Arc Bolt Spacing (in.)	3.43829863
Number of bolts	180
Force per Bolt (lbs.)	12692.0343
Pressure Fruntrum Angle (rad)	0.52359878

Bolt Stiffness	A (in.^2)	l (in.)	kb (kips/in.)
	0.30679616	2.25	4090.61543

Member Stiffness*	k, L-bracket	k, Trans. Cyl.	km (kips/in)
	10311.6286	37087.6108	8068.35034

Joint Constant	C
	0.33642791

Recommended Preload/Torque*	Fp (lbs.)	Fi (lbs.)	T (in.-lbs.)
	19210	14407.5	1800.9375

Bolt Load Factor	Sp	n
	19210	1.12471923

* Following assumptions are made:

- 1) joint frustrum angles assumed to be 30 degrees.
- 2) use washer with diameter 1.5 times bolt diameter
- 3) for Fi calculation, expect reused connection
- 4) for T, use K=0.2

Figure A.1. Example spreadsheet for bolted joint in tension.

Bolt Grade: SAE 5, ASTM A325 (Type 1)

INPUT

Bolt Diameter (in.)	0.5
Bolt Yield (psi)	92000
Bolt Ultimate (psi)	120000
Cylinder Radius (in.)	48
Arc per Bolt (degrees)	4
Number of Rows	1
Row Spacing (in.)	1.75
Specimen Thickness (in.)	0.25
Specimen Yield (psi)	66000
Specimen Ultimate (psi)	73000
Flange Thickness (in.)	0.5
Flange Yield (psi)	36000
Flange Ultimate (psi)	55000
Axial Running Load (lbs./in.)	5050

OUTPUT

Cylinder Circumference (in.)	301.592895
Arc Bolt Spacing (in.)	3.35103216
Number of bolts	90
Force per Bolt (lbs.)	16922.7124

Joint Bending - Bolt

t (grip)	M	I	c	Stress	FS (yield)	MS (yield)	FS (ult.)	MS (ult.)
0.75	6346.01716	0.04908739	0.25	32320	2.84653465	1.84653465	3.71287129	2.71287129

Joint Bending - Specimen

t (grip)	M	I	c	Stress	FS (yield)	MS (yield)	FS (ult.)	MS (ult.)
0.75	6346.01716	0.00436332	0.125	181800	0.3630363	-0.6369637	0.40154015	-0.59845985

Joint Bending - Flange

t (grip)	M	I	c	Stress	FS (yield)	MS (yield)	FS (ult.)	MS (ult.)
0.75	6346.01716	0.03490659	0.25	45450	0.79207921	-0.20792079	1.21012101	0.21012101

Bolt Shear

A	Stress	FS (yield)	MS (yield)	FS (ult.)	MS (ult.)
0.19634954	86186.6667	0.61591894	-0.38408106	0.80337252	-0.19662748

Net Tension Failure

A	F	Stress	FS (yield)	MS (yield)	FS (ult.)	MS (ult.)
0.71275804	16922.7124	23742.5767	2.77981623	1.77981623	3.07464523	2.07464523

Bearing* - Specimen

A	Stress	FS (yield)	MS (yield)	FS (ult.)	MS (ult.)
0.125	135381.699	0.73126575	-0.26873425	0.80882424	-0.19117576

Bearing* - Flange

A	Stress	FS (yield)	MS (yield)	FS (ult.)	MS (ult.)
0.25	67690.8497	0.79774445	-0.20225555	1.21877625	0.21877625

Shear Out

Neglected due to requiring first row of bolts being at least 2 bolt diameters from land edge.

Tensile Tear Out

Neglected due to requiring first row of bolts being at least 2 bolt diameters from land edge.

Minimum MS: -0.6369637

* Bearing allowable assumed to be 1.5 times Fu and Fy even though provided data suggests a factor of 2.0

Figure A.2. Example spreadsheet for bolted joint in single shear.

IN-LINE BOLTS, DOUBLE SHEAR

Bolt Grade: SAE 5, ASTM A325 (Type 1)
Flange Material: 1025 Low Carbon Steel
Specimen Material: Al-Li-2195

INPUT

Bolt Diameter (in.)	0.5
Bolt Yield (psi)	92000
Bolt Ultimate (psi)	120000
Cylinder Radius (in.)	48
Arc per Bolt (degrees)	20
Number of Rows	1
Row Spacing (in.)	1.75
Specimen Thickness (in.)	0.25
Specimen Yield (psi)	66000
Specimen Ultimate (psi)	73000
Flange Thickness (in.)	0.5
Flange Yield (psi)	36000
Flange Ultimate (psi)	55000
Axial Running Load (lbs./in.)	46.152

OUTPUT

Cylinder Circumference (in.)	301.592895
Arc Bolt Spacing (in.)	16.7551608
Number of bolts	18
Force per Bolt (lbs.)	773.284182

Bolt Shear

A	Stress	FS (yield)	MS (yield)	FS (ult.)	MS (ult.)
0.39269908	1969.152	26.9577971	25.9577971	35.162344	34.162344

Net Tension Failure

A	F	Stress	FS (yield)	MS (yield)	FS (ult.)	MS (ult.)
4.0637902	773.284182	190.286443	346.845519	345.845519	383.632165	382.632165

Bearing* - Specimen

A	Stress	FS (yield)	MS (yield)	FS (ult.)	MS (ult.)
0.125	6186.27346	16.0031723	15.0031723	17.7004784	16.7004784

Bearing* - Flange

A	Stress	FS (yield)	MS (yield)	FS (ult.)	MS (ult.)
0.25	1546.56836	34.9160123	33.9160123	53.3439077	52.3439077

Shear Out

Neglected due to requiring first row of bolts being at least 2 bolt diameters from land edge.

Tensile Tear Out

Neglected due to requiring first row of bolts being at least 2 bolt diameters from land edge.

Minimum MS: 15.0031723

* Bearing allowable assumed to be 1.5 times Fu and Fy even though provided data suggests a factor of 2.0

Figure A.3. Example spreadsheet for bolted joint in double shear.

Appendix B: Bolt Pattern Design FEM

B-1 Two-Row, In-Line

The FEM used to analyze the bolt load distribution between bolt rows for the two-row, in-line bolt pattern is shown in Figure B.1. It was analyzed in MSC/NASTRAN (Ref. 8) and consisted of quadrilateral and triangular shell elements, along with bar elements. The shell elements represent the test article and therefore have a thickness of 0.25 inch and are Al-Li-2195. The bar elements are used to distribute the bolt load around the bolt hole circumference and to connect the shell model to ground. In the figure, shell elements are black and the bar elements are orange. The bar elements used to transfer load to the bolt hole circumference were given very large stiffness so as to remain as rigid entities. At the center of the bolt locations, bars were used to provide an elastic connection so as to provide a more accurate load distribution. The properties for the elastic connection bars were such that the axial stiffness was representative of a single, steel attachment flange that was 0.5 inch thick, and they were given bending stiffness sufficient to prevent numerical problems. These elastic connection bars connect the inner row of bolt centers to the edge row of bolt centers, and the edge row of bolt centers to ground points. The ground points are fixed in all degrees of freedom. A uniform compression or tension displacement was applied to the edge opposite the bolts and the bolt load distribution determined.

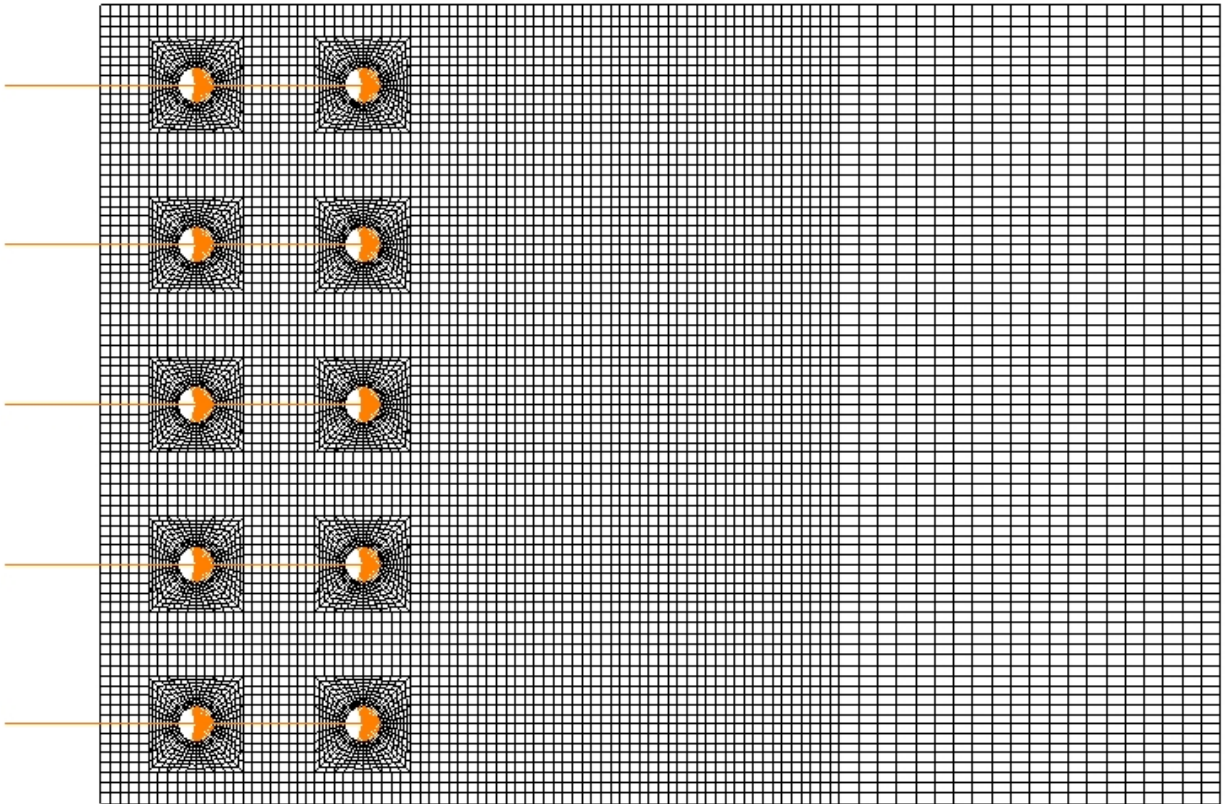


Figure B.1. Two-row, in-line bolt pattern FEM (compression case).

B-2 Two-Row, Staggered

The FEM used to analyze the bolt load distribution between bolt rows for the two-row, staggered bolt pattern is shown in Figure B.2. Modeling was the same as that for the two-row, in-line pattern as described in Section B-1 with the exception of the elastic connection bars. In this model, the elastic connection bars were all attached to the ground point because it was quicker and easier than trying to connect the centers of the inner row of bolts to the centers of the edge row of bolts. Boundary conditions and loading were the same as for the two-row, in-line analysis.

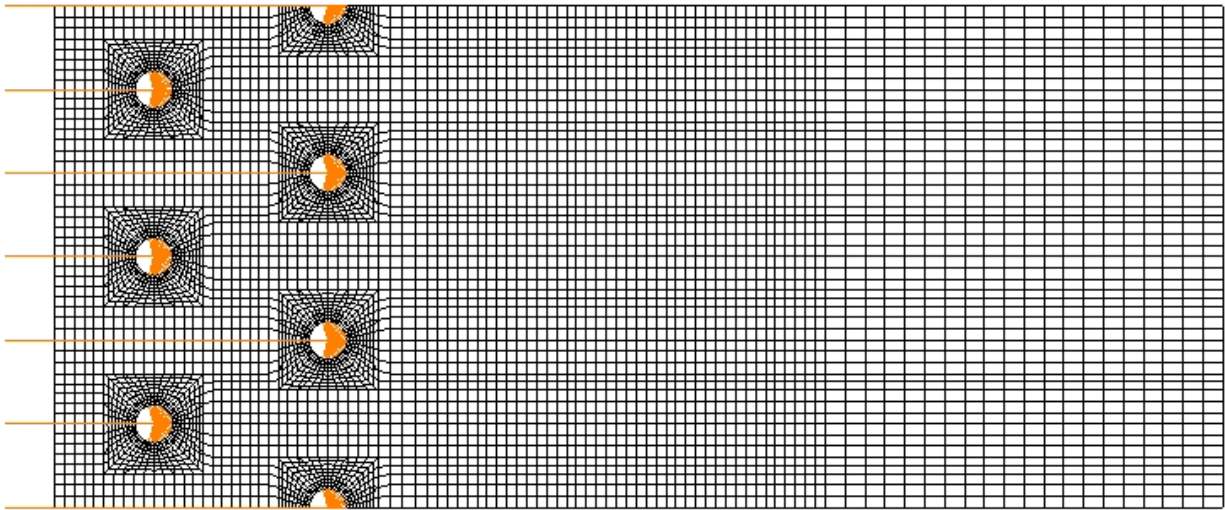


Figure B.2. Two-row, staggered bolt pattern FEM (compression case).

B-3 Two-Row, Staggered, Gapped

The FEM used to analyze the bolt load distribution between bolt rows for the two-row, staggered and gapped bolt pattern is shown in Figure B.3. Modeling, boundary conditions and loading were the same as that for the two-row, staggered pattern as described in Section B-2.

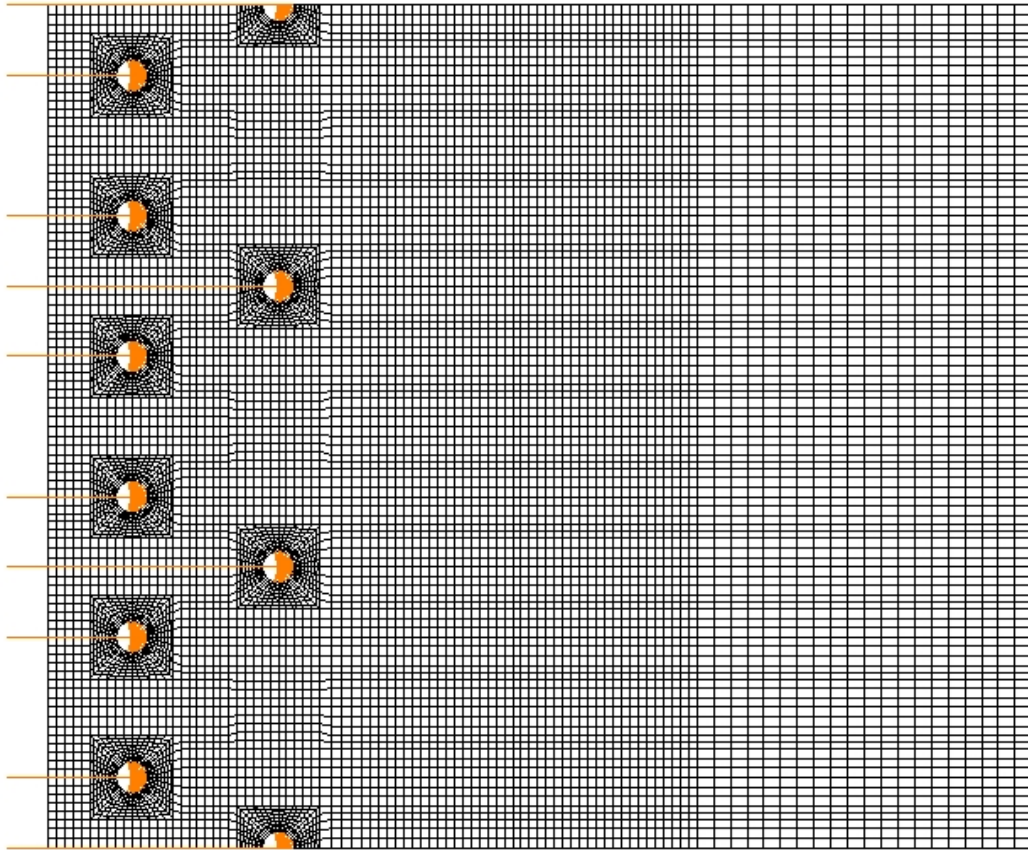
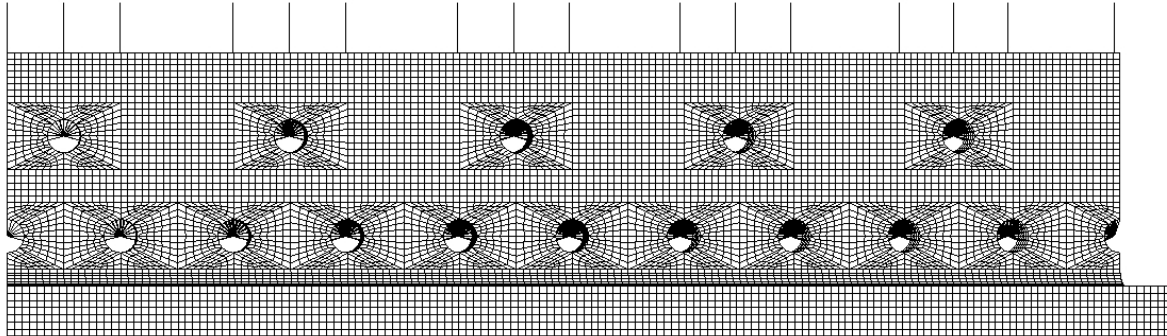


Figure B.3. Two-row, staggered, gapped bolt pattern FEM (compression case).

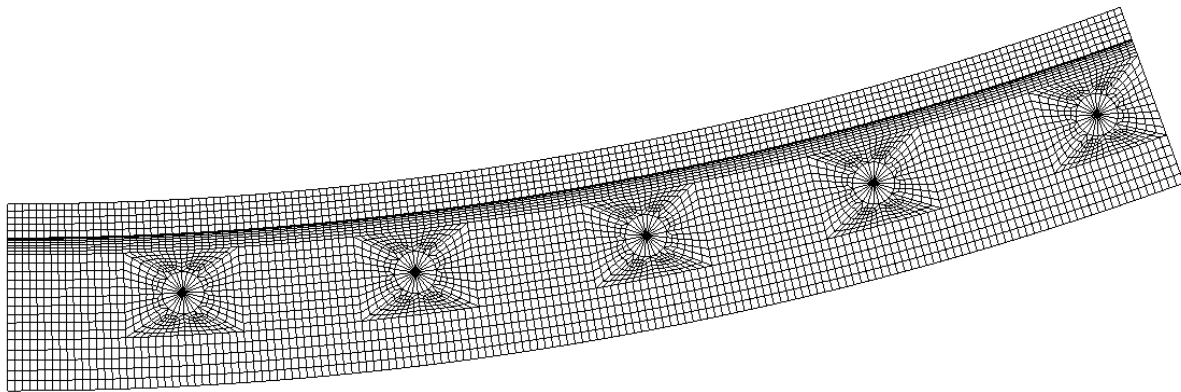
Appendix C: Multiple-Piece Design FEM

C-1 Design MP-1

A 20-degree arc segment solid model of the attachment ring was created to examine the stresses within the L-shaped section. Only the outer attachment ring was modeled under the assumption that the response of the inner ring would be similar. The FEM is shown in Figures C.1 and C.2. Loads applied at the bolt locations are shown in Figure C.3, where only tension loads were applied because they were expected to produce the largest stresses, particularly at the fillet.



a) View looking radial.



b) View looking axial.

Figure C.1. MP-1 FEM.

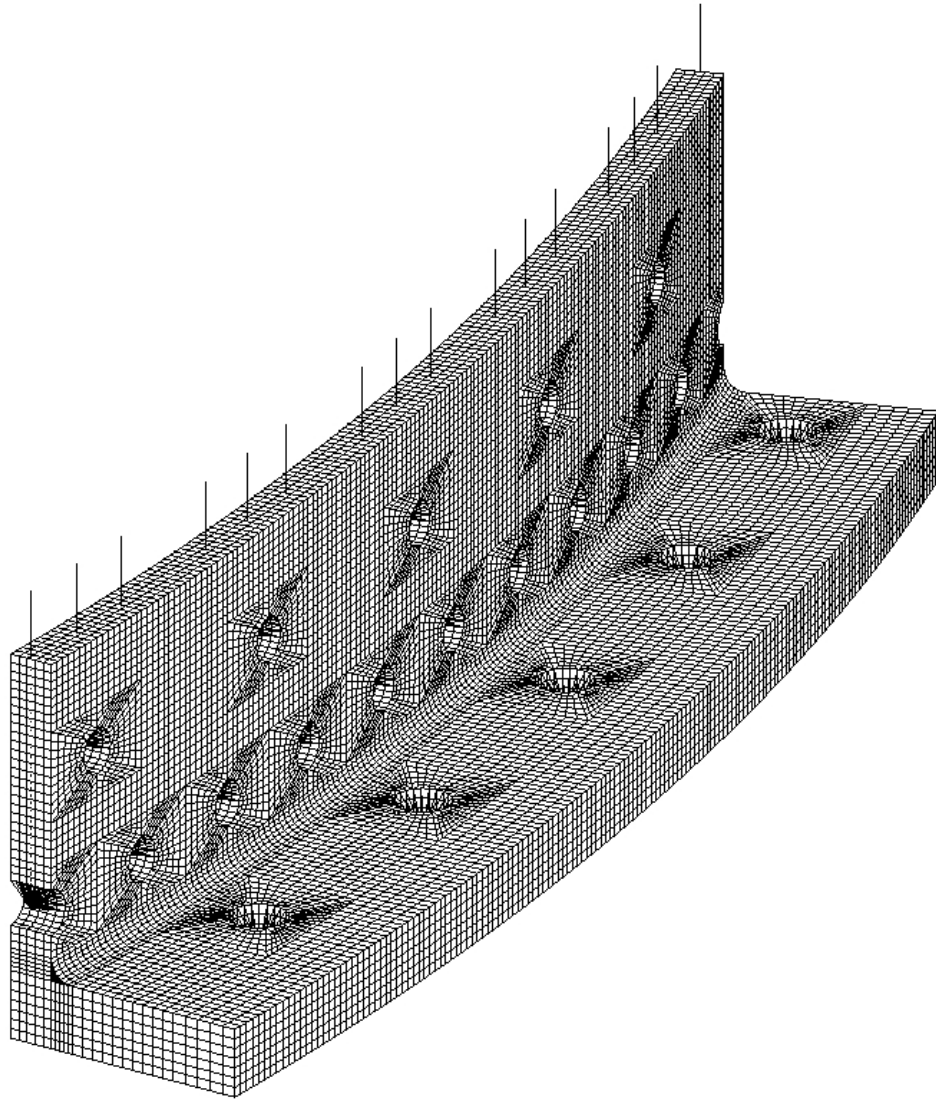


Figure C.2. MP-1 FEM isometric view.

values in the 0.001-inch layers providing the surface values. Additionally, to provide the proper offset for the components, a dummy layer was used to generate laminates that positioned the component material at the proper location. This dummy layer was fabricated from a dummy material having $E = 0.001$ psi and $\nu = 0.3$. Figure C.6 shows how the dummy ply is applied to remove the offset for a three-ply laminate that was modeled at the OML with an offset. For boundary conditions, the model was assumed to be clamped at both ends, where all degrees of freedom were fixed with the exception of the axial displacement at one end. At the load end, the axial displacement was free and a uniform distributed line load was applied. Buckling analyses used a uniform compressive axial load of -1000 lb/in, while a uniform compressive axial load of -2500 lb/in was used in the nonlinear analyses. At the loaded end, a set of beams was created around the circumference to keep the edge planar. These beams were modeled using the AISI 1025 steel, and were given in the plane of the shell bending stiffness by assigning $I = 100$ in⁴. The area, moment of inertia out-of-plane of the shell and the torsional constant were assigned values of 0.0001. Typical nonlinear analysis deformed shape is shown in Figure C.7, and typical nonlinear vonMises stress results are shown in Figures C.8 to C.17 for the various parts of the attachment ring and test article. The figures show the stresses for the design with 0.25-inch thick L-shaped ring and band components, where each component was modeled using three plies.

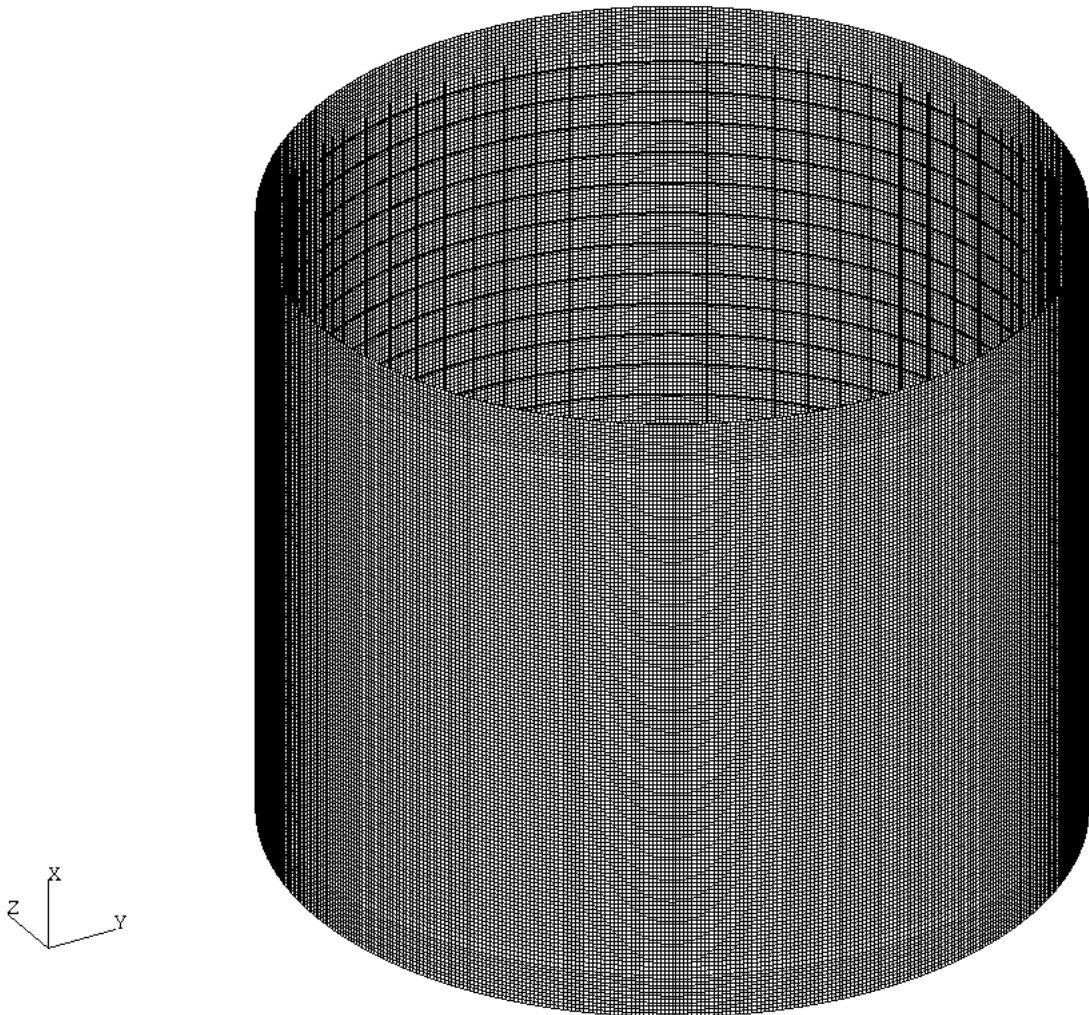


Figure C.4. MP-2 FEM to examine thickness of L-bracket web and band.

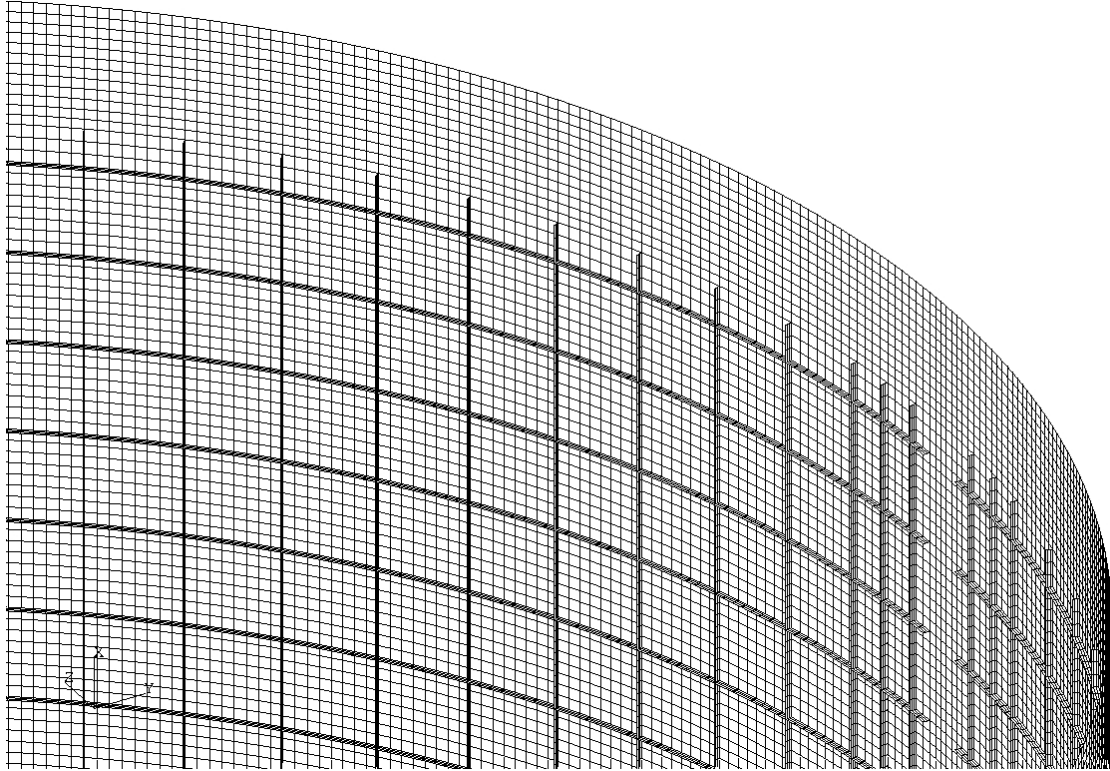
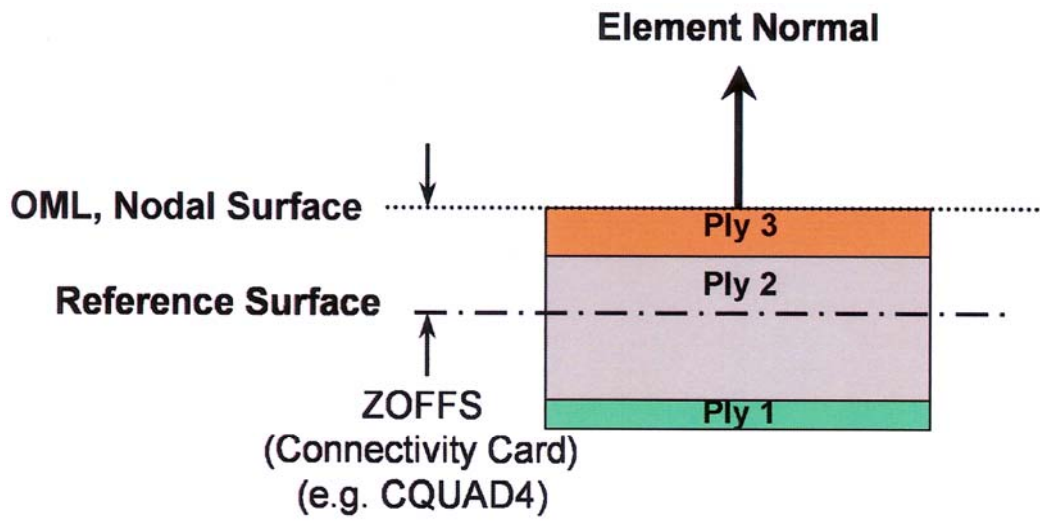
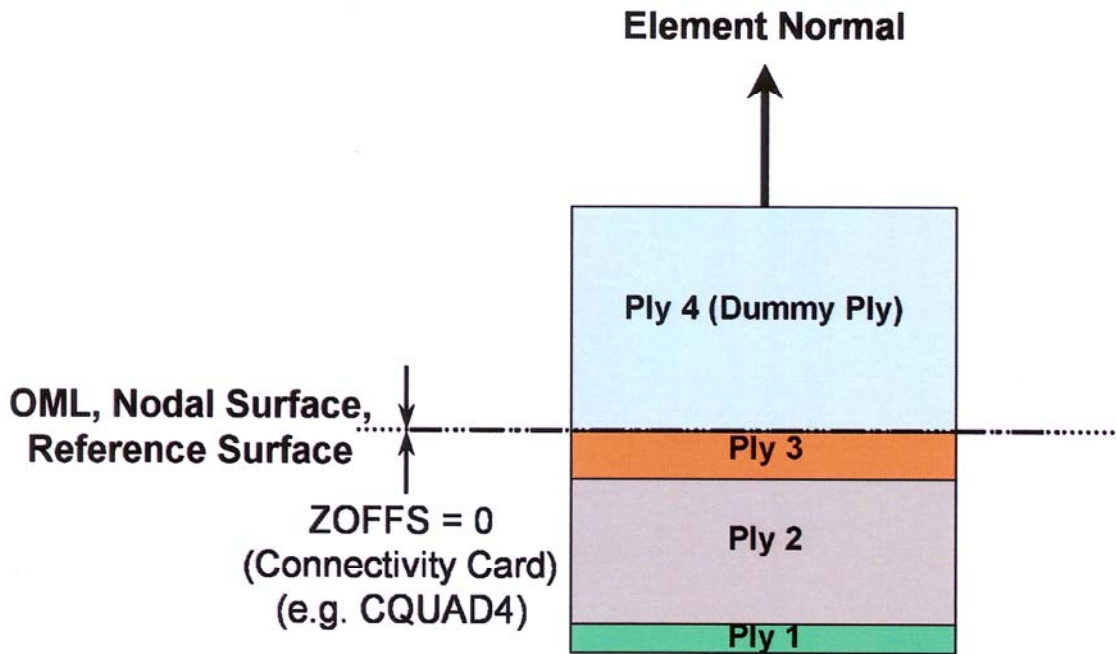


Figure C.5. Close-up of MP-2 FEM to determine required thickness of L-bracket web and band.



a) With offset.



b) Without offset, with dummy ply.

Figure C.6. Use of dummy ply to remove offsets.

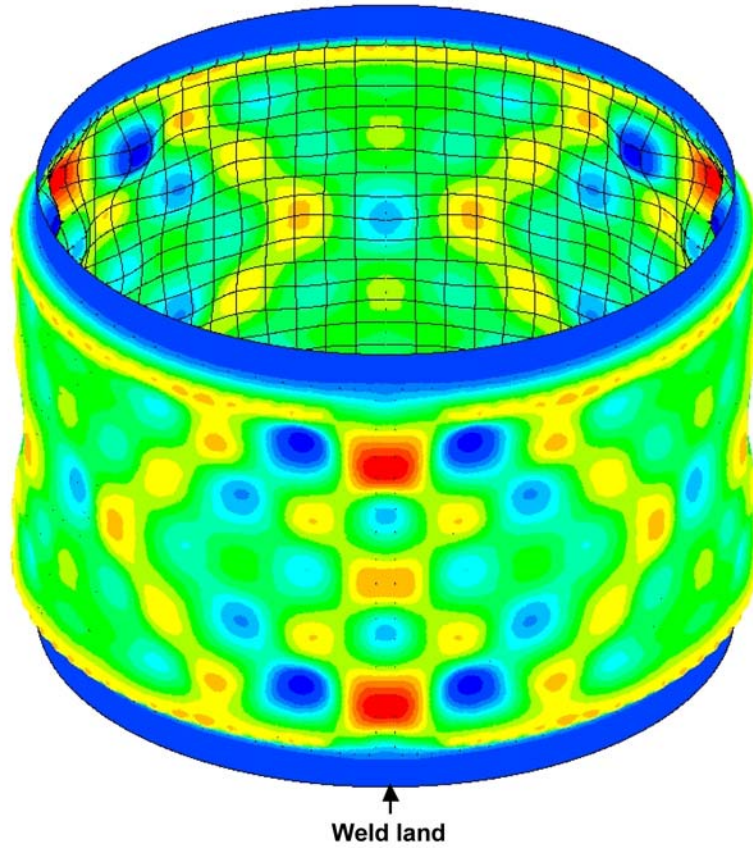


Figure C.7. Nonlinear deformation for design MP-2 at 2,300 lb/in with $t_{w,L} = t_{w,B} = 0.25$ inch (contours indicate radial displacement).

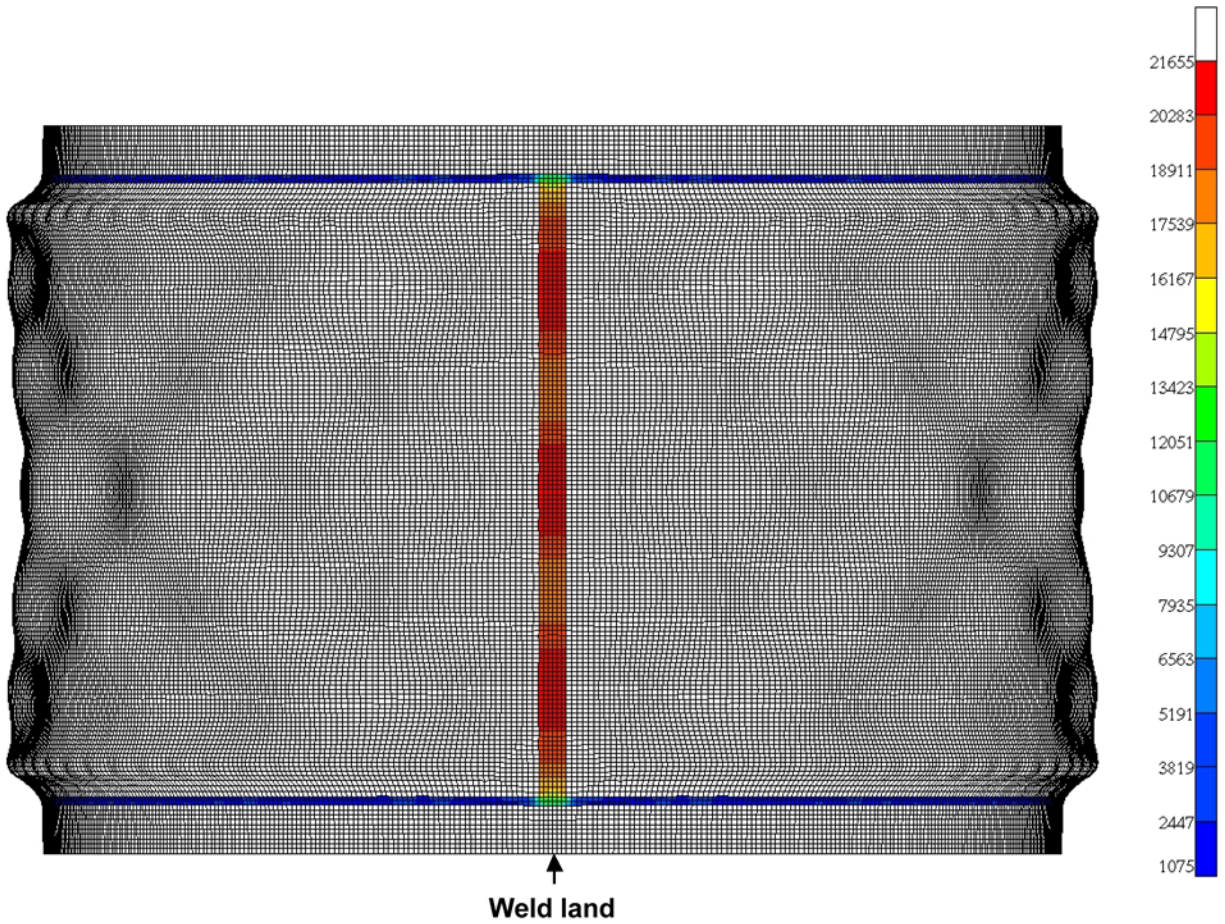


Figure C.8. vonMises stress for design MP-2 at 2,300 lb/in with $t_{w,L} = t_{w,B} = 0.25$ inch, test article weld land inner surface.

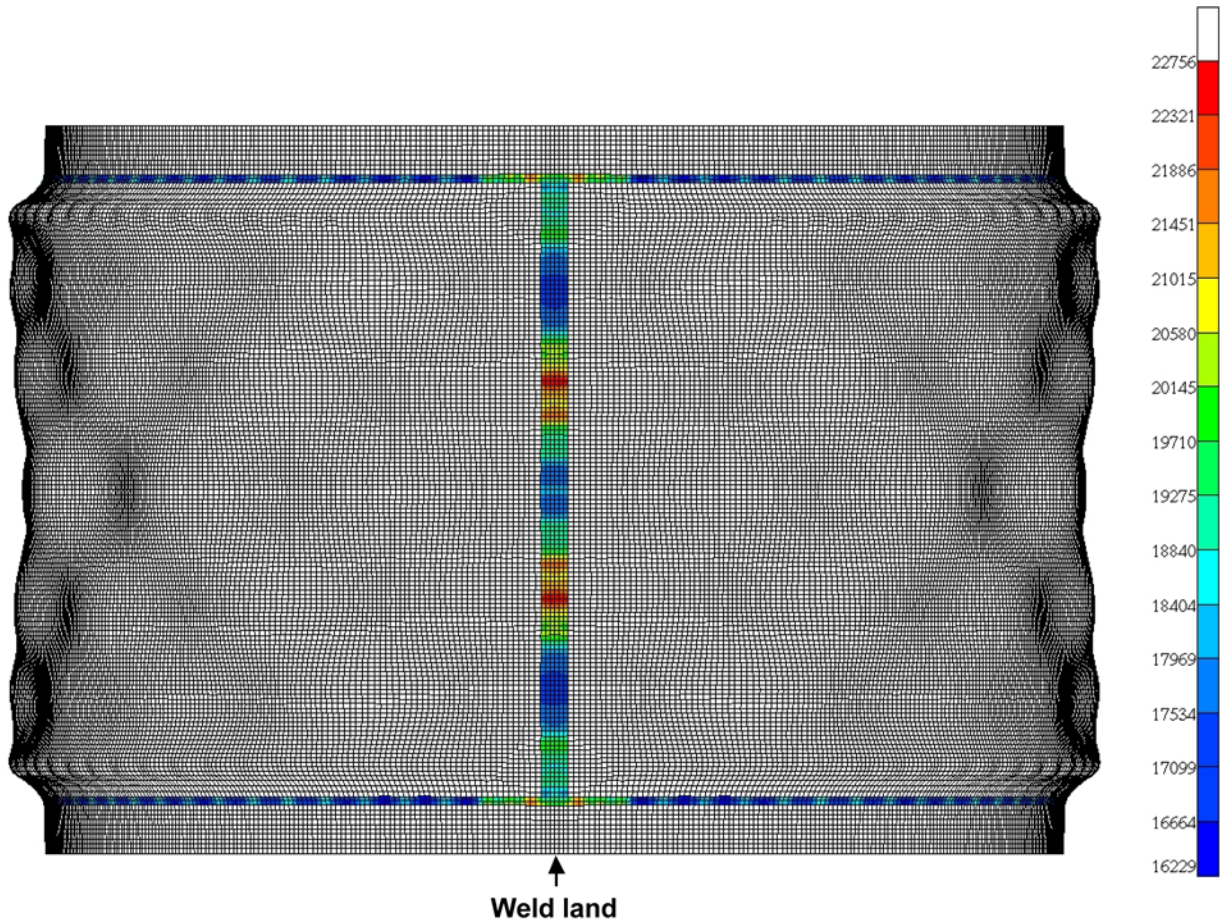


Figure C.9. vonMises stress for design MP-2 at 2,300 lb/in with $t_{w,L} = t_{w,B} = 0.25$ inch, test article weld land outer surface.

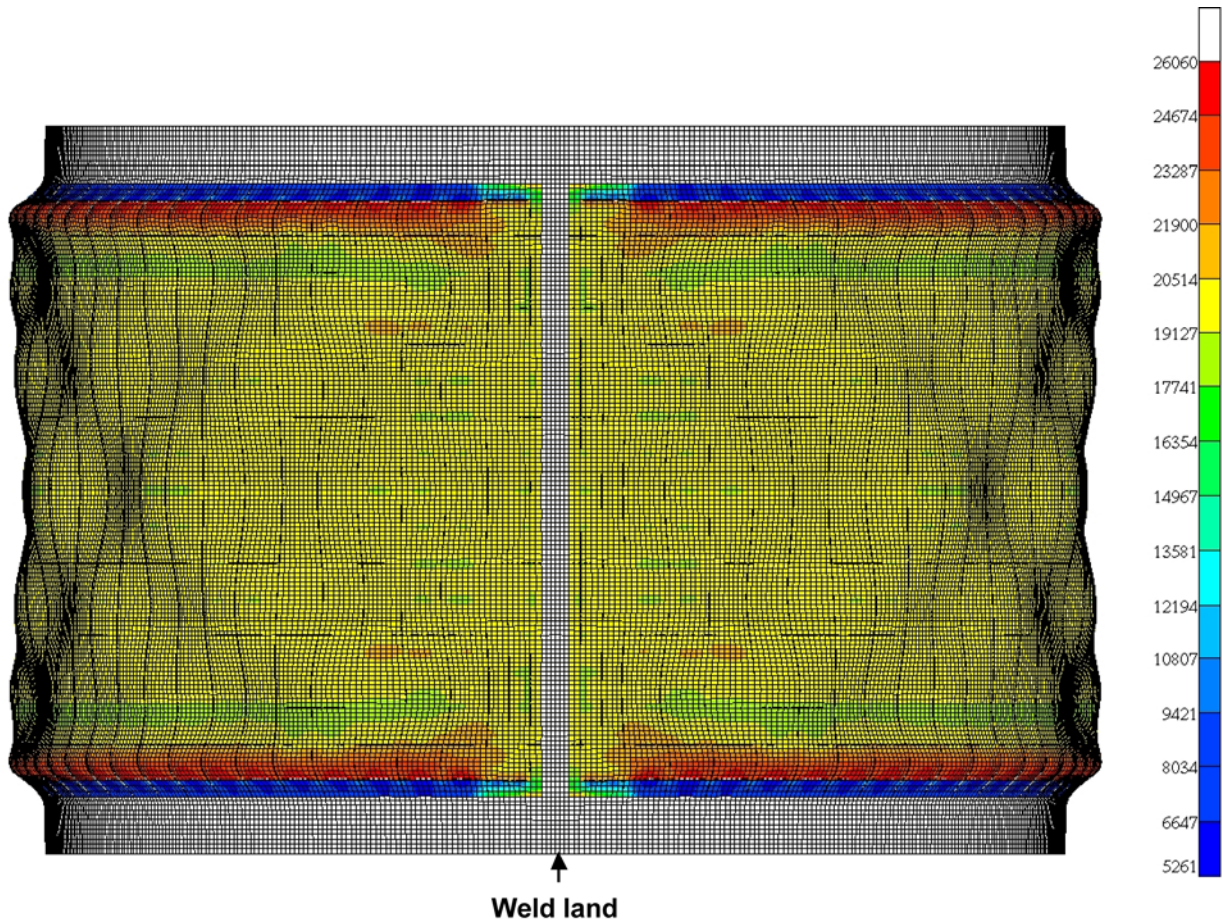


Figure C.10. vonMises stress for design MP-2 at 2,300 lb/in with $t_{w,L} = t_{w,B} = 0.25$ inch, test article skin inner surface.

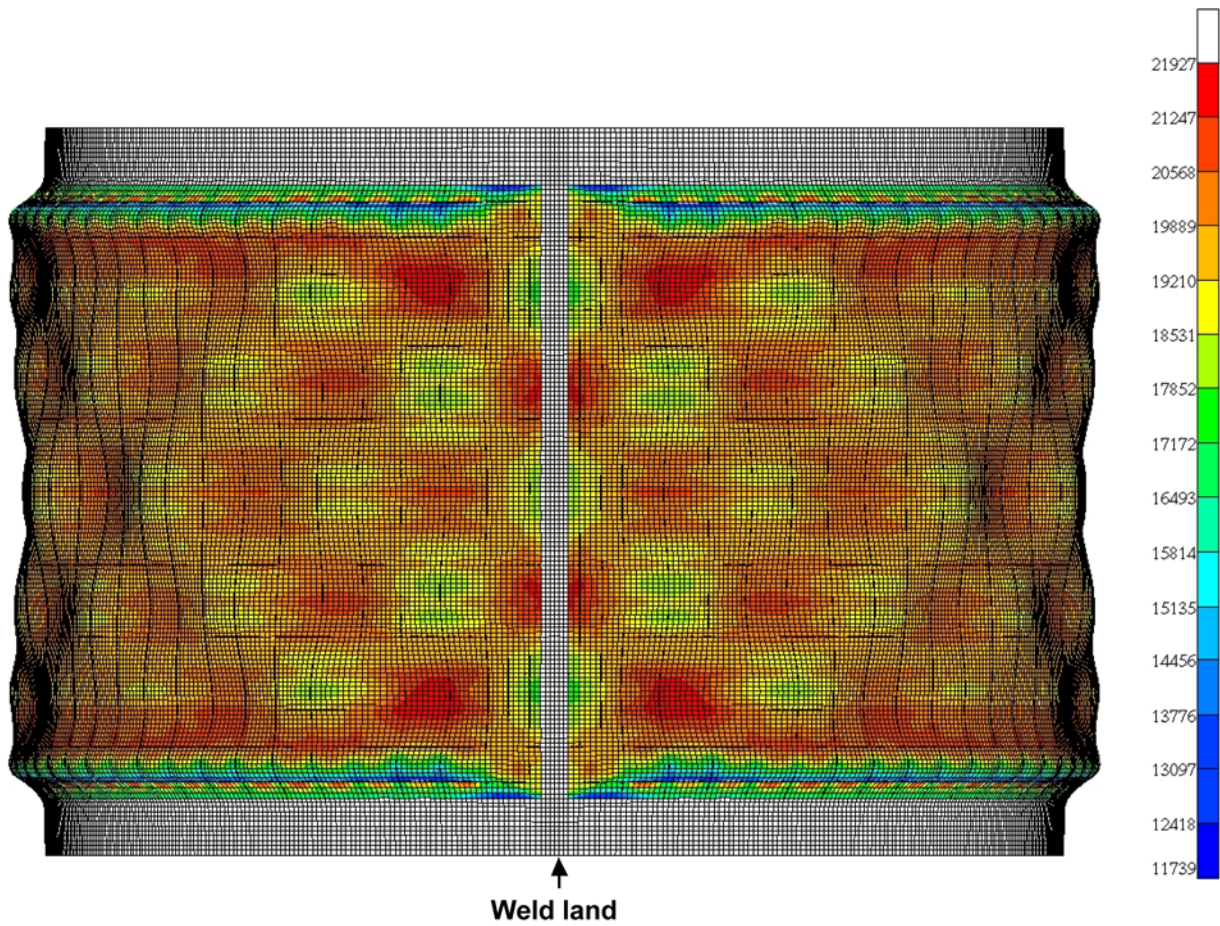


Figure C.11. vonMises stress for design MP-2 at 2,300 lb/in with $t_{w,L} = t_{w,B} = 0.25$ inch, test article skin outer surface.

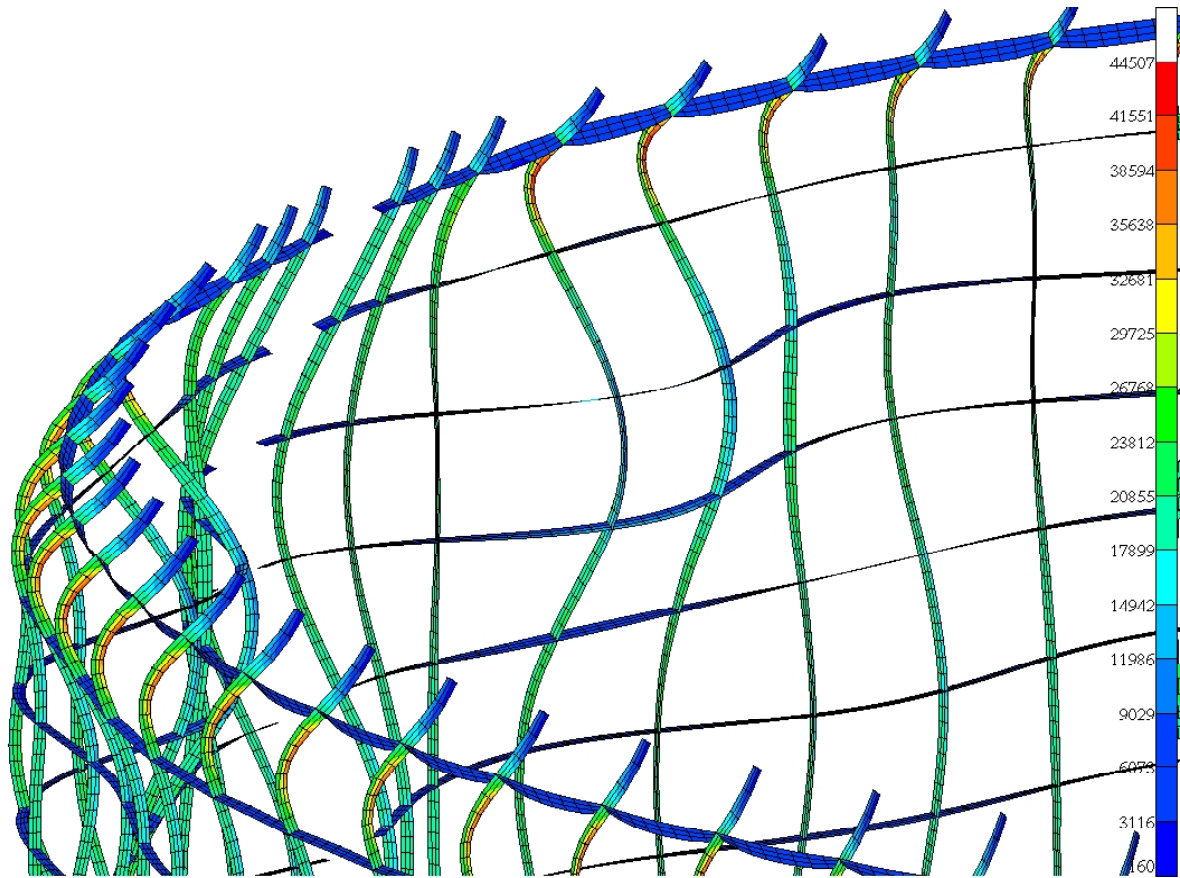


Figure C.12. vonMises stress for design MP-2 at 2,300 lb/in with $t_{w,L} = t_{w,B} = 0.25$ inch, test article stringer Z_1 ("bottom" of element) surface.

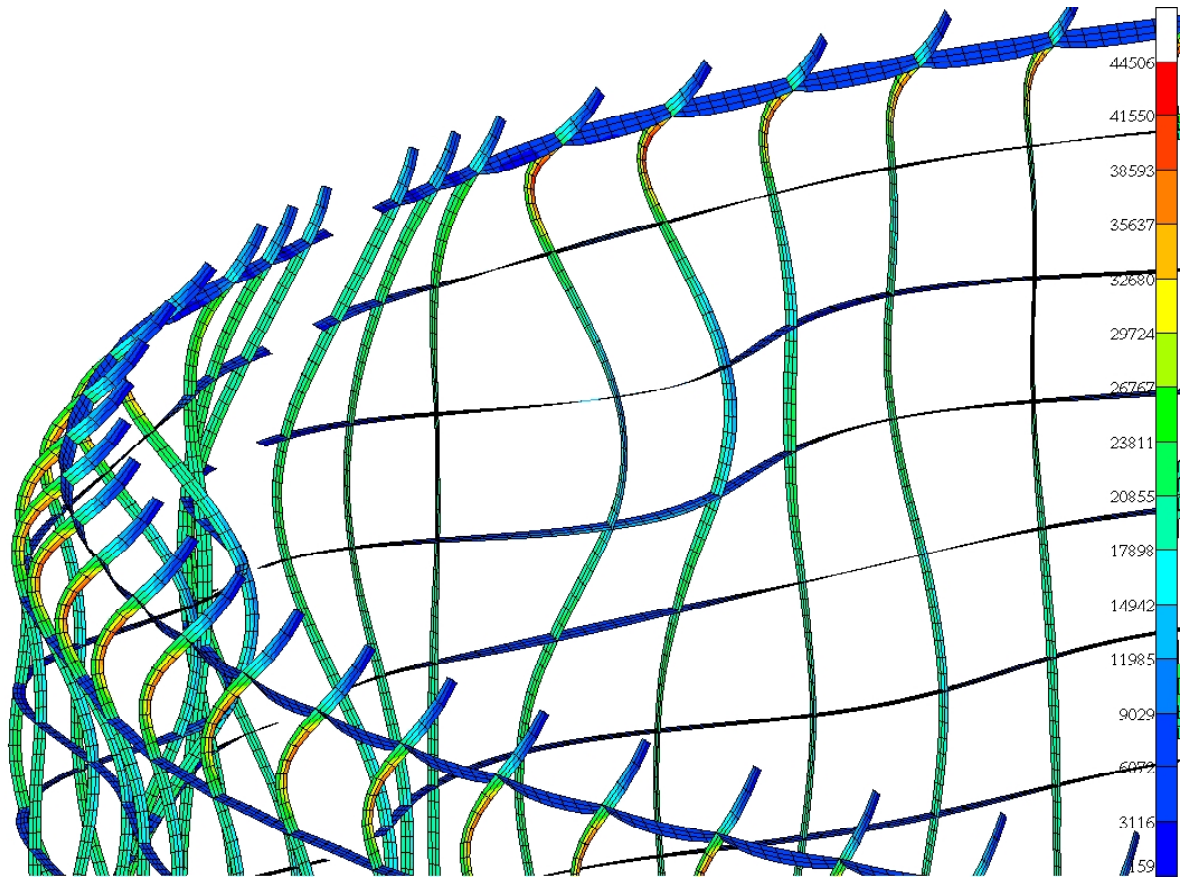


Figure C.13. vonMises stress for design MP-2 at 2,300 lb/in with $t_{w,L} = t_{w,B} = 0.25$ inch, test article stringer Z_2 ("bottom" of element) surface.

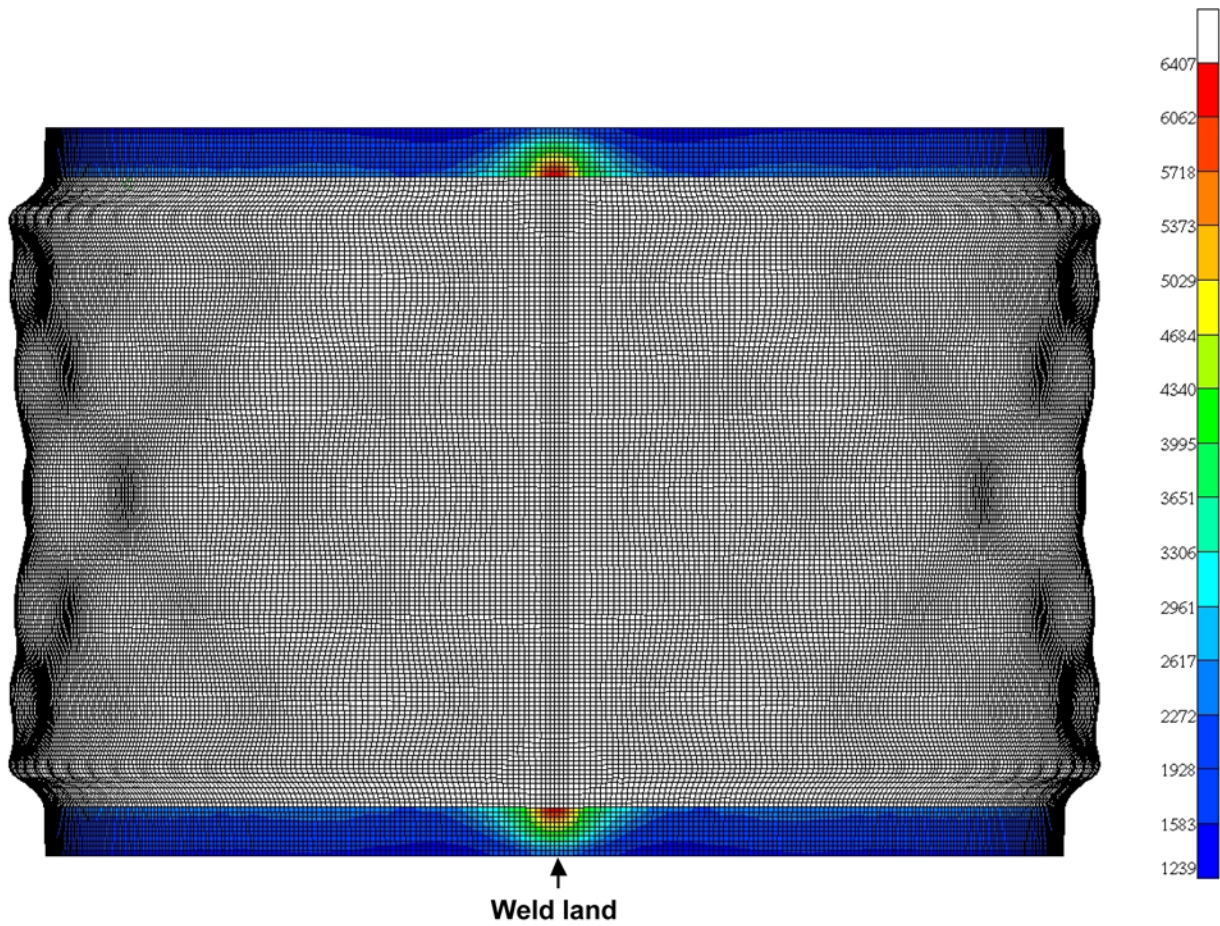


Figure C.14. vonMises stress for design MP-2 at 2,300 lb/in with $t_{w,L} = t_{w,B} = 0.25$ inch, test article L-shaped ring web inner surface.

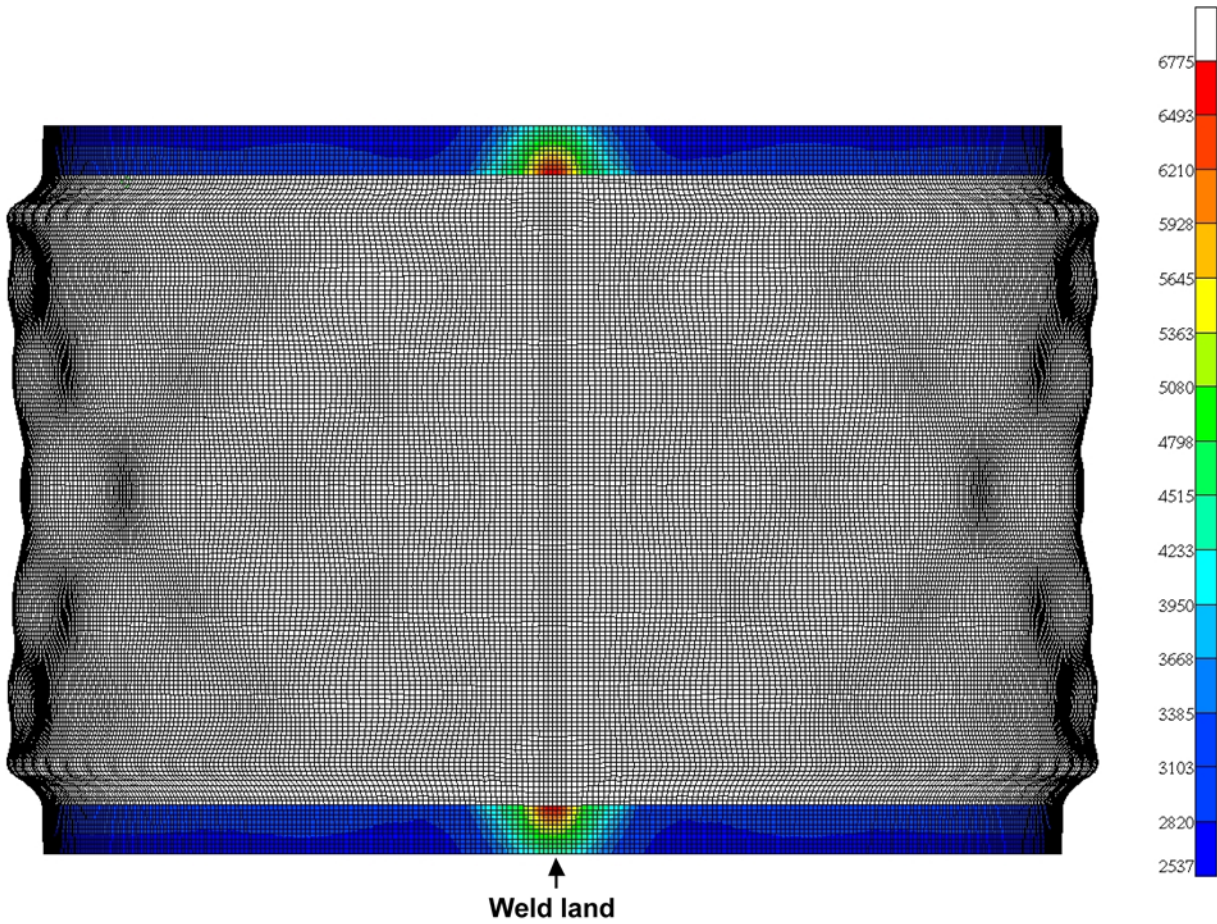


Figure C.15. vonMises stress for design MP-2 at 2,300 lb/in with $t_{w,L} = t_{w,B} = 0.25$ inch, test article L-shaped ring web outer surface.

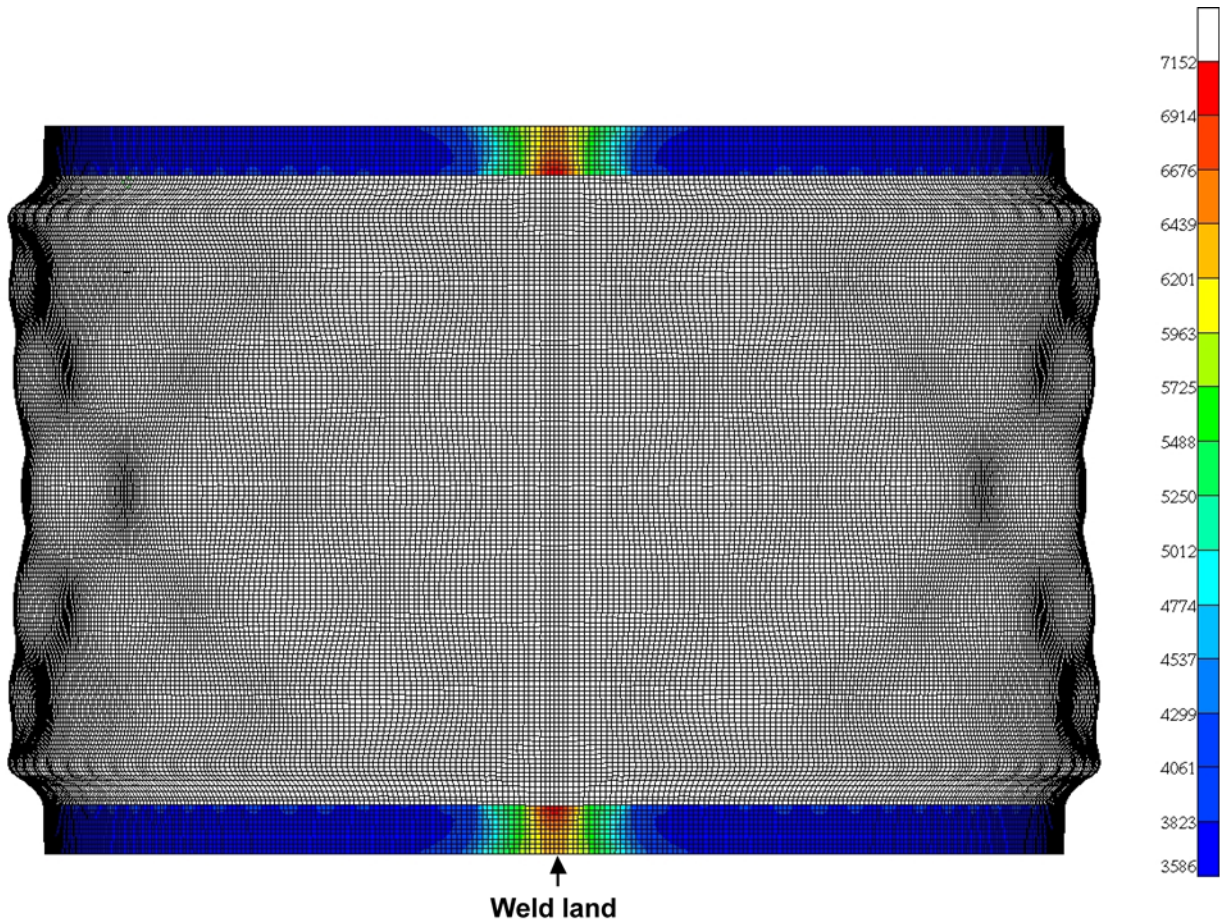


Figure C.16. vonMises stress for design MP-2 at 2,300 lb/in with $t_{w,L} = t_{w,B} = 0.25$ inch, test article band inner surface.

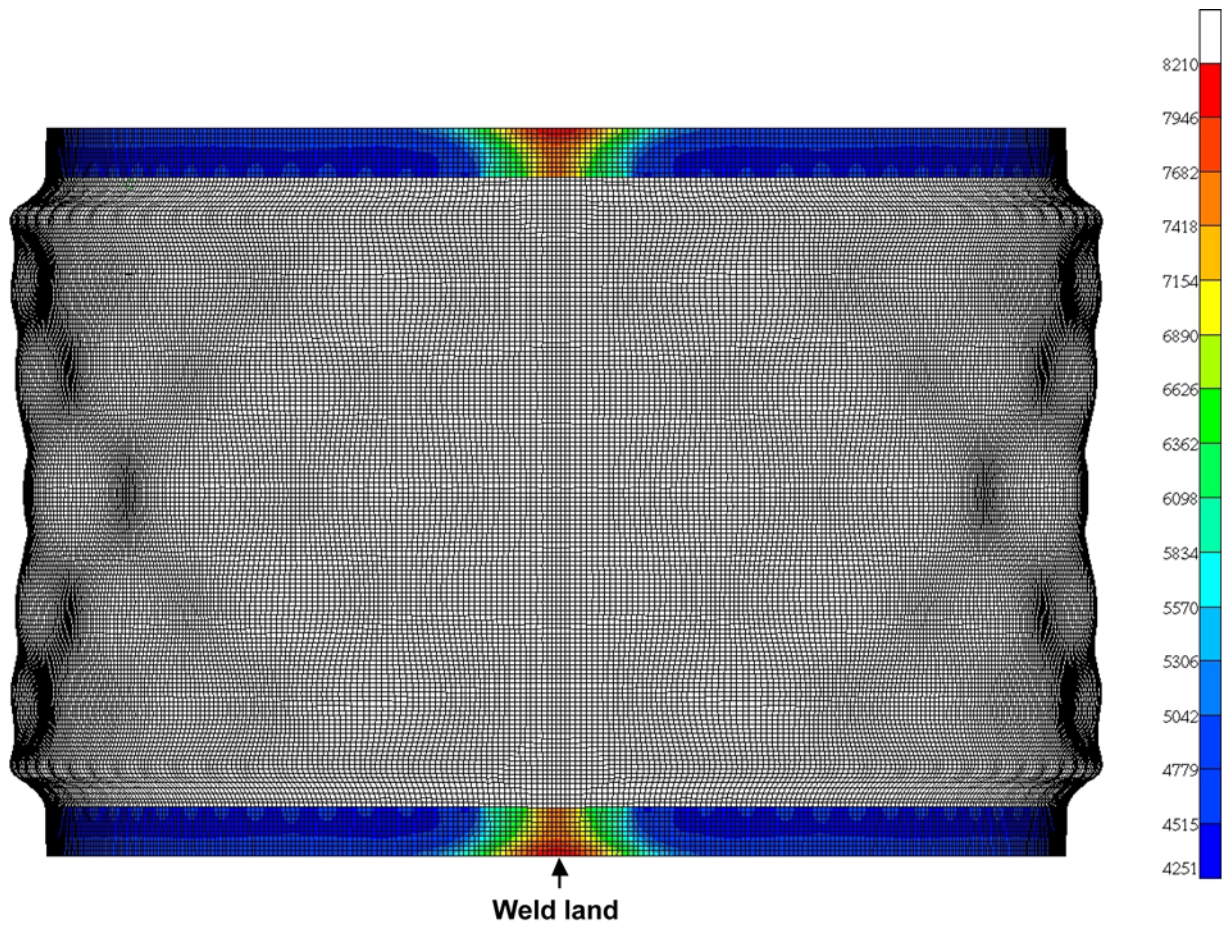


Figure C.17. vonMises stress for design MP-2 at 2,300 lb/in with $t_{w,L} = t_{w,B} = 0.25$ inch, test article band outer surface.

A 24-degree arc-length solid model of the L-shaped ring and band was created to examine the stresses within the sections if no adhesive was used between the test article and the attachment ring. The FEM is shown in Figure C.18. The inner L-shaped ring and the outer band are attached to each other via beams to represent the half-inch diameter attachment bolts. The ends of these beams are attached to the edges of the bolt holes in the L-shaped ring and band that are farthest from the test article, as shown in Figure C.19. The test article portion of the FEM is free and independent from these bolt representations.

Boundary conditions were applied to various parts of the model. The bolts attaching the L-shaped ring to the transition section were not modeled, so the entire base of the L-shaped ring was constrained as clamped. A clamped surface was used since it was assumed that subjected to compression, the base face of the L-shaped ring would be in contact with the transition section in all places. However, the bases of the test article and outer ring were constrained in the axial direction, only, and were free to move along the plane representing the transition section flange. Symmetry boundary conditions were applied to the ends of the three components. To provide interaction between the test article and the attachment ring parts, contact pairs were created at the interfaces between the test article and attachment ring as shown in Figure C.20. Lastly, a uniform end shortening of 0.2 inches was applied to the test cylinder edge.

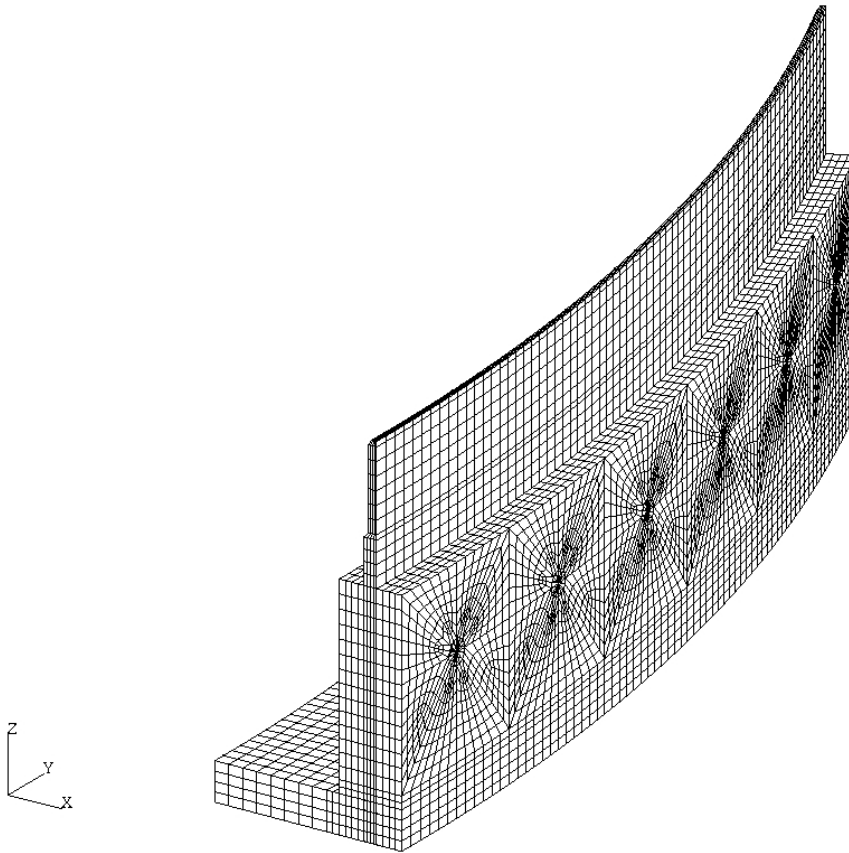


Figure C.18. Local MP-2 FEM to examine contact response of L-bracket web and band.

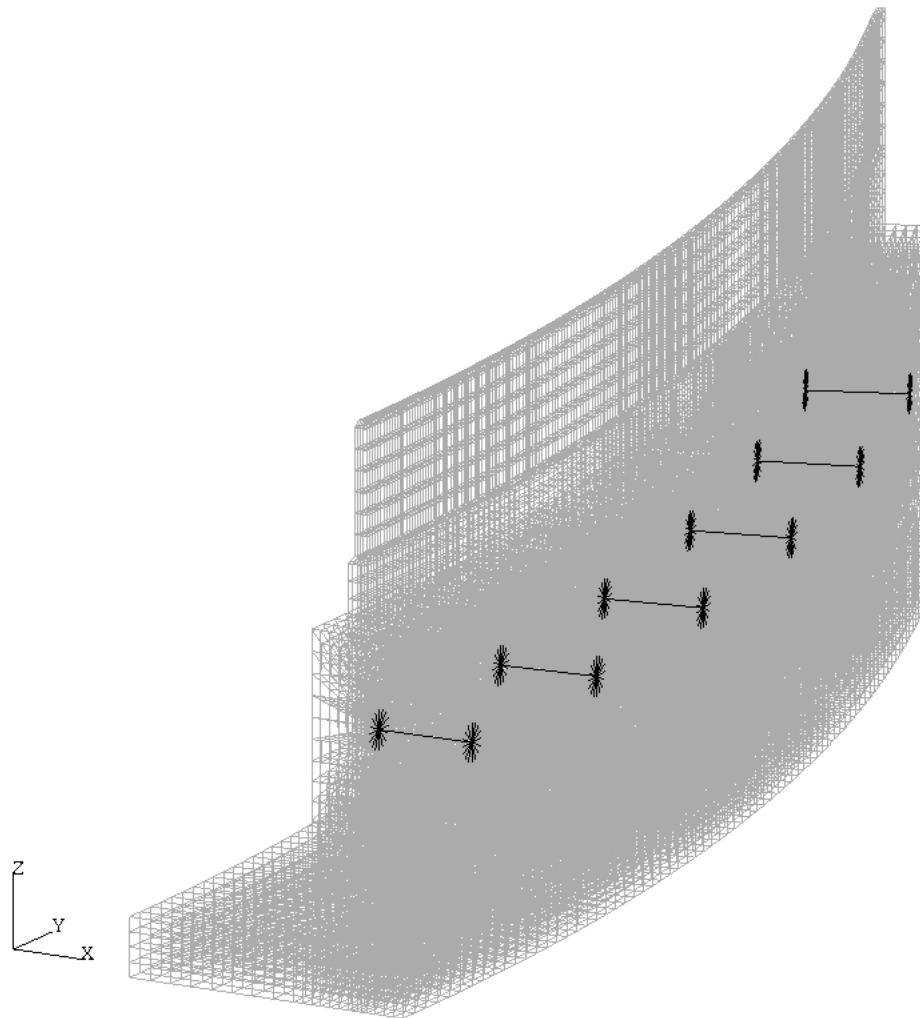


Figure C.19. Locations of bolts (black) in local MP-2 FEM.

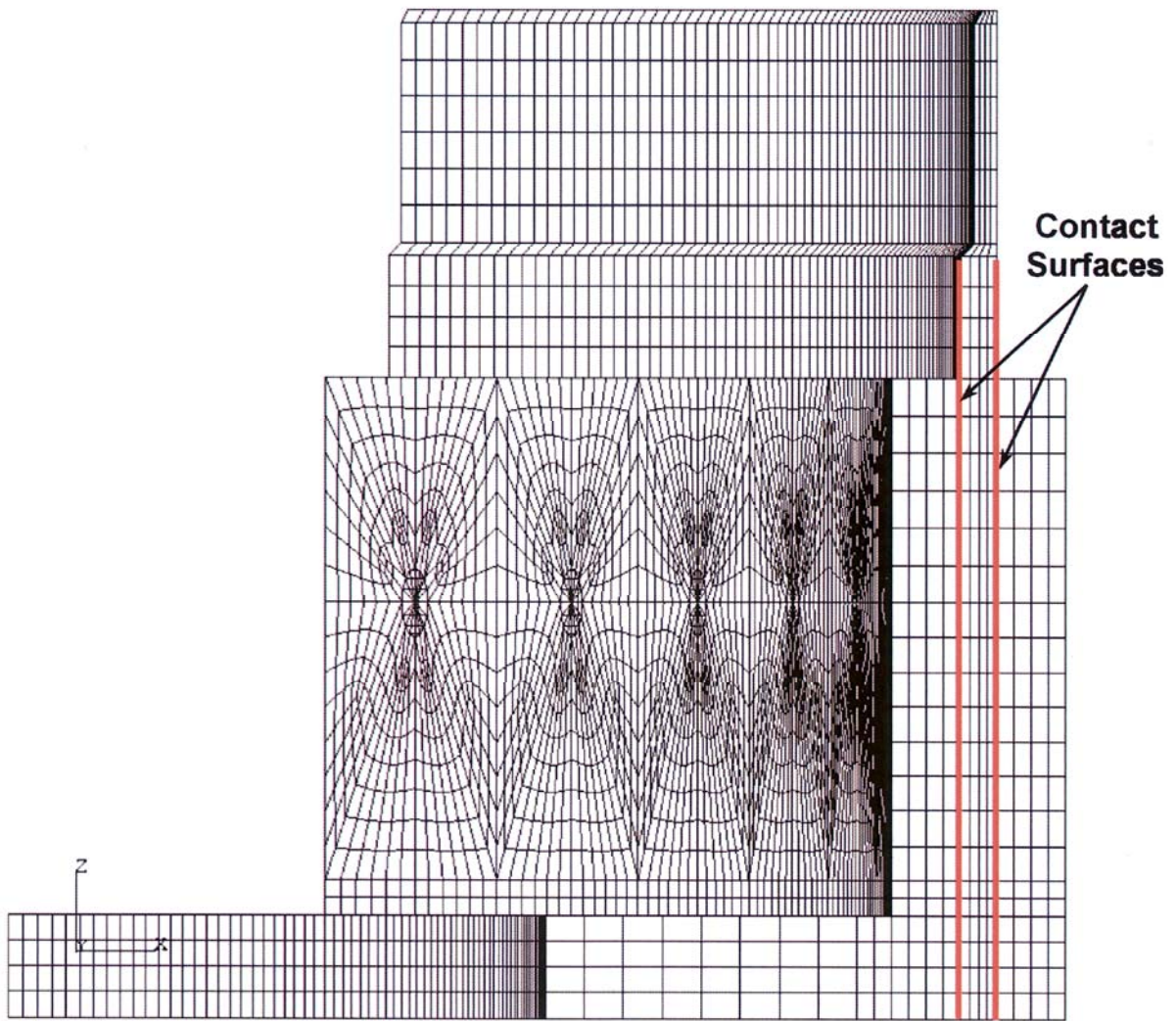


Figure C.20. Contact surface locations for local MP-2 FEM.

C-3 Design MP-3

The multiple-piece MP-3 design was analyzed using a shell FEM identical to the one used for the MP-2 design and described above. This model was chosen because previous analyses have shown the test article response is not significantly influenced by the boundary conditions on the attachment ring. This model equates to removing the legs of the L-shaped rings and the base annular ring as shown in Figure C.21, and clamping the shell model at the base of the webs. Since only the attachment ring webs are included in the shell model, and because the webs are attached to the test article using EA-9394, the resulting shell FEM is identical to the MP-2 design shell model and is shown in Figures 6.4 and 6.5.

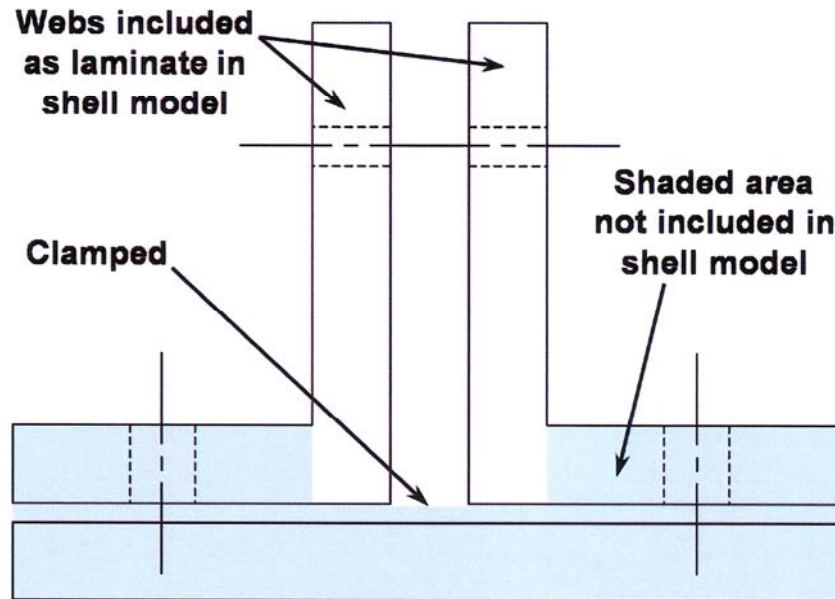


Figure C.21. Attachment ring modeled in MP-3 shell FEM.

Appendix D: Single-Piece Design FEM

The SP-1 design was analyzed using an ABAQUS™ shell FEM, shown in Figures D.1, D.2 and D.3. Each end of the model was modeled differently, with one end examining the response for a completely adhesive joint at the test article attachment ring interface, and the other examining the response for a completely bolted joint at the same location. At the adhesively-attached end, the webs of the attachment ring were considered to be adhesively bonded to the test article using the EA-9394. The EA-9394 was included in the analysis by creating a laminate consisting of the attachment ring webs, test article, and EA-9394 with their appropriate thicknesses. Modeling in this manner separated the attachment ring webs the proper distance from the test article. Similar to the previous model, to determine the stresses/strains at the surfaces of the components to assess bending, each component was broken up into three layers. The outermost layers were given a thickness of 0.001 inch, with the central layer given a thickness appropriate to yield the total component thickness. Values of stress and strain were then examined in all three layers for a component, with the values in the 0.001-inch layers providing the surface values. Although not necessary in the ABAQUS™ analysis, since the model was derived from the NASTRAN™ for MP-2 and MP-3, a dummy layer was included to generate a laminate having no offsets (recall Figure C.5). This dummy layer was fabricated from a dummy material having $E = 0.001$ psi and $\nu = 0.3$. All remaining shell elements were defined as single layers with the appropriate offsets. At the bolted end, the inner and outer flanges were attached at the 18 bolt locations using beam elements to approximate the bolt stiffness as shown in Figure D.4. Appropriate boundary conditions were applied to each end. At the laminated end, which was the load end, all degrees of freedom except for the axial displacement were restrained. At the bolted end, each of the three components (inner flange, test article and outer flange) was clamped. Additionally, contact pairs were defined between the inner and outer flanges and the test article. A uniform compressive axial load of -2500 lb/in was used at the laminated end in the nonlinear analyses. As previously, at the loaded end, a set of beams was created around the circumference to keep the edge planar. These beams were modeled using the AISI 1025 steel, and were given in the plane of the shell bending stiffness by assigning $I = 100$ in⁴. The area, moment of inertia out-of-plane of the shell and the torsional constant were assigned values of 0.0001. Lastly, response was examined using both the ABAQUS™ S4 and S4R5 shell elements.

The typical nonlinear analysis deformed shape is shown in Figures D.4 and D.5. Typical nonlinear vonMises stress results are shown in Figures D.6 to D.24 for the various parts of the attachment ring and test article. Cross-section deformed plots in the vicinity of the contact region between the attachment ring flanges and test article are shown in Figure D.25 and D.26 at the weld land and in the center of a panel, respectively. The figures show the results for the design having AISI 1025 steel attachment rings subjected to LC1 at $N_x = 2220$ lb/in uniform loading that was analyzed using the S4R5 shell elements.

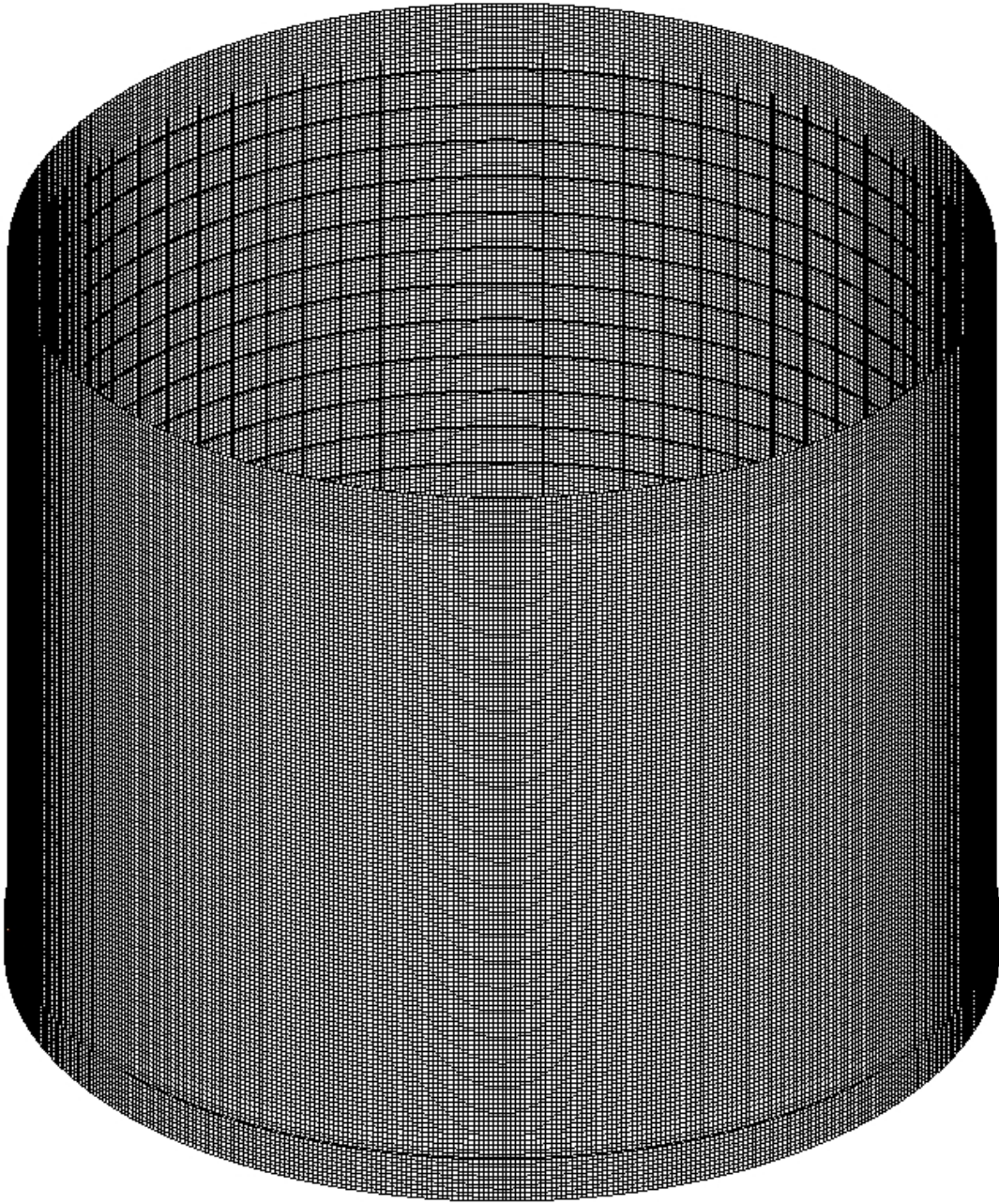


Figure D.1. SP-1 ABAQUS™ shell FEM.

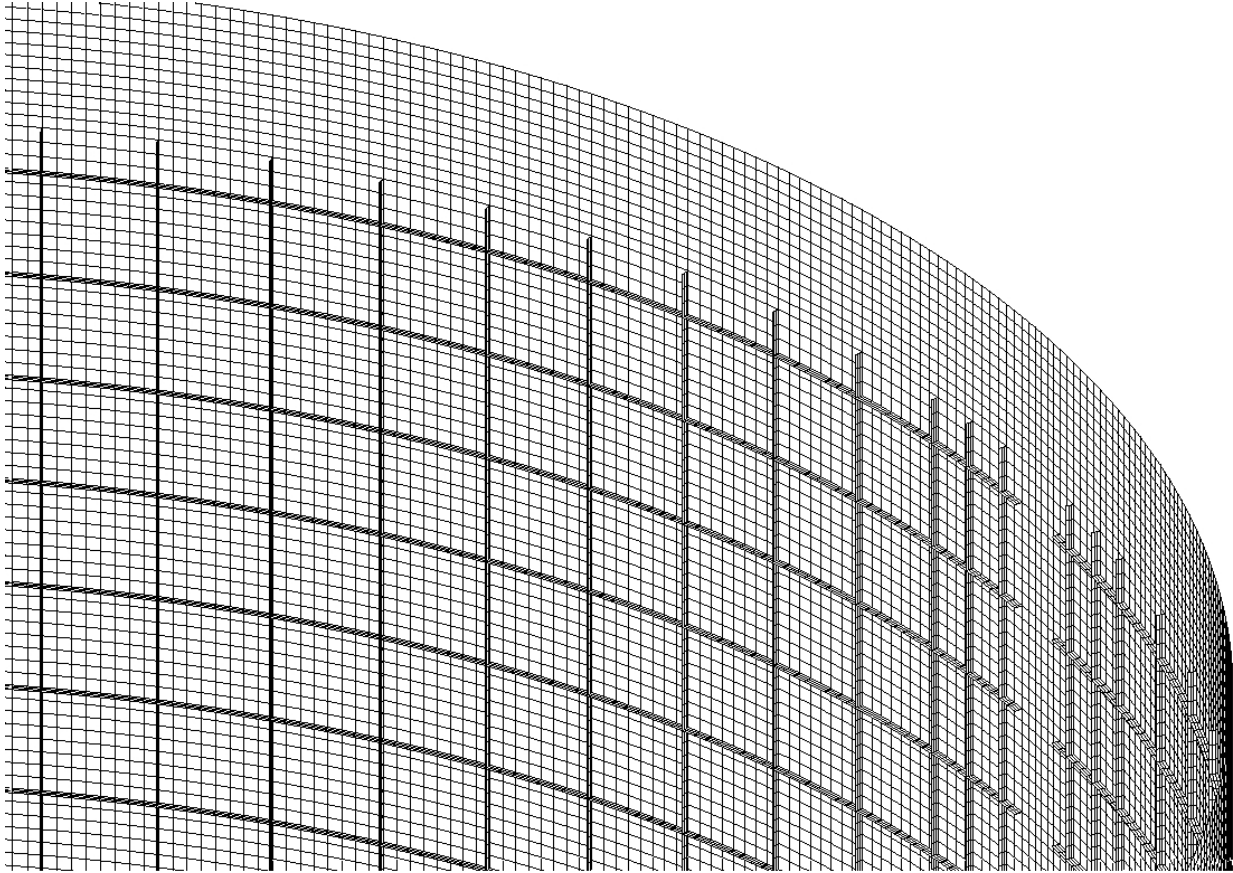


Figure D.2. SP-1 ABAQUS™ shell FEM, laminated end.

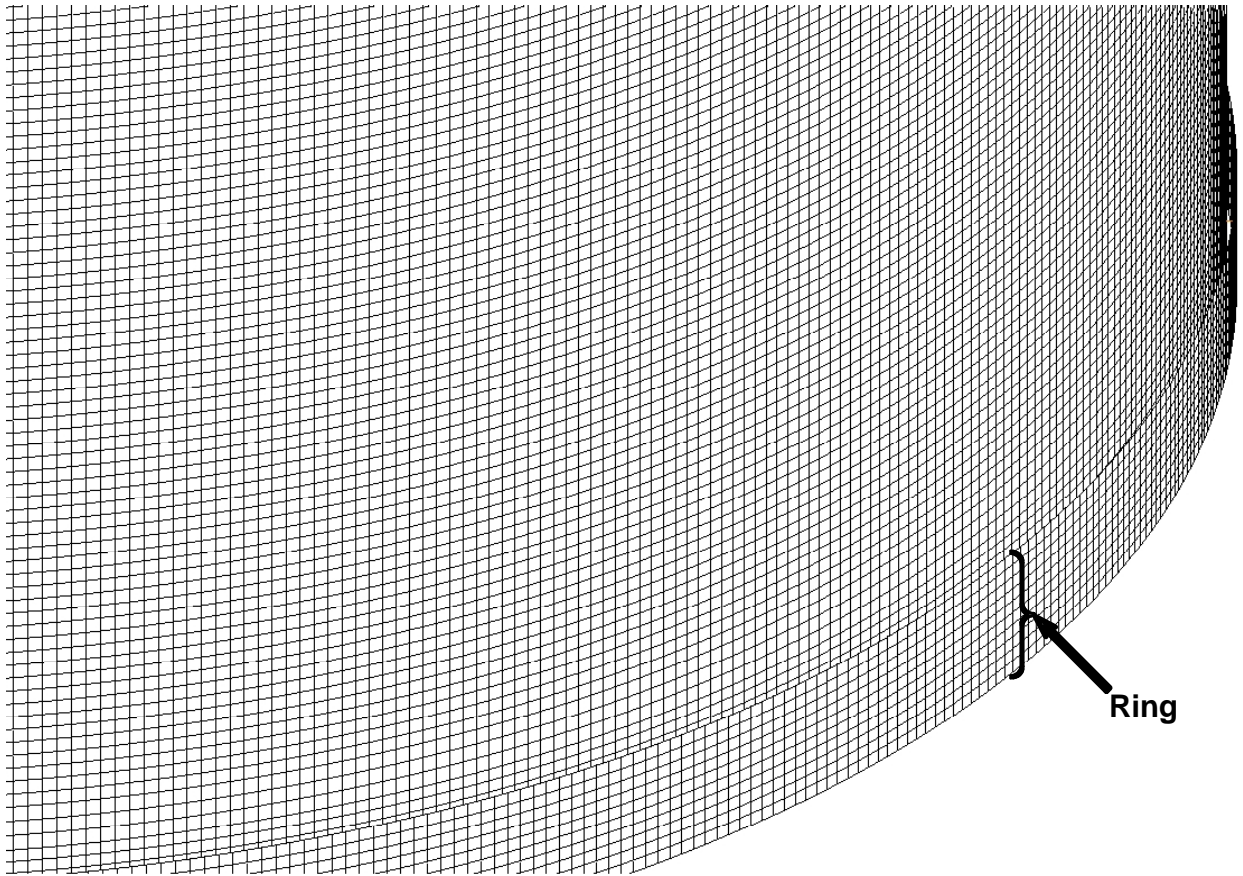


Figure D.3. SP-1 ABAQUS™ shell FEM, bolted end.

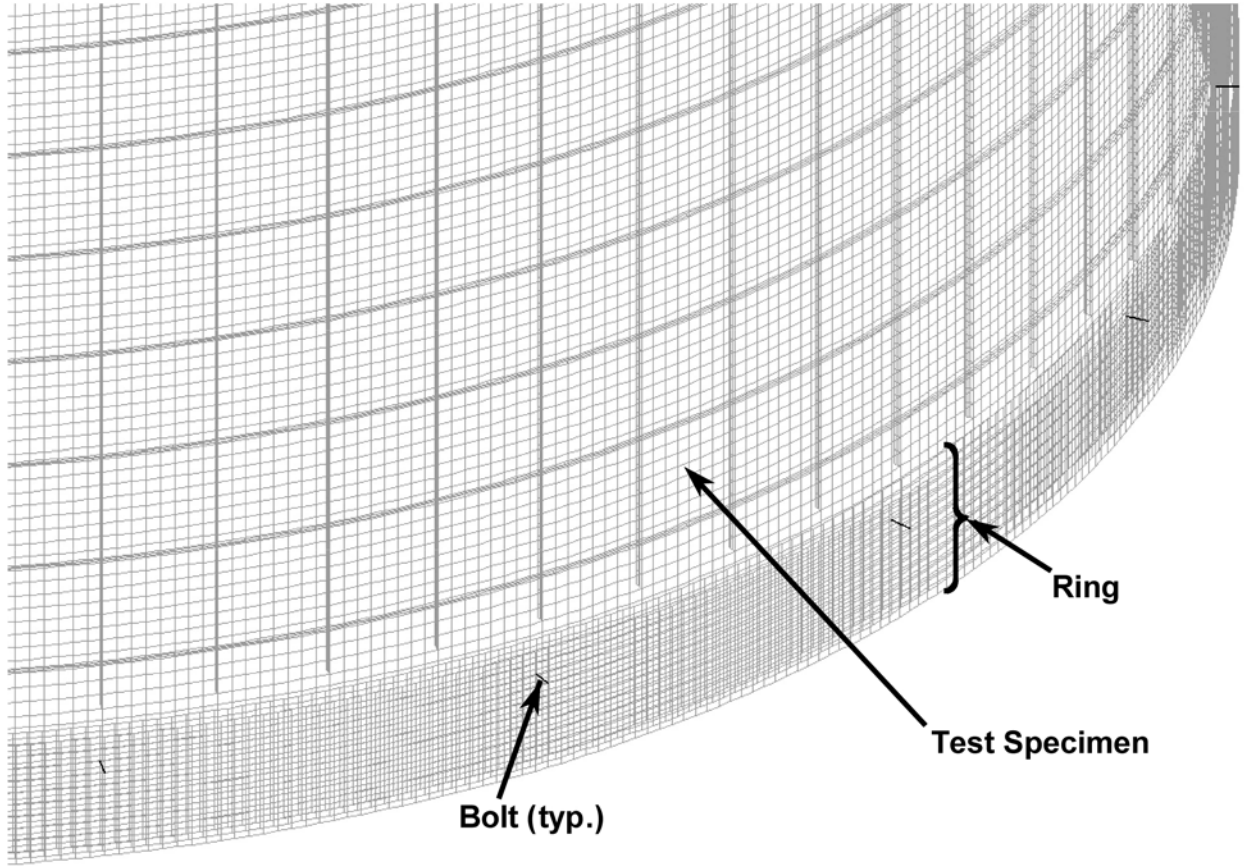


Figure D.4. SP-1 ABAQUS™ shell FEM attachment bolt beams (shown in black).

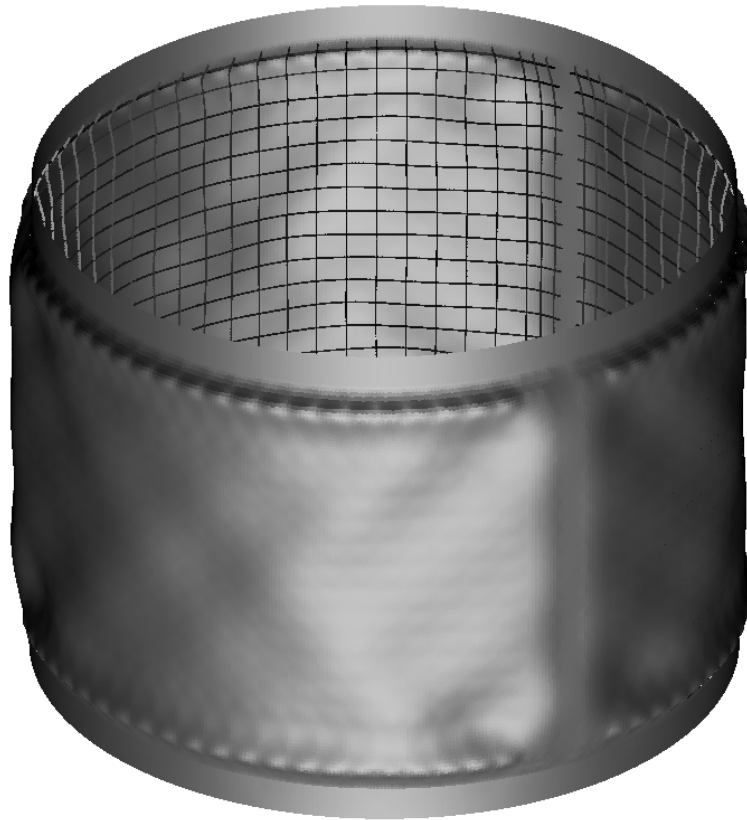


Figure D.5. SP-1 nonlinear deformed shape, LC1 at 2220 lb/in, AISI 1025 steel attachment rings (deformations magnified x50).

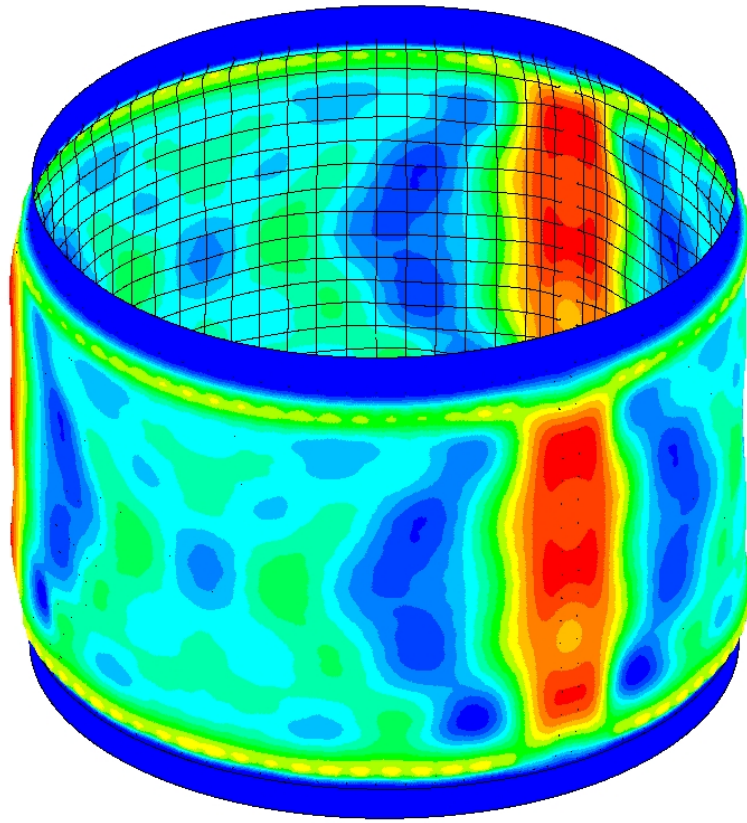


Figure D.6. SP-1 nonlinear deformed shape with radial deflection contours, LC1 at 2220 lb/in, AISI 1025 steel attachment rings (deformations magnified x50).

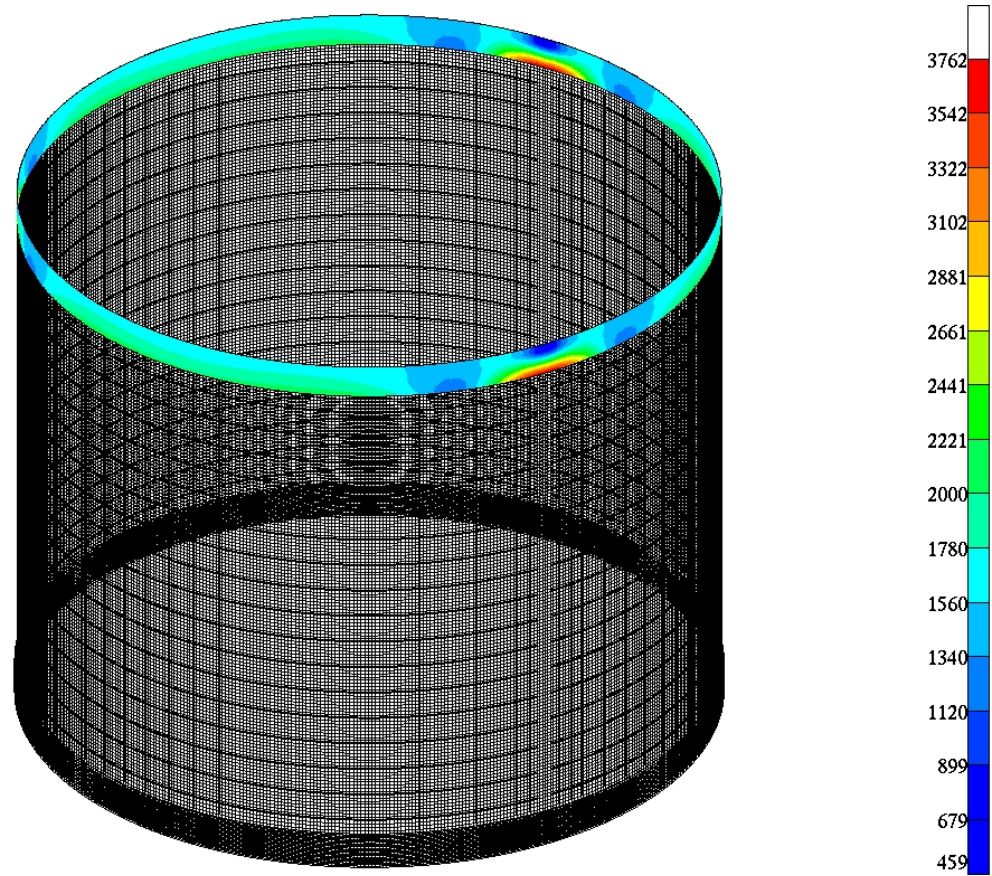


Figure D.7. SP-1 vonMises stress (psi) in inner flange inner surface at laminated end, LC1 at 2220 lb/in, AISI 1025 steel attachment rings.

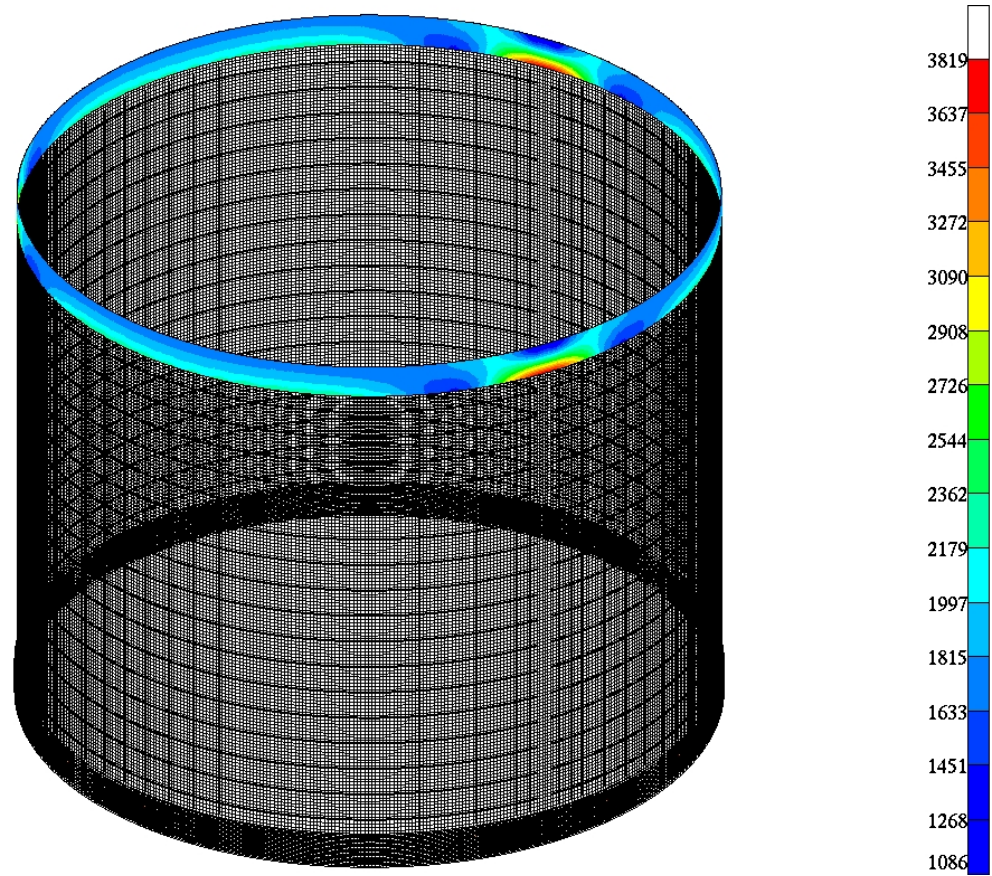


Figure D.8. SP-1 vonMises stress (psi) in inner flange outer surface at laminated end, LC1 at 2220 lb/in, AISI 1025 steel attachment rings.

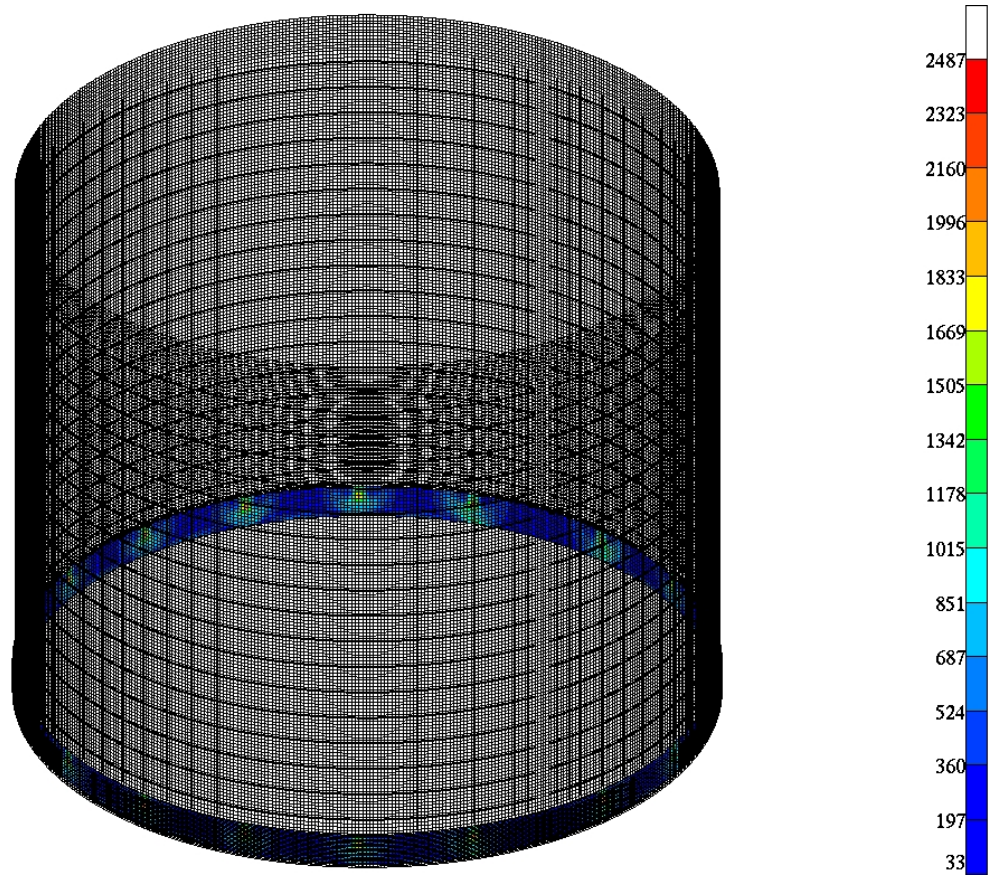


Figure D.9. SP-1 vonMises stress (psi) in inner flange inner surface at bolted end, LC1 at 2220 lb/in, AISI 1025 steel attachment rings.

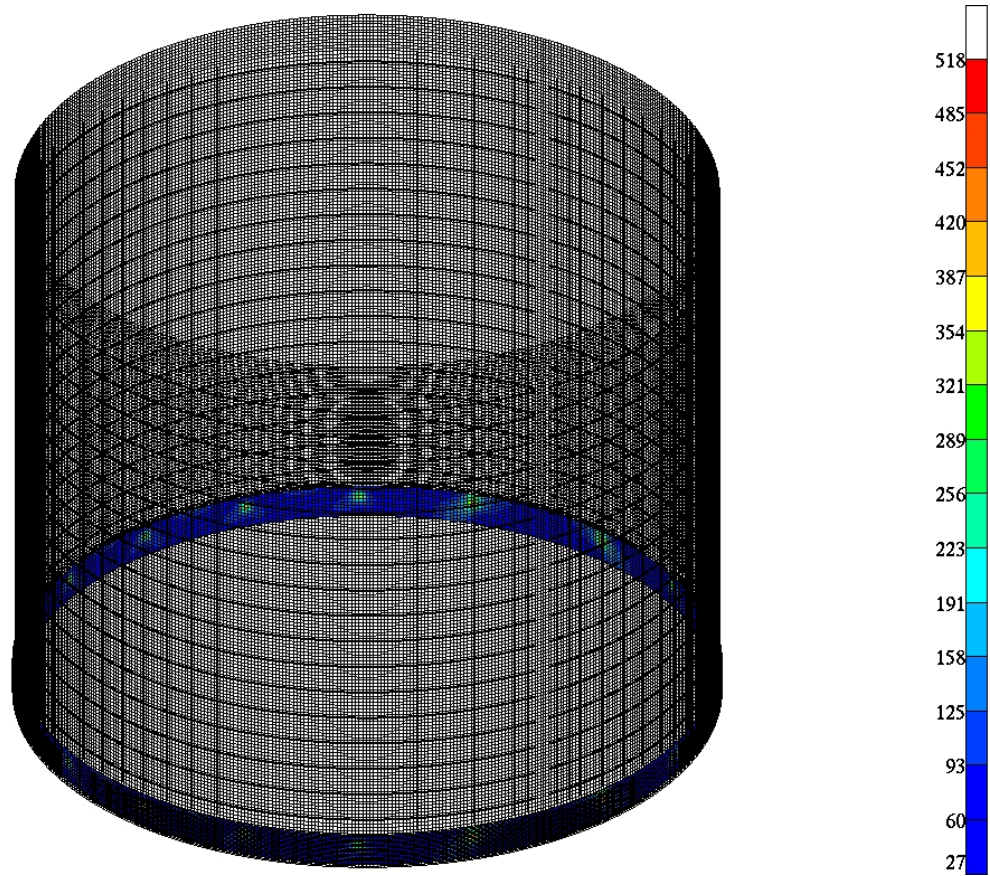


Figure D.10. SP-1 vonMises stress (psi) in inner flange outer surface at bolted end, LC1 at 2220 lb/in, AISI 1025 steel attachment rings.

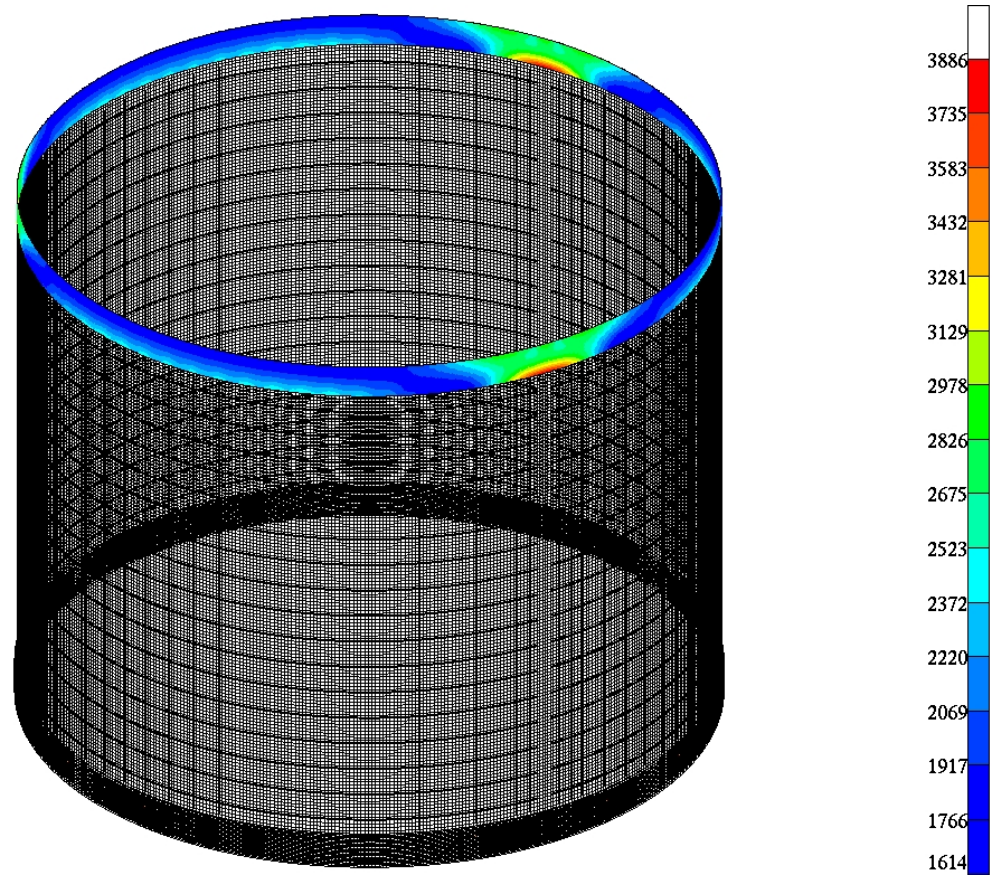


Figure D.11. SP-1 vonMises stress (psi) in outer flange inner surface at laminated end, LC1 at 2220 lb/in, AISI 1025 steel attachment rings.

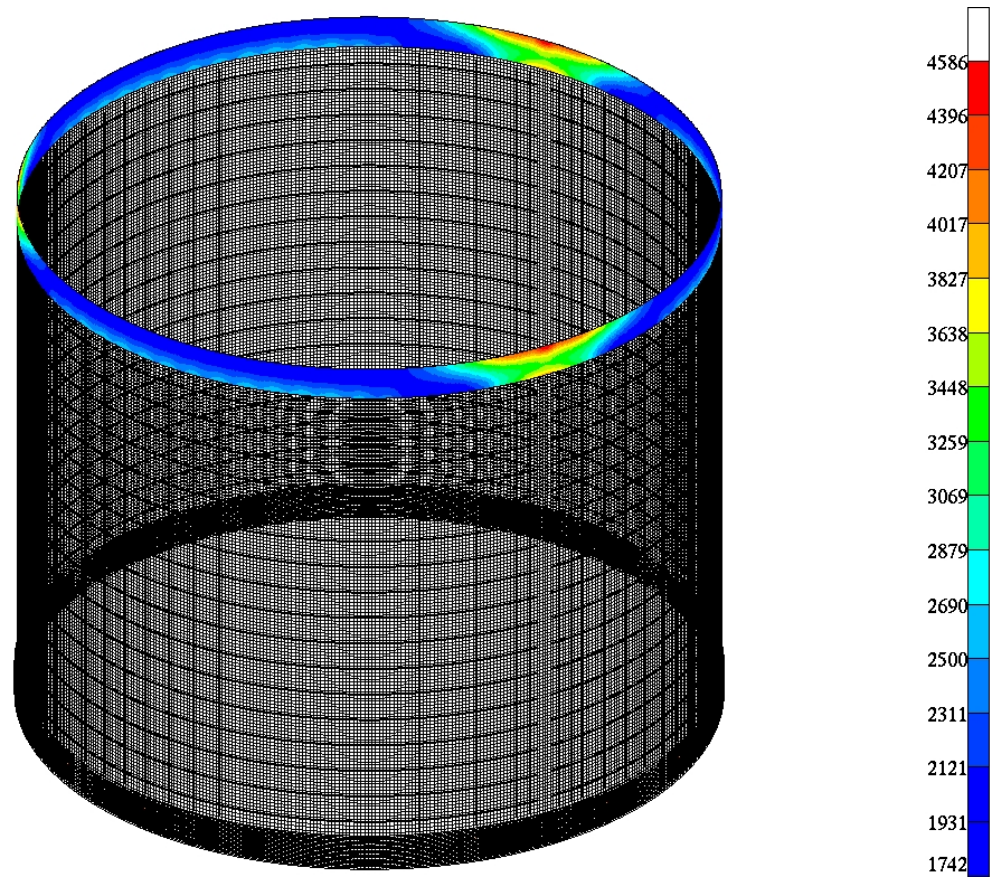


Figure D.12. SP-1 vonMises stress (psi) in outer flange outer surface at laminated end, LC1 at 2220 lb/in, AISI 1025 steel attachment rings.

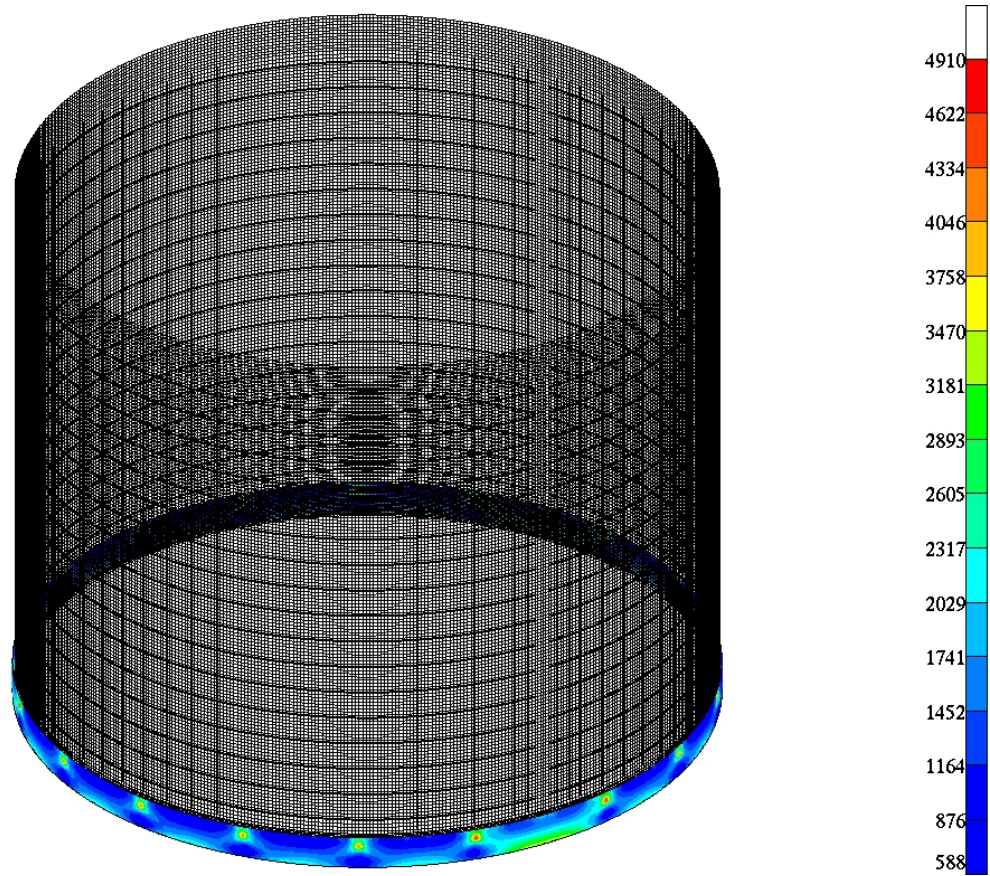


Figure D.13. SP-1 vonMises stress (psi) in outer flange inner surface at bolted end, LC1 at 2220 lb/in, AISI 1025 steel attachment rings.

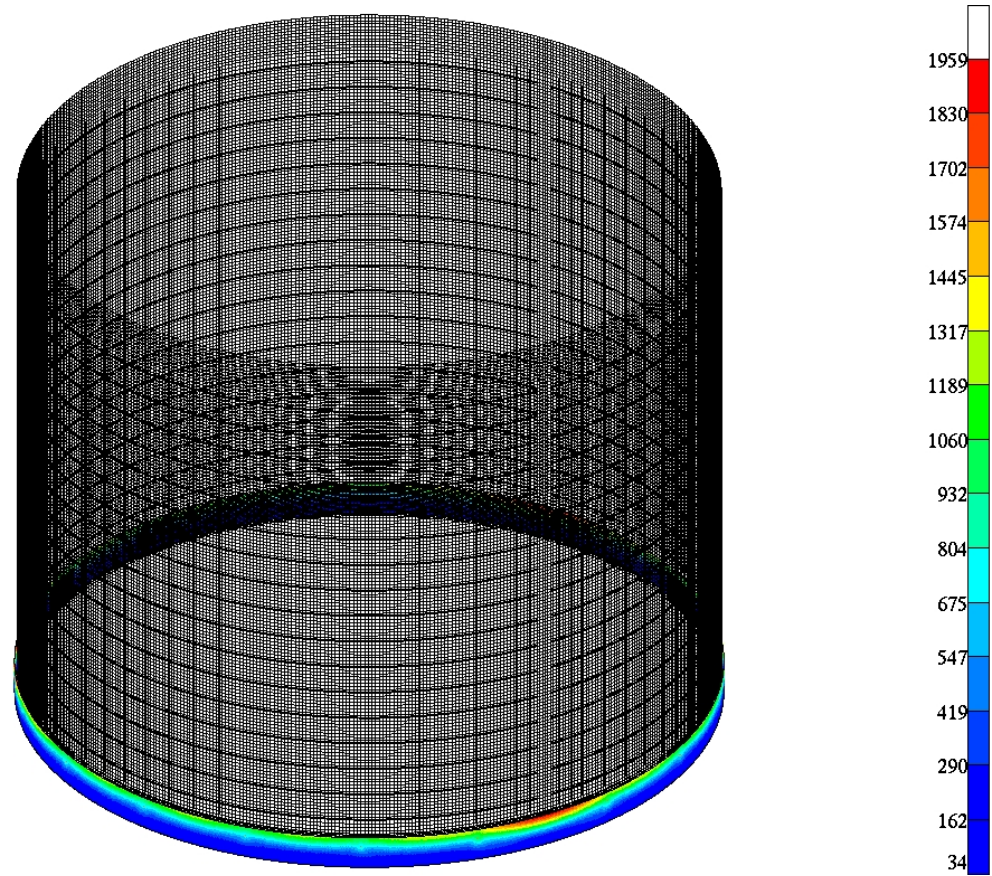


Figure D.14. SP-1 vonMises stress (psi) in outer flange outer surface at bolted end, LC1 at 2220 lb/in, AISI 1025 steel attachment rings.

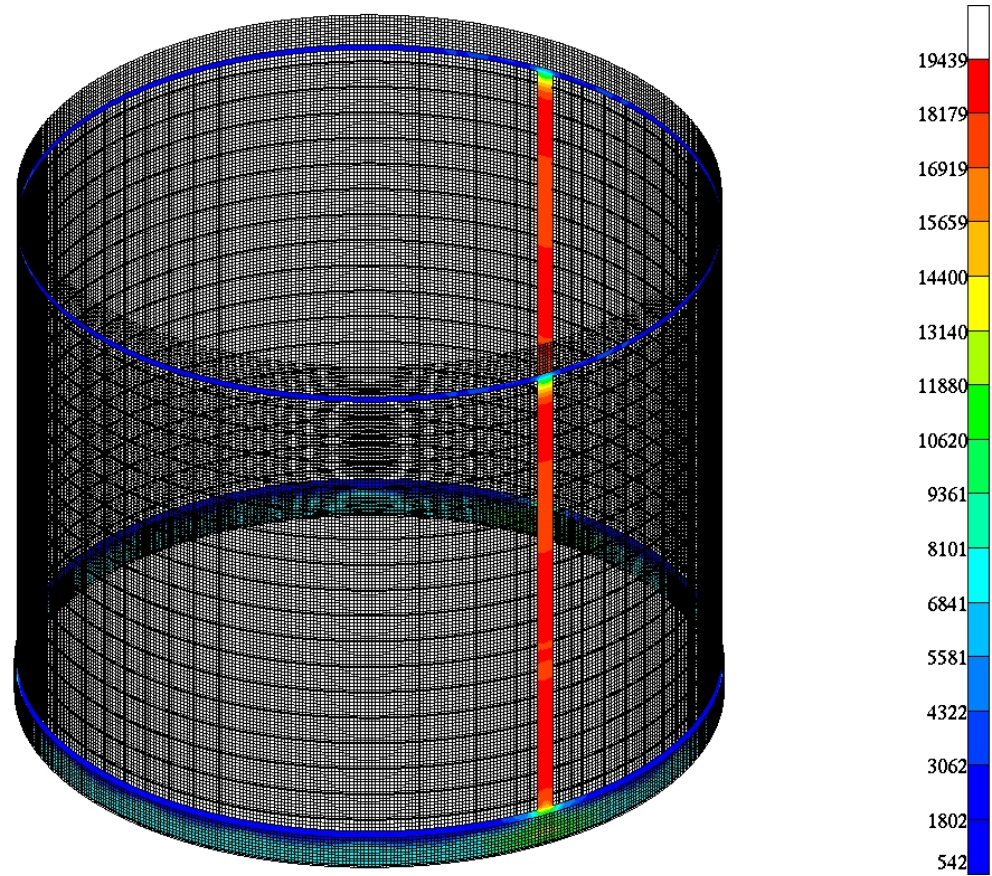


Figure D.15. SP-1 vonMises stress (psi) in weld land inner surface, LC1 at 2220 lb/in, AISI 1025 steel attachment rings.

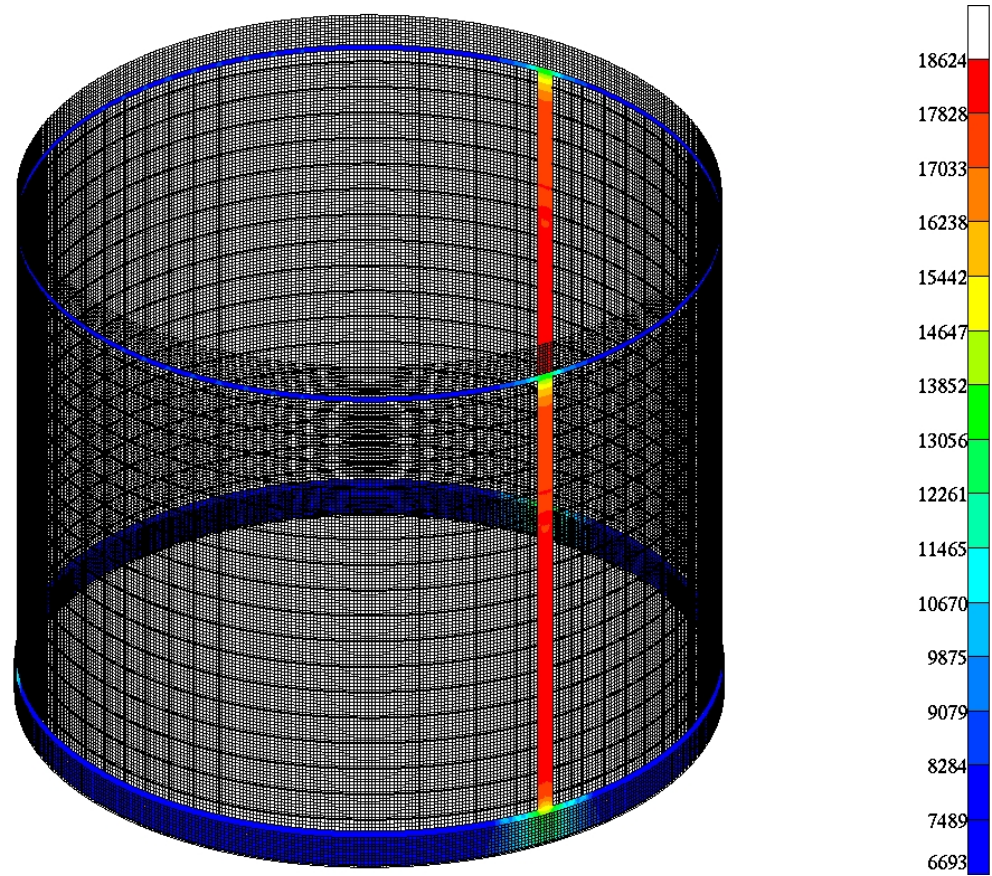


Figure D.16. SP-1 vonMises stress (psi) in weld land outer surface, LC1 at 2220 lb/in, AISI 1025 steel attachment rings.

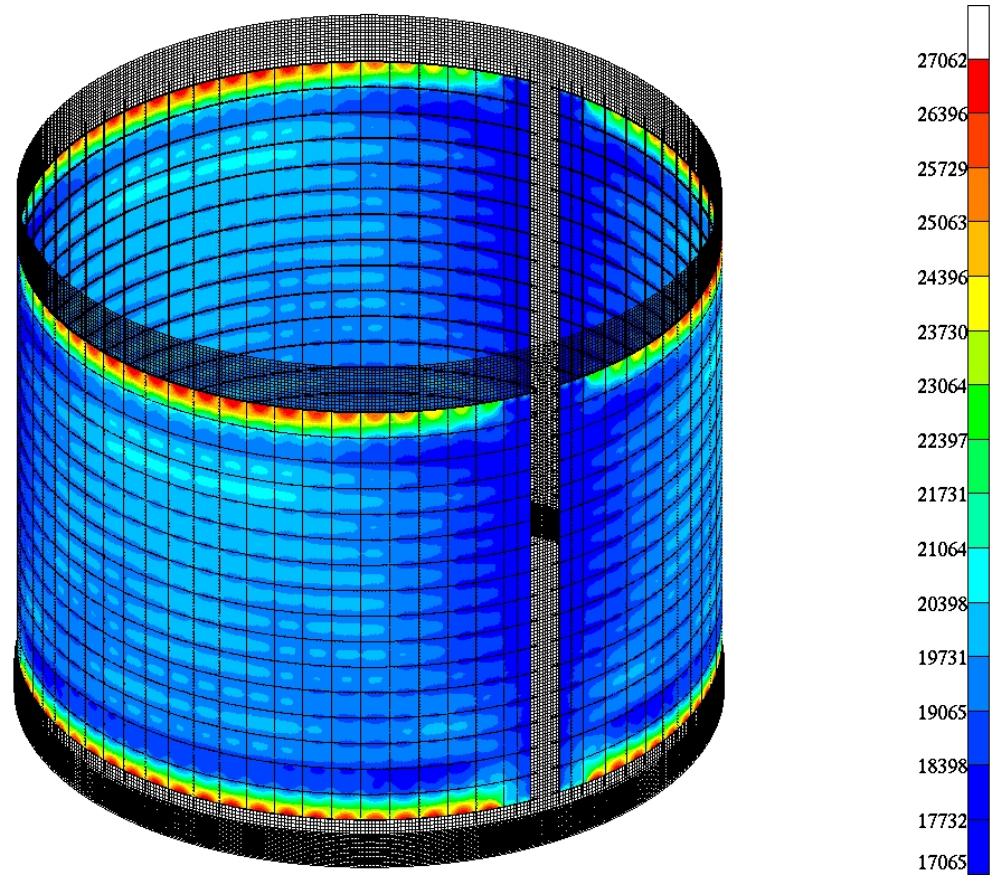


Figure D.17. SP-1 vonMises stress (psi) in acreage skin inner surface, LC1 at 2220 lb/in, AISI 1025 steel attachment rings.

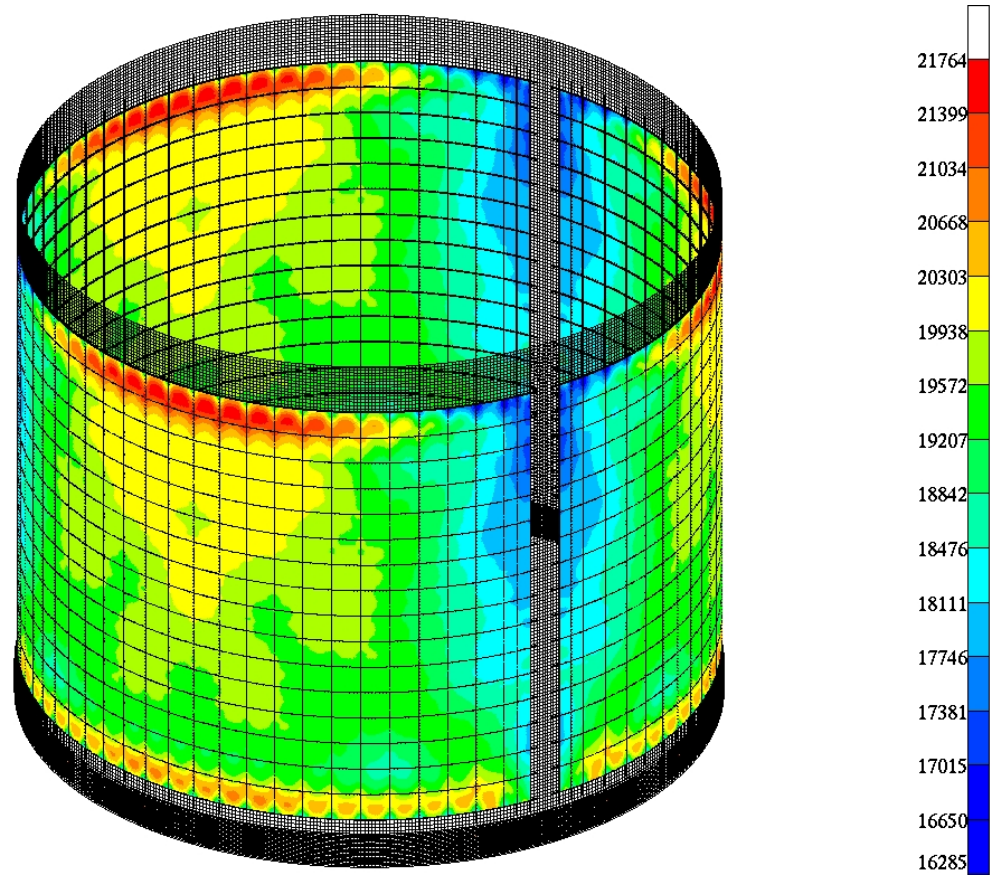


Figure D.18. SP-1 vonMises stress (psi) in acreage skin outer surface, LC1 at 2220 lb/in, AISI 1025 steel attachment rings.

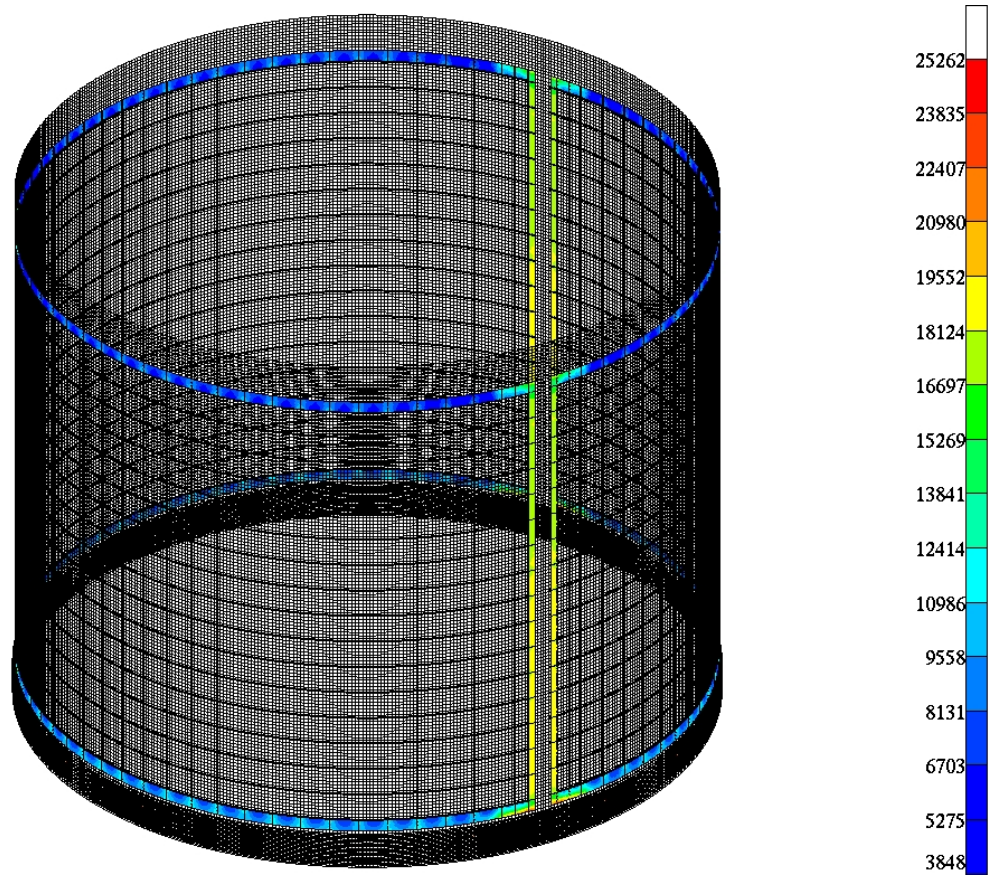


Figure D.19. SP-1 vonMises stress (psi) in intermediate skin inner surface, LC1 at 2220 lb/in, AISI 1025 steel attachment rings.

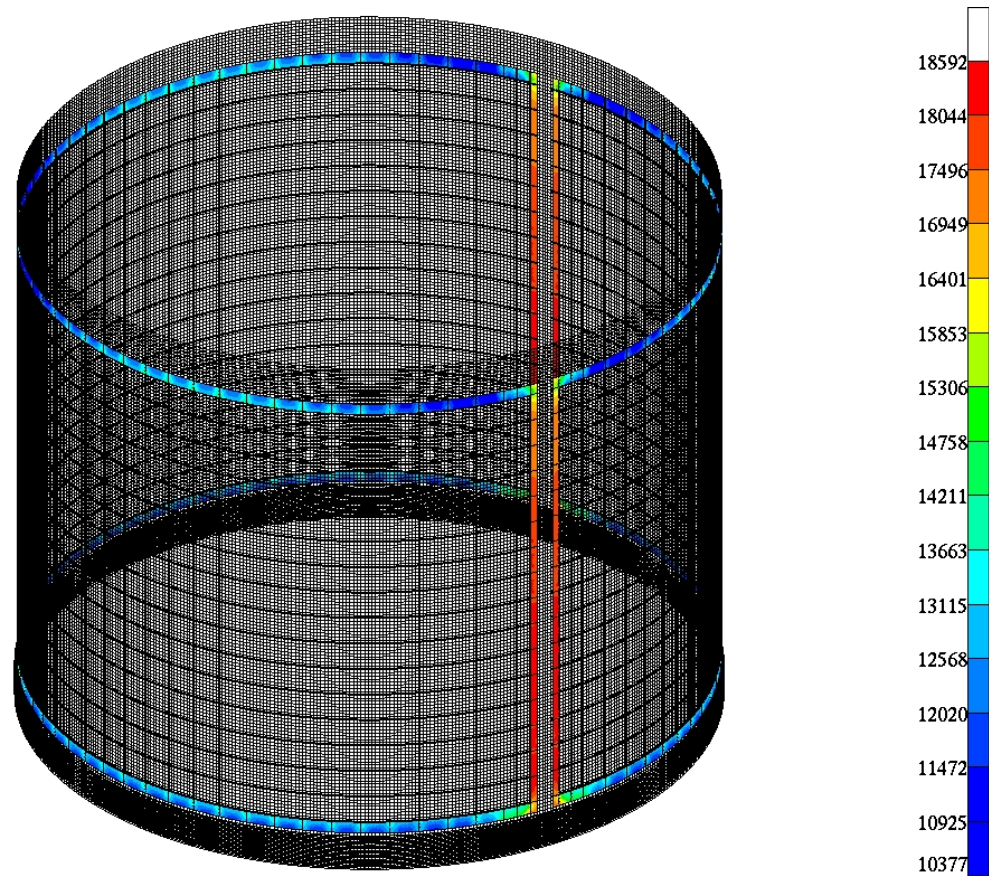


Figure D.20. SP-1 vonMises stress (psi) in intermediate skin outer surface, LC1 at 2220 lb/in, AISI 1025 steel attachment rings.

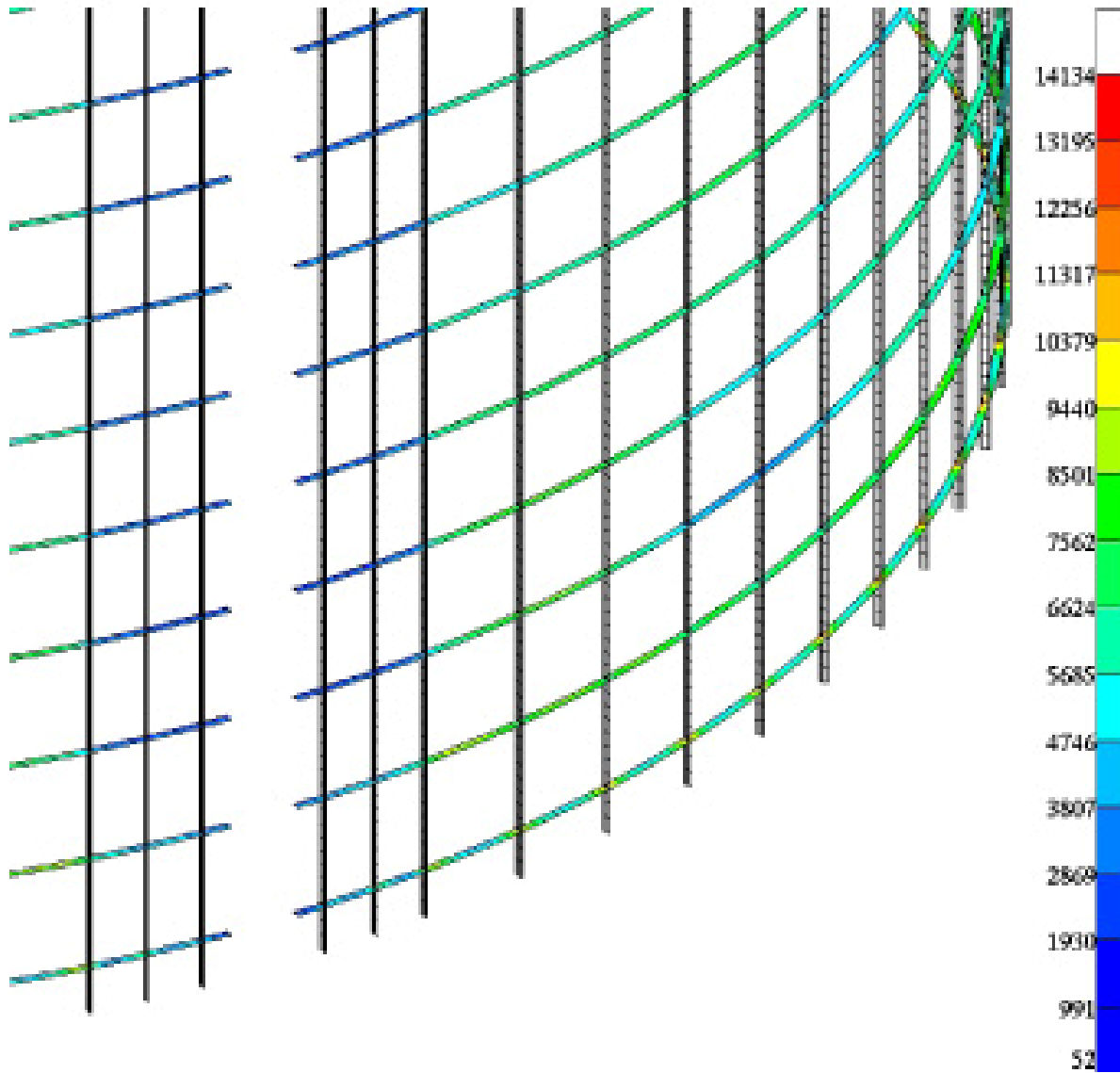


Figure D.21. SP-1 vonMises stress (psi) in ring inner surface, LC1 at 2220 lb/in, AISI 1025 steel attachment rings.

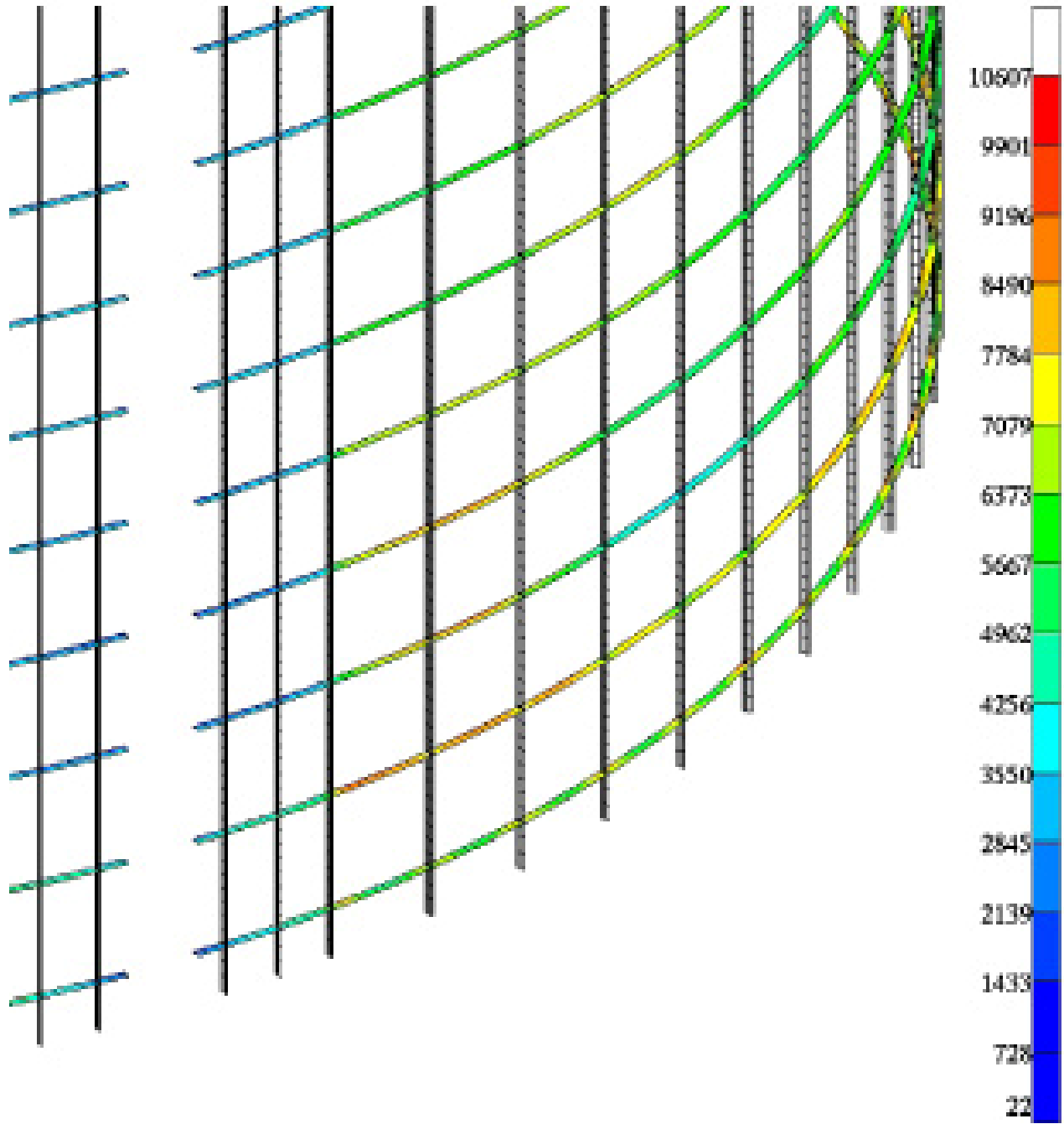


Figure D.22. SP-1 vonMises stress (psi) in ring outer surface, LC1 at 2220 lb/in, AISI 1025 steel attachment rings.

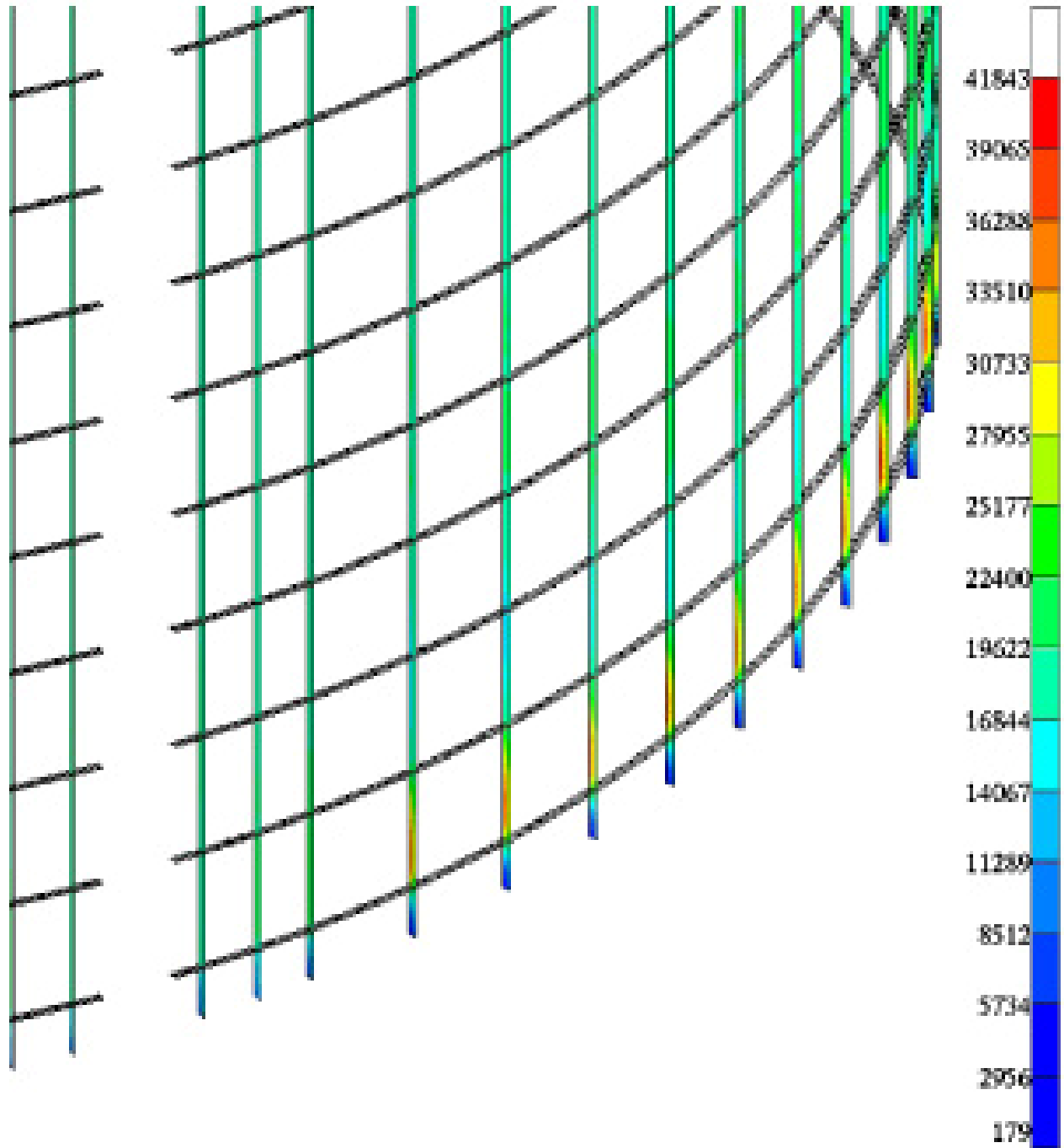


Figure D.23. SP-1 vonMises stress (psi) in stringer inner surface, LC1 at 2220 lb/in, AISI 1025 steel attachment rings.

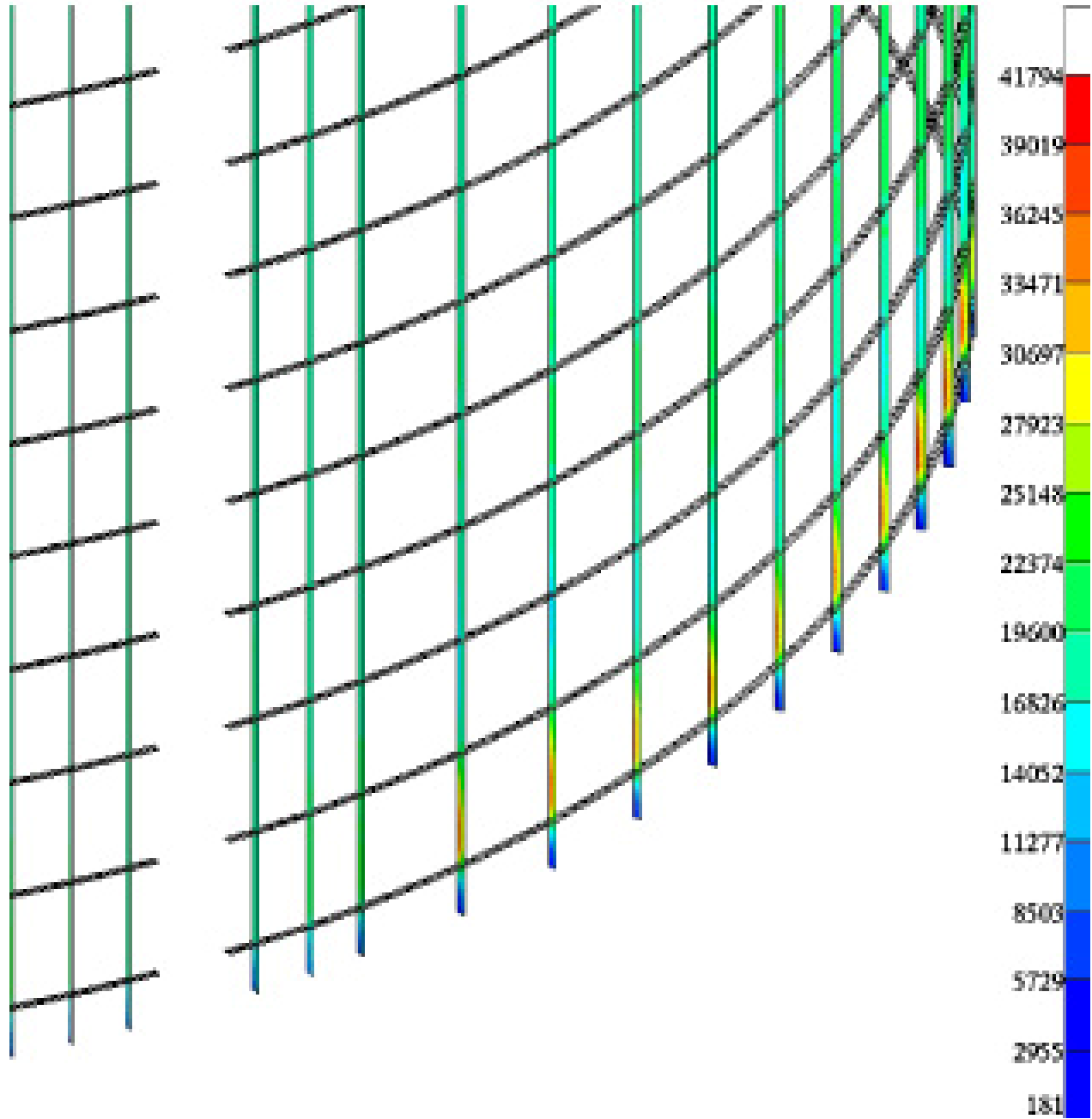


Figure D.24. SP-1 vonMises stress (psi) in stringer skin outer surface, LC1 at 2220 lb/in, AISI 1025 steel attachment rings.

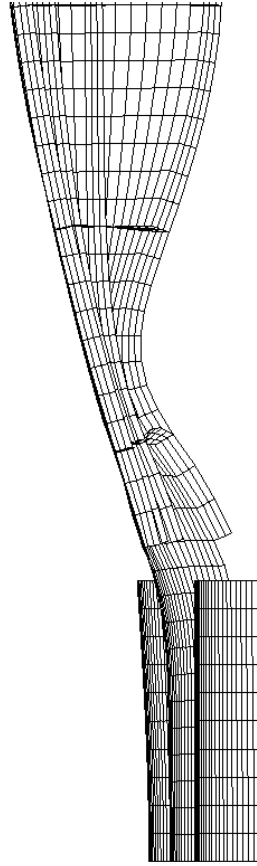


Figure D.25. SP-1 nonlinear contact region deformation at weld land, LC1 at 2220 lb/in, AISI 1025 steel attachment rings (deformations magnified x50).

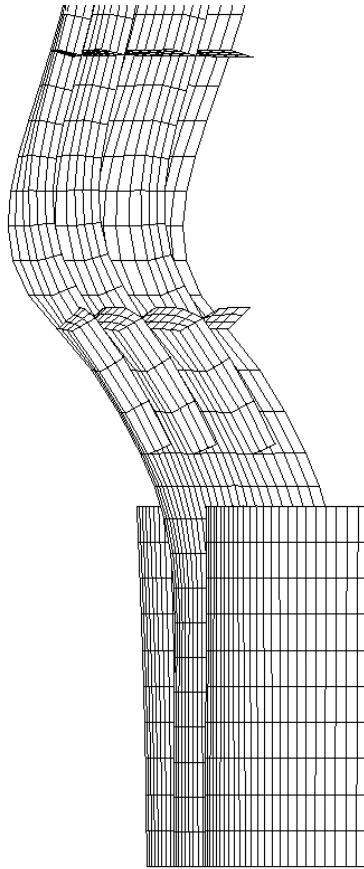


Figure D.26. SP-1 nonlinear contact region deformation at acreage (center of panel), LC1 at 2220 lb/in, AISI 1025 steel attachment rings (deformations magnified x50).

REPORT DOCUMENTATION PAGE

*Form Approved
OMB No. 0704-0188*

The public reporting burden for this collection of information is estimated to average 1 hour per response, including the time for reviewing instructions, searching existing data sources, gathering and maintaining the data needed, and completing and reviewing the collection of information. Send comments regarding this burden estimate or any other aspect of this collection of information, including suggestions for reducing this burden, to Department of Defense, Washington Headquarters Services, Directorate for Information Operations and Reports (0704-0188), 1215 Jefferson Davis Highway, Suite 1204, Arlington, VA 22202-4302. Respondents should be aware that notwithstanding any other provision of law, no person shall be subject to any penalty for failing to comply with a collection of information if it does not display a currently valid OMB control number.
PLEASE DO NOT RETURN YOUR FORM TO THE ABOVE ADDRESS.

1. REPORT DATE (DD-MM-YYYY) 01-08-2010		2. REPORT TYPE Technical Memorandum		3. DATES COVERED (From - To)	
4. TITLE AND SUBTITLE Design of 8-ft-diameter Barrel Test Article Attachment Rings for Shell Buckling Knockdown Factor Project				5a. CONTRACT NUMBER	
				5b. GRANT NUMBER	
				5c. PROGRAM ELEMENT NUMBER	
6. AUTHOR(S) Lovejoy, Andrew E.; Hilburger, Mark W.				5d. PROJECT NUMBER	
				5e. TASK NUMBER	
				5f. WORK UNIT NUMBER 869021.04.07.01.13	
7. PERFORMING ORGANIZATION NAME(S) AND ADDRESS(ES) NASA Langley Research Center Hampton, VA 23681-2199				8. PERFORMING ORGANIZATION REPORT NUMBER L-19913	
9. SPONSORING/MONITORING AGENCY NAME(S) AND ADDRESS(ES) National Aeronautics and Space Administration Washington, DC 20546-0001				10. SPONSOR/MONITOR'S ACRONYM(S) NASA	
				11. SPONSOR/MONITOR'S REPORT NUMBER(S) NASA/TM-2010-216839	
12. DISTRIBUTION/AVAILABILITY STATEMENT Unclassified - Unlimited Subject Category 16-Space Transportation and Safety Availability: NASA CASI (443) 757-5802					
13. SUPPLEMENTARY NOTES					
14. ABSTRACT The Shell Buckling Knockdown Factor (SBKF) project includes the testing of sub-scale cylinders to validate new shell buckling knockdown factors for use in the design of the Ares-I and Ares-V launch vehicles. Test article cylinders represent various barrel segments of the Ares-I and Ares-V vehicles, and also include checkout test articles. Testing will be conducted at Marshall Space Flight Center (MSFC) for test articles having an eight-foot diameter outer mold line (OML) and having lengths that range from three to ten feet long. Both ends of the test articles will be connected to the test apparatus using attachment rings. Three multiple-piece and one single-piece design for the attachment rings were developed and analyzed. The single-piece design was chosen and will be fabricated from either steel or aluminum (Al) depending on the required safety factors (SF) for test hardware. This report summarizes the design and analysis of these attachment ring concepts.					
15. SUBJECT TERMS Constellation Program; Shell buckling knockdown factor; Test article attachment rings; Testing methodologies					
16. SECURITY CLASSIFICATION OF:			17. LIMITATION OF ABSTRACT	18. NUMBER OF PAGES	19a. NAME OF RESPONSIBLE PERSON
a. REPORT	b. ABSTRACT	c. THIS PAGE			STI Help Desk (email: help@sti.nasa.gov)
U	U	U	UU	94	19b. TELEPHONE NUMBER (Include area code) (443) 757-5802